

000 VARIATIONAL DEEP LEARNING VIA IMPLICIT REGU- 001 LARIZATION 002 003 004

005 **Anonymous authors**

006 Paper under double-blind review

007 008 ABSTRACT 009

011 Modern deep learning models generalize remarkably well in-distribution, despite
012 being overparametrized and trained with little to no *explicit* regularization. In-
013 stead, current theory credits *implicit* regularization imposed by the choice of ar-
014 chitecture, hyperparameters and optimization procedure. However, deep neural
015 networks can be surprisingly non-robust, resulting in overconfident predictions
016 and poor out-of-distribution generalization. Bayesian deep learning addresses this
017 via model averaging, but typically requires significant computational resources as
018 well as carefully elicited priors to avoid overriding the benefits of implicit regu-
019 larization. Instead, in this work, we propose to regularize variational neural net-
020 works solely by relying on the *implicit bias of (stochastic) gradient descent*. We
021 theoretically characterize this inductive bias in overparametrized linear models as
022 generalized variational inference and demonstrate the importance of the choice
023 of parametrization. Empirically, our approach demonstrates strong in- and out-
024 of-distribution performance without additional hyperparameter tuning and with
025 minimal computational overhead.

027 1 INTRODUCTION

029 The success of deep learning across many application domains is, on the surface, remarkable, given
030 that deep neural networks are usually overparameterized and trained with little to no *explicit* regular-
031 ization. The generalization properties observed in practice have been explained by *implicit* regular-
032 ization instead, resulting from the choice of architecture [1], hyperparameters [2, 3], and optimizer
033 [4–10]. Notably, the corresponding inductive biases often require no additional computation, in
034 contrast to enforcing a desired inductive bias through explicit regularization.

035 In the last two decades, there has been an increasing focus on improving the reliability and robust-
036 ness of deep learning models via (approximately) Bayesian approaches [11] to improve performance
037 on out-of-distribution data [12], in continual learning [13] and sequential decision-making [14].
038 However, despite its promise, in practice, Bayesian deep learning can suffer from issues with prior
039 elicitation [15], can be challenging to scale [16], and explicit regularization via a prior combined
040 with approximate inference may result in pathological inductive biases and uncertainty [17–20].

041 In this work, we demonstrate both theoretically and empirically how to exploit the implicit bias of
042 optimization for approximate inference in probabilistic neural networks, thus regularizing training
043 implicitly rather than explicitly via the prior. This not only narrows the gap to how standard neural
044 networks are trained, but also reduces the computational overhead of training compared to varia-
045 tional inference. More specifically, we propose to learn a variational distribution over the weights
046 of a deep neural network by maximizing the *expected* log-likelihood in analogy to training via max-
047 imum likelihood in the standard case. However, in contrast to variational Bayes, there is *no explicit*
048 regularization via a Kullback-Leibler divergence to the prior. Surprisingly, we show theoretically
049 and empirically that training this way does not cause uncertainty to collapse away from the training
050 data, if initialized and parametrized correctly. More so, for overparametrized linear models we rigor-
051 ously characterize the implicit bias of SGD as generalized variational inference with a 2-Wasserstein
052 regularizer penalizing deviations from the prior. Figure 1 illustrates our approach on a toy example.

053 **Contributions** In this work, we propose a new approach to Bayesian deep learning that gener-
054 alizes robustly by exploiting the implicit regularization of (stochastic) gradient descent. We fully

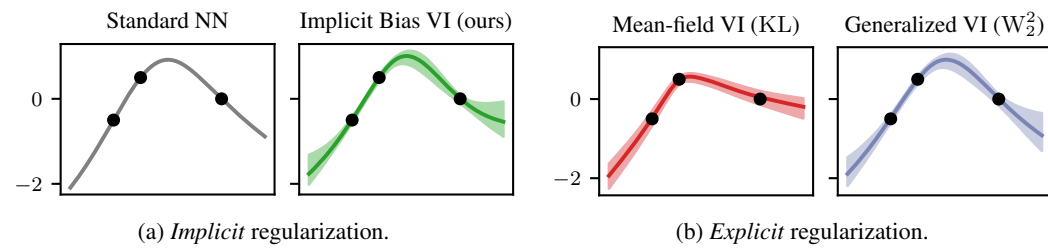


Figure 1: *Variational deep learning via implicit regularization.* Neural networks generalize well without explicit regularization due to implicit regularization from the architecture and optimization. We can exploit this implicit bias for variational deep learning, removing the computational overhead of explicit regularization and narrowing the gap to deep learning practice. As illustrated for a two-hidden layer MLP and proven rigorously for overparametrized linear models in Theorems 1 and 2, the implicit bias of (S)GD in variational networks (see (a)) can be understood as generalized variational inference with a 2-Wasserstein regularizer (see (b)). This differs from the standard ELBO objective with a KL divergence to the prior as used for example in mean-field VI (see (b)).

characterize this implicit bias for regression (Theorem 1) and binary classification (Theorem 2) in overparameterized linear models, generalizing results for non-probabilistic models and drawing a rigorous connection to generalized Bayesian inference. We also demonstrate the importance of the parametrization for the inductive bias and its impact on hyperparameter choice. In several benchmarks, we demonstrate competitive performance to state-of-the-art baselines for Bayesian deep learning, at minimal computational overhead compared to standard neural networks. Finally, we provide an open-source implementation of our approach as a standalone library: `inferno`.

2 BACKGROUND

Given a training dataset $(\mathbf{X}, \mathbf{y}) = \{(\mathbf{x}_n, y_n)\}_{n=1}^N$ of input-output pairs, supervised learning seeks a function $f_{\mathbf{w}}(\mathbf{x})$ to predict the corresponding output $y(\mathbf{x})$ for a test input \mathbf{x} . The parameters $\mathbf{w} \in \mathbb{R}^P$ of the function are typically trained via empirical risk minimization, i.e.

$$\mathbf{w}_* \in \arg \min_{\mathbf{w}} \ell_r(\mathbf{w}) \quad \text{with} \quad \ell_r(\mathbf{w}) = \ell(\mathbf{y}, f_{\mathbf{w}}(\mathbf{X})) + \lambda r(\mathbf{w}), \quad (1)$$

where the loss $\ell(\mathbf{y}, f_{\mathbf{w}}(\mathbf{X}))$ encourages fitting the training data and the regularizer $r(\mathbf{w})$, given some $\lambda > 0$, discourages overfitting, which can lead to poor generalization on test data.

Implicit Bias of Optimization One remarkable observation in deep learning is that training overparametrized neural networks ($P > N$) with gradient descent without *explicit* regularization can nonetheless lead to effective (in-distribution) generalization, despite there being many global minima of the loss corresponding to functions $f_{\mathbf{w}}$ which achieve zero training error [21]. This can be explained by the optimizer, initialization, and parametrization *implicitly* regularizing the optimization problem $\arg \min_{\mathbf{w}} \ell(\mathbf{y}, f_{\mathbf{w}}(\mathbf{X}))$, thereby preferring certain global minima [e.g. 4, 5, 7, 22, 23]. Nonetheless, deep neural networks can be surprisingly brittle when predicting *out-of-distribution*, often displaying overconfidence and a significant drop in generalization performance.

Bayesian Deep Learning Approximate Bayesian techniques like the Laplace approximation [24–26], stochastic weight averaging [27, 28], deep ensembles [29], and variational approaches [30–33] attempt to address the aforementioned shortcomings of deep learning by learning a distribution over functions as opposed to merely a point estimate. The idea being that a weighted combination of models, all of which achieve low training error, generalizes more robustly while at the same time providing uncertainty quantification.

Variational Inference In Bayesian inference this weighted combination is defined by the posterior distribution $p(\mathbf{w} | \mathbf{X}, \mathbf{y}) \propto p(\mathbf{y} | \mathbf{X}, \mathbf{w})p(\mathbf{w})$ over weights, induced by a likelihood $p(\mathbf{y} | \mathbf{w})$ and a choice of prior $p(\mathbf{w})$ that expresses an explicit preference for some models over others. Approximating the posterior with $q_{\boldsymbol{\theta}}(\mathbf{w}) \approx p(\mathbf{w} | \mathbf{X}, \mathbf{y})$ by maximizing a lower bound to the log-evidence leads to the following variational optimization problem [34]:

$$\boldsymbol{\theta}_* \in \arg \min_{\boldsymbol{\theta}} \ell_r(\boldsymbol{\theta}) \quad \text{s.t.} \quad \ell_r(\boldsymbol{\theta}) = \mathbb{E}_{q_{\boldsymbol{\theta}}(\mathbf{w})}(-\log p(\mathbf{y} | \mathbf{w})) + \text{KL}(q_{\boldsymbol{\theta}}(\mathbf{w}) \parallel p(\mathbf{w})) \quad (2)$$

108 Equation (2) is an instance of the empirical risk minimization objective in Equation (1), with the key
 109 difference that one optimizes over variational parameters θ of a family of distributions $q_\theta(\mathbf{w}) \in \mathcal{Q}$.
 110 If that family includes the posterior, $q_\theta(\mathbf{w}) = p(\mathbf{w} \mid \mathbf{X}, \mathbf{y})$ is the unique global minimum. In
 111 the case of a potentially misspecified prior or likelihood, the variational formulation (2) can be
 112 generalized to arbitrary loss functions ℓ and statistical distances D to the prior [35–37], such that

$$\ell_r(\theta) = \mathbb{E}_{q_\theta(\mathbf{w})}(\ell(\mathbf{y}, f_\mathbf{w}(\mathbf{X}))) + \lambda D(q_\theta, p). \quad (3)$$

3 VARIATIONAL DEEP LEARNING VIA IMPLICIT REGULARIZATION

117 Our overarching goal is to enable deep neural networks to generalize robustly out-of-distribution
 118 without sacrificing their in-distribution performance, at minimal computational overhead. We ap-
 119 proach this goal within the framework of Bayesian deep learning, by learning a distribution over
 120 neural networks $f_\mathbf{w}$, induced by a parametrized variational distribution $q_\theta(\mathbf{w})$ over its weights.
 121 However, rather than approximating the Bayesian posterior, which trades off training error against
 122 an explicit, a priori preference for certain models, we enforce that *all models have zero training*
 123 *error* while using *implicit* regularization to weight them. Doing so preserves the implicit regulari-
 124 zation of the optimizer, which determines the generalization performance of neural networks to a
 125 substantial degree, rather than purely relying on explicit regularization induced by the prior. Impor-
 126 tantly, this approach leads to robust out-of-distribution generalization, while providing uncertainty
 127 quantification at small computational overhead over standard deep learning.

3.1 TRAINING VIA THE EXPECTED LOSS

130 We propose to train a variational neural network defined by an architecture $f_\mathbf{w}$ and a variational
 131 distribution over weights $q_\theta(\mathbf{w})$ by *minimizing the expected loss* $\bar{\ell}(\theta)$ in analogy to how deep neural
 132 networks are usually trained. In other words, the optimal variational parameters are given by

$$\theta_* \in \arg \min_{\theta} \underbrace{\mathbb{E}_{q_\theta(\mathbf{w})}(\ell(\mathbf{y}, f_\mathbf{w}(\mathbf{X})))}_{:=\bar{\ell}(\theta)} + \lambda D(q_\theta, p). \quad (4)$$

136 At first glance removing the divergence term from the variational objective in Eq. (3) seems prob-
 137 lematic because the new objective is clearly minimized when the variational distribution is a point
 138 mass at the minimum loss solution, i.e. $q_{\theta_*}(\mathbf{w}) = \delta_{\mathbf{w}_*}(\mathbf{w})$ where $\mathbf{w}_* \in \arg \min_{\mathbf{w}} \ell(\mathbf{y}, f_\mathbf{w}(\mathbf{X}))$.
 139 This seemingly defeats the point of a Bayesian deep learning framework, given that there is no
 140 variability in predictions on test data. Moreover, the new objective no longer involves a prior dis-
 141 tribution, ostensibly removing the ability to manually favor some models over others entirely. The
 142 key to understanding our approach is that, in the overparameterized setting, a point mass is only one
 143 of many optima corresponding to distributions $q_{\theta_*}(\mathbf{w})$, and it is the implicit bias of the optimiza-
 144 tion procedure that chooses among them. As we will see, if one trains an overparametrized linear
 145 model via the expected loss using (stochastic) gradient descent, this implicit bias can be explicitly
 146 characterized to depend on the initialization.

3.2 IMPLICIT BIAS OF SGD AS GENERALIZED VARIATIONAL INFERENCE

147 Assume we train an overparametrized linear model with a Gaussian variational family via the ex-
 148 pected loss. For an appropriate learning rate sequence, (stochastic) gradient descent converges to a
 149 global minimum $\theta_*^{\text{GD}} \in \arg \min \bar{\ell}(\theta)$ of the training objective. As we show in Section 4, if SGD is
 150 *initialized to the prior*, i.e. $q_{\theta_0}(\mathbf{w}) = p(\mathbf{w})$, its implicit bias can be understood as selecting the
 151 distribution over models with zero training error which is closest to the prior in 2-Wasserstein distance:

$$q_{\theta_*^{\text{GD}}} = \arg \min_{q_\theta} \text{W}_2^2(q_\theta, p) \text{ s.t. } \theta \in \arg \min \bar{\ell}(\theta)$$

152 Therefore, we can interpret the implicit bias of (S)GD when training a variational linear model as
 153 performing *generalized variational inference*. More precisely, the above is equivalent to $q_{\theta_*^{\text{GD}}}$ mini-
 154 mizing the objective in Equation (3) for a certain regularization strength, but with a regularizer that
 155 is *not* a KL divergence as it would be for standard variational inference, but rather a 2-Wasserstein
 156 distance to the prior. This characterization directly generalizes results for (non-probabilistic) mod-
 157 els, where the implicit bias of SGD selects minima that are close to the initialization in Euclidean
 158 distance [5, 21]. We therefore call our method **Implicit Bias Variational Inference (IBVI)**. From a

practical perspective, by exploiting the implicit regularization of SGD, rather than performing generalized variational inference directly, we no longer need to compute the regularizer explicitly or allocate memory for the prior hyperparameters.¹

Section 4 provides a detailed version of the regression result introduced here and proves a similar result for binary classification. Our experiments in Section 5 focus on the application to deep neural networks, where we generally expect the implicit regularization to be more complex.

3.3 COMPUTATIONAL EFFICIENCY

In practice, we minibatch the expected loss both over training data and parameter samples w_m drawn from the variational distribution $q_{\theta}(w)$ such that

$$\bar{\ell}(\theta) = \mathbb{E}_{q_{\theta}(w)}(\ell(y, f_w(X))) \approx \frac{1}{N_b M} \sum_{n=1}^{N_b} \sum_{m=1}^M \ell(y_n, f_{w_m}(x_n)). \quad (5)$$

The training cost is primarily determined by two factors. The number of parameter samples M we draw for each evaluation of the objective, and the variational family, which determines the number of additional parameters of the model and the cost for sampling a set of parameters in each forward pass. We wish to keep the overhead compared to a vanilla deep neural network as small as possible.

Training With A Single Parameter Sample ($M = 1$) When drawing fewer parameter samples w_m the training objective in Eq. (5) becomes noisier similar to using a smaller batch size. This is concerning since the optimization procedure may not converge given this additional noise. However, one can *train with a single parameter sample only*, simply by reducing the learning rate appropriately, as we show experimentally in Figure 2 and Section S3.2. Therefore, given a set of sampled parameters, the cost of a forward and backward pass is identical to a standard neural network (up to the overhead of the covariance parameters). When using fewer parameter samples in the expected loss, training is unstable unless the learning rate is chosen sufficiently small. For a fixed number of optimizer steps this decreases performance, but either training for more steps, or using momentum closes this gap.

Variational Family and Covariance Structure We choose a Gaussian variational distribution $q_{\theta}(w)$ over (a subset of the) weights of the neural network. While at first glance this may seem restrictive, there is ample evidence that variational families in deep neural networks do not need to be complex to be expressive [38, 39]. In fact, in analogy to deep feedforward NNs with ReLU activations being universal approximators [40], one can show that Bayesian neural networks with ReLU activations and at least one Gaussian hidden layer are universal conditional distribution approximators, meaning they can approximate any continuous conditional distribution arbitrarily well [39]. As we show in Section 4, training an overparametrized linear model with SGD via the expected loss amounts to generalized variational inference *if the covariance is factorized*, i.e. $\Sigma = \bar{S}S^T$ where $S \in \mathbb{R}^{P \times R}$ is a dense matrix with rank $R \leq P$. The implicit bias of SGD for arbitrary parametrizations of the covariance matrix remains an open problem. Throughout our experiments we use Gaussian layers with factorized covariances for all architectures.

3.4 PARAMETRIZATION, FEATURE LEARNING AND HYPERPARAMETER TRANSFER

The inductive bias of SGD depends on the initialization and choice of *parametrization*, a bijective map $\rho : \Theta' \rightarrow \Theta$ reparametrizing a (variational) model such that $f_{\theta} \equiv f_{\rho(\theta')}$. When training deep neural networks, it is not unusual to use layer-specific learning rates. These can be absorbed into the weights of the model and the initialization, meaning they effectively just define a different

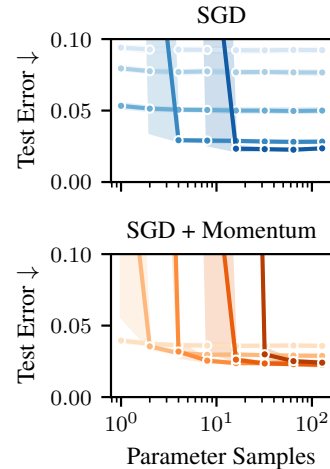


Figure 2: *Training with a single parameter sample given a small enough learning rate.* Lighter color shades correspond to smaller learning rates. See also Section S3.2.

¹We only need them to initialize the optimizer after which we can free up the allocated memory.

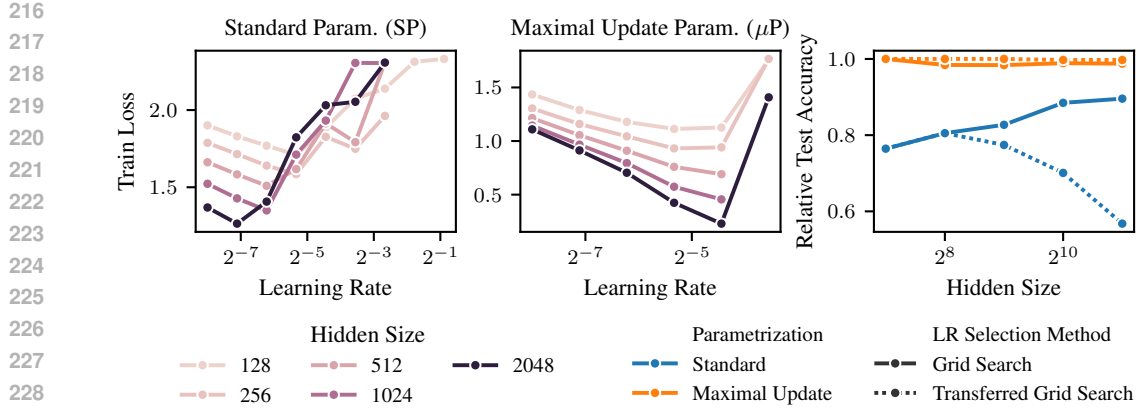


Figure 3: *Hyperparameter Transfer*. When scaling the size of a neural network, one has to re-tune the hyperparameters, such as the learning rate, when using the standard parametrization (SP). The same is true for probabilistic networks as we show here on CIFAR-10 (left). However, when using our proposed extension of the maximal update parametrization (μ P) [41] to probabilistic networks, one can tune the learning rate on a small model and achieve optimal generalization for larger models by “transferring” the optimal learning rate from a smaller model (center and right).

parametrization [Lemma J.1, 41]. While parameterization is well-studied for non-probabilistic deep learning, it has been identified as one of the “grand challenges of Bayesian computation” [42].

In deep learning, the “standard parameterization” (SP) initializes the weights of a neural network randomly from a distribution with variance $\propto 1/\text{fan_in}$ (e.g., as in Kaiming initialization, the PyTorch default) and makes no further adjustments to the forward pass or learning rate. In contrast, the maximal update parametrization (μ P) [43] ensures feature learning even as the width of the network tends to infinity. In addition, under μ P, hyperparameters like the learning rate, can be tuned on a small model and transferred to a large-scale model [41].

Given our interpretation of training via the expected loss as generalized variational inference with a prior implied by the parametrization and initialization, a natural question is whether we can extend μ P to the variational setting and thus inherit its inductive bias. In the probabilistic setting, feature learning occurs when the *distribution* over hidden units changes from initialization. At any point during training, the i th hidden unit in layer l is a function of four random variables: the variational mean and covariance parameters (μ, S) , Gaussian noise z , and the previous layer hidden units:

$$\mathbf{h}_i^{(l)}(\mathbf{x}) = \mathbf{W}_i \mathbf{h}^{(l-1)}(\mathbf{x}) = (\mu_i + S_i z) \mathbf{h}^{(l-1)}(\mathbf{x}). \quad (6)$$

The parameters are random because of the stochasticity in the initialization and/or optimization procedure, while the noise is randomly drawn during each forward pass. Since the $S_i z$ term is a sum over R terms, where R is the rank of $S \in \mathbb{R}^{P \times R}$, applying the central limit theorem we propose scaling this term by $R^{-1/2}$ and then applying μ P to the mean and covariance parameters. In practice, we implement the scaling via an adjustment to the covariance initialization and learning rate. Section S2 in the supplement provides empirical investigating of this scaling, demonstrating feature learning in the last hidden layer as the width is increased.

Figure 3 demonstrates that our proposed maximal update parametrization enables hyperparameter transfer in a probabilistic model. We train two-hidden-layer MLPs on CIFAR10, using a low rank covariance in the final two layers. Under standard parametrization (left panel), the learning rate that results in the smallest training loss decreases with hidden size. In contrast, under μ P (middle panel), it remains the same across hidden sizes. The right panel of Fig. 3 demonstrates the practical implications for model selection. For each parametrization and each hidden size D , we select the learning rate based on a grid search. In “transferred grid search” we do a grid search using the smallest model (hidden size 128) and transfer the best validating learning rate to the hidden size D model, whereas in “grid search” we perform the grid search on the hidden size D model. Relative to the test accuracy of the best performing model across learning rate and parametrization, we see

270 that (a) μ P outperforms SP, though the gap decreases with hidden size, and (b) the transfer strategy
 271 works well for μ P but poorly for SP once the hidden size exceeds 256.
 272

273 **3.5 RELATED WORK**

274 Variational inference in the context of Bayesian deep learning has seen rapid development in re-
 275 cent years [30–33, 44, 45]. Using a Wasserstein regularizer [37] in the context of generalized VI
 276 [36] is arguably most related to our work, given our theoretical results. Structure in the variational
 277 parameters has always played an important role for computational reasons [38, 46, 47] and often
 278 only a few layers are treated probabilistically [39], with some methods only considering the last
 279 layer, effectively treating the neural network as a feature extractor [48, 49]. The Laplace approxi-
 280 mation if applied in the last-layer also falls under this category, which has the advantage that it can
 281 be applied post-hoc [13, 24–26, 50–54]. Deep ensembles repeat the standard training process using
 282 multiple random initializations [29, 55] and have been linked to Bayesian methods [56, 57] with cer-
 283 tain caveats [58, 59]. While we use SGD only to optimize the variational parameters and arguably
 284 average over samples by using momentum, SGD has also been used widely to directly approximate
 285 samples from a target distribution [27, 56, 60, 61], a popular example being stochastic weight aver-
 286 aging (SWA) [27, 28]. Our theoretical analysis extends recent developments on the implicit bias of
 287 overparameterized linear models [4, 5, 7] to the probabilistic setting. For classification, works have
 288 focused on convergence rates [6], SGD [7], SGD with momentum [8], and the multiclass setting
 289 [10]. Results on the implicit bias of neural network training [22] often assume large widths [9, 62–
 290 65] allowing similar arguments as for linear models. The former is exemplified by the neural tangent
 291 parametrization, under which neural networks behave like kernel methods in the infinite width limit
 292 [66]. Yang et al. [41, 43, 64, 65] developed an alternative parameterization that still admits feature
 293 learning in the infinite width limit, which we extended to the case of variational networks.
 294

295 **4 THEORETICAL ANALYSIS**

296 Consider an overparameterized linear model with a Gaussian prior, trained via the expected loss
 297 using (stochastic) gradient descent. We show that, in both regression (Theorem 1) and binary clas-
 298 sification (Theorem 2), our approach can be understood as generalized variational inference with a
 299 2-Wasserstein regularizer, which penalizes deviation from the prior among models with zero training
 300 error. Theorems 1 and 2 recover analogous results for non-probabilistic models [4, 5, 21].
 301

302 **4.1 LINEAR REGRESSION**

303 **Theorem 1** (Implicit Bias in Regression)

304 Let $f_w(x) = x^\top w$ be an overparametrized linear model with $P > N$. Define a Gaussian prior
 305 $p(w) = \mathcal{N}(w; \mu_0, S_0 S_0^\top)$ and likelihood $p(y | w) = \mathcal{N}(y; f_w(x), \sigma^2 I)$ and assume a varia-
 306 tional family $q_\theta(w) = \mathcal{N}(w; \mu, S S^\top)$ with $\theta = (\mu, S)$ such that $\mu \in \mathbb{R}^P$ and $S \in \mathbb{R}^{P \times R}$ where
 307 $R \leq P$. If the learning rate sequence $(\eta_t)_t$ is chosen such that the limit point $\theta_*^{\text{GD}} = \lim_{t \rightarrow \infty} \theta_t^{\text{GD}}$
 308 identified by gradient descent, initialized at $\theta_0 = (\mu_0, S_0)$, is a (global) minimizer of the expected
 309 log-likelihood $\bar{\ell}(\theta)$, then

$$\theta_*^{\text{GD}} \in \arg \min_{\substack{\theta = (\mu, S) \\ s.t. \theta \in \arg \min \bar{\ell}(\theta)}} W_2^2(q_\theta, p). \quad (7)$$

310 Further, this also holds in the case of stochastic gradient descent and when using momentum.
 311

312 *Proof.* See Section S1.1.1. □

313 Theorem 1 states that, among those variational parameters which minimize the expected loss, SGD
 314 (with momentum) converges to the unique variational distribution which is closest in 2-Wasserstein
 315 distance to the prior. This characterization of the implicit regularization of SGD as generalized vari-
 316 ational inference differs from a standard ELBO objective (2) in VI via the choice of regularizer. Since
 317 the variational parameters minimize the expected loss in Equation (7), all samples from the predic-
 318 tive distribution interpolate the training data (see Figure 1(b), right panel), the same way a standard
 319 neural network would. In contrast, when training with a KL regularizer, the uncertainty does not
 320 collapse at the training data (see Figure 1(b), left panel), in fact a KL regularizer would diverge to
 321 infinity for a Gaussian with vanishing variance. Now, for test points that are increasingly out-of-
 322 distribution, i.e. less aligned with the span of the training data, the variational predictive matches
 323

324 the prior predictive more closely. Interestingly, $q_{\theta_{\text{GD}}}$ is equal to the distribution over weights of an
 325 ensemble of linear models initialized from the prior and trained independently (see Section S1.1.3).
 326 Next, we prove a similar result for binary classification.
 327

328 4.2 BINARY CLASSIFICATION OF LINEARLY SEPARABLE DATA

329 Consider a binary classification problem with labels $y_n \in \{-1, 1\}$, a linear model $f_{\mathbf{w}}(\mathbf{x}) = \mathbf{x}^T \mathbf{w}$
 330 and a variational distribution $q_{\theta}(\mathbf{w})$ with variational parameters θ . The expected empirical loss
 331 is $\bar{\ell}(\theta) = \sum_{n \in [N]} \mathbb{E}_{q_{\theta}(\mathbf{w})}(\ell(y_n \mathbf{x}_n^T \mathbf{w}))$. We assume without loss of generality² that all labels are
 332 positive, i.e. $y_n = 1$ for all n , and that the dataset is linearly separable.
 333

334 **Assumption 1** The dataset is *linearly separable*: $\exists \mathbf{w} \in \mathbb{R}^P$ such that $\forall n : \mathbf{w}^T \mathbf{x}_n > 0$.

335 For an overparametrized linear model, if $\mathbf{X} \in \mathbb{R}^{N \times P}$ has full row rank the dataset is guaranteed to
 336 be linearly separable.³ Define the solution to the hard margin SVM, the *L₂ max margin vector* as
 337

$$338 \hat{\mathbf{w}} = \arg \min_{\mathbf{w} \in \mathbb{R}^P} \|\mathbf{w}\|_2^2 \quad \text{s.t.} \quad \mathbf{w}^T \mathbf{x}_n \geq 1, \quad (8)$$

340 and the set of *support vectors* $\mathcal{S} = \arg \min_{n \in [N]} \mathbf{x}_n^T \hat{\mathbf{w}}$ indexing the data points on the margin.
 341 We make the following additional assumption which is satisfied with high probability under mild
 342 assumptions on the training data distribution and degree of overparametrization [67, 68].

343 **Assumption 2** The SVM support vectors span the dataset: $\text{span}(\{\mathbf{x}_n\}_{n \in [N]}) = \text{span}(\{\mathbf{x}_n\}_{n \in \mathcal{S}})$.
 344

345 We can now characterize the implicit bias in the case of binary classification.

346 **Theorem 2** (Implicit Bias in Binary Classification)

347 Let $f_{\mathbf{w}}(\mathbf{x}) = \mathbf{x}^T \mathbf{w}$ be an (overparametrized) linear model and define a Gaussian prior $p(\mathbf{w}) =$
 348 $\mathcal{N}(\mathbf{w}; \mu_0, \mathbf{S}_0 \mathbf{S}_0^T)$. Assume a variational distribution $q_{\theta}(\mathbf{w}) = \mathcal{N}(\mathbf{w}; \mu, \mathbf{S} \mathbf{S}^T)$ over the weights
 349 $\mathbf{w} \in \mathbb{R}^P$ with variational parameters $\theta = (\mu, \mathbf{S})$ such that $\mathbf{S} \in \mathbb{R}^{P \times R}$ and $R \leq P$. Assume we
 350 are using the exponential loss $\ell(u) = \exp(-u)$ and optimize the expected empirical loss $\bar{\ell}(\theta)$ via
 351 gradient descent initialized at the prior, i.e. $\theta_0 = (\mu_0, \mathbf{S}_0)$, with a sufficiently small learning rate η .
 352 Then for almost any dataset which is linearly separable (Assumption 1) and for which the support
 353 vectors span the data (Assumption 2), the rescaled gradient descent iterates (rGD)
 354

$$354 \theta_t^{\text{rGD}} = (\mu_t^{\text{rGD}}, \mathbf{S}_t^{\text{rGD}}) = \left(\frac{1}{\log(t)} \mu_t^{\text{GD}} + \mathbf{P}_{\text{null}(\mathbf{X})} \mu_0, \mathbf{S}_t^{\text{GD}} \right) \quad (9)$$

355 converge to a limit point $\theta_*^{\text{rGD}} = \lim_{t \rightarrow \infty} \theta_t^{\text{rGD}}$ for which it holds that

$$358 \theta_*^{\text{rGD}} \in \arg \min_{\substack{\theta = (\mu, \mathbf{S}) \\ \text{s.t. } \theta \in \Theta_*}} W_2^2(q_{\theta}, p). \quad (10)$$

360 where the feasible set $\Theta_* = \{(\mu, \mathbf{S}) \mid \mathbf{P}_{\text{range}(\mathbf{X}^T)} \mu = \hat{\mathbf{w}} \text{ and } \forall n : \text{Var}_{q_{\theta}}(f_{\mathbf{w}}(\mathbf{x}_n)) = 0\}$
 361 consists of mean parameters which, if projected onto the training data, are equivalent to the *L₂ max*
 362 *margin vector* and covariance parameters such that there is no uncertainty at training data.
 363

364 *Proof.* See Section S1.2. □

366 Theorem 2 states that the mean parameters μ_t converge to the *L₂ max-margin vector* $\hat{\mathbf{w}}$ in the span
 367 of the training data, i.e. the data manifold, and there uncertainty collapses to zero. This is analogous
 368 to the regression case, where zero training loss enforces interpolation of the training data. In the
 369 null space of the training data, i.e. off of the data manifold, the model falls back on the prior as
 370 enforced by the 2-Wasserstein distance. The assumption of an exponential loss is standard in the
 371 literature and we expect this to extend to (binary) cross-entropy in the same way it does in results
 372 for standard neural networks [4, 6–8, 10]. Similarly, we conjecture that Theorem 2 can be extended
 373 to SGD with momentum [cf. 7, 8]. While Theorem 2 is similar to Theorem 1, there are some subtle
 374 differences. First, the feasible set for the minimization problem in Equation (10) is not the set of
 375 minima of the expected loss. This is because the exponential function does not have an optimum
 376 in contrast to a quadratic function. However, the sequence of variational parameters identified by
 377

²This is not a restriction since we can always absorb the sign into the inputs, such that $\mathbf{x}'_n := y_n \mathbf{x}_n$.

³We can always choose $\mathbf{w} = \mathbf{X}^T (\mathbf{X} \mathbf{X}^T)^{-1} \mathbf{1}$, i.e. the weights linearly interpolating $\mathbf{y} = \mathbf{1} = (1, \dots, 1)^T$.

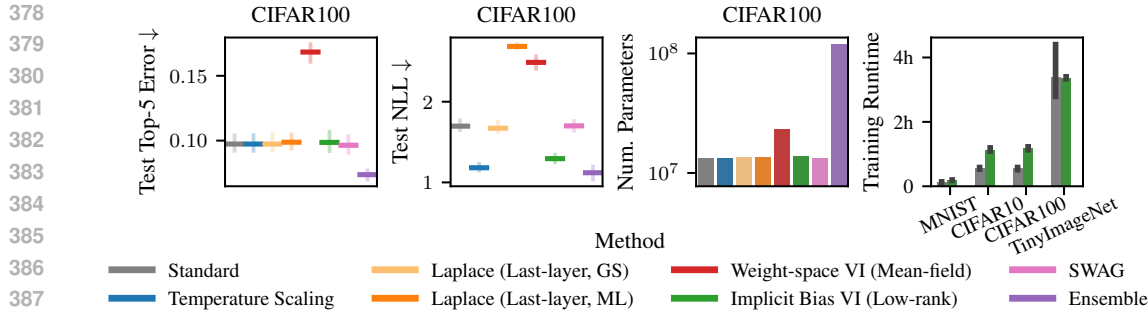


Figure 4: *In-distribution generalization and uncertainty quantification.* Implicit Bias VI (IBVI) has similar test error to other Bayesian deep learning approaches and achieves competitive uncertainty quantification on in-distribution data. While ensembles have improved accuracy, they come at an additional memory overhead. Training a probabilistic model via IBVI has only a minor computational overhead during training, both in time and memory, over standard deep learning.

gradient descent still satisfies $\lim_{t \rightarrow \infty} \bar{\ell}(\theta_t) = 0$. Second, without transformation of the mean parameters, the exponential loss results in the mean parameters being unbounded. This necessitates the transformation in Equation (9) as we explain in detail in Section S1.3.

5 EXPERIMENTS

We benchmark the *generalization* and *robustness* of our approach, **Implicit Bias VI (IBVI)**, against standard neural networks and several baselines for uncertainty quantification, namely **Temperature Scaling (TS)** [69], **Laplace approximation (LA-GS) & (LA-ML)** [24–26], **Weight-Space VI (WSVI)** [30, 31], **SWA-Gaussian (SWAG)** [28] and **Deep Ensembles (DE)** [29], on a set of standard benchmark datasets for image classification and robustness to input corruptions. We use convolutional architectures (LeNet5 [70] or ResNet34 [71]), which, for all datasets but MNIST, are initialized with pretrained weights except for the input and output layer. All models were trained with SGD with momentum $\gamma = 0.9$ and a batch size of $N_b = 128$ for 200 epochs in single precision on an NVIDIA GH200 GPU. Results shown are averaged across five random seeds. A detailed description of the datasets, metrics, models and training can be found in Section S3. An implementation of our method is contained in the supplementary material and will be open-sourced upon publication.

In-Distribution Generalization and Uncertainty Quantification In order to assess the in-distribution generalization, we measure the test error, negative log-likelihood (NLL) and calibration error (ECE) on MNIST, CIFAR10, CIFAR100 and TinyImageNet. As Figure 4 shows for CIFAR100, and Figure S10 for all datasets, the test error for post-hoc methods (TS, LA-GS, LA-ML) is unchanged. As expected, SWAG and IBVI perform similarly with only Ensembles providing an increase in accuracy, but at substantial memory overhead compared to most other approaches. Similarity of IBVI to Ensembles is perhaps expected in light of their equivalence for linear models (see Proposition S1). In-distribution uncertainty quantification measured in terms of NLL is improved substantially by TS, DE and IBVI with only LA and WSVI showing occasional worsening of NLL compared to the base model. The full results in Figure S10 show that TS, DE and IBVI consistently are also the best calibrated. As described in Section 3.3, for IBVI we train with a single sample only and a probabilistic input and output layer with low-rank covariance, reducing the memory overhead compared to a standard neural network to as little as $\approx 10\%$ with similar training time (see Figure 4). See Section S3.3.2 for the full experimental results including different parametrizations (SP vs μ P).

Robustness to Input Corruptions We evaluate the robustness of the different models on MNISTC [72], CIFAR10C, CIFAR100C and TinyImageNetC [73]. These are corrupted versions of the original datasets, where the images are modified via a set of 15 corruptions, such as impulse noise, blur, pixelation etc. We selected the maximum severity for each corruption and averaged the performance across all. As expected, the performance of all models drops compared to the in-distribution performance measured on the standard test sets as Figure 5 shows. Besides DE which consistently show lower test error, also IBVI shows improved accuracy on corrupted data compared to all other approaches. When using the maximal update parametrization, SWAG shows good ac-

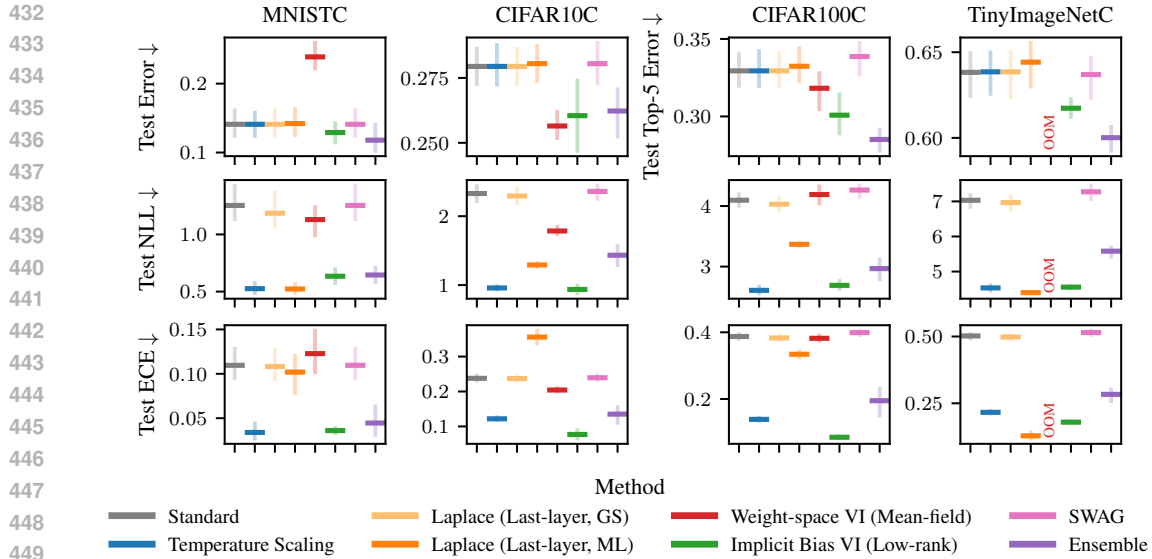


Figure 5: *Generalization on robustness benchmark problems.* When comparing different methods for Bayesian deep learning with regards to robustness to 15 different input corruptions, our approach, Implicit Bias VI, consistently has competitive uncertainty quantification across different datasets and metrics without sacrificing accuracy compared to a non-probabilistic network.

curacy on the two larger datasets (see Figure S12). **TS**, **DE** and **IBVI** perform consistently well in terms of uncertainty quantification (both for NLL and ECE) across all datasets, with **LA-ML** being somewhat competitive in terms of NLL. However, compared to the in-distribution setting **IBVI** has better uncertainty quantification than the **Ensembles** across all datasets.

Limitations Compared to standard neural networks, when training via Implicit Bias VI, we observed that often lower learning rates were necessary due to the additional stochasticity in the objective (see also Section 3.3). While this does not have a significant impact on generalization, it sometimes requires slightly more epochs to achieve similar in-distribution performance to standard neural networks. Effectively, early in training it takes a bit more time for IBVI to become sufficiently certain about those features which are critical for in-distribution performance. This also means that folk knowledge on learning rate settings for specific architectures may not immediately transfer. In the experiments we train models with probabilistic in- and output layers with our approach, but we have so far not explored other covariance structures or where in the network probabilistic layers are most beneficial. While there is theoretical evidence that even just a single probabilistic hidden layer may be sufficient [39], we believe there is potential for improvement. Beyond the prior induced by the choice of parametrization, we did not experiment with more informative or learned priors, which could potentially give significant performance improvements on certain tasks [15].

6 CONCLUSION

In this paper, we demonstrated how to improve the robustness of deep neural networks and while quantifying predictive uncertainty by exploiting the implicit regularization of (stochastic) gradient descent. We rigorously characterized this implicit bias for an overparametrized linear model and showed that our approach is equivalent to generalized variational inference with a 2-Wasserstein regularizer at reduced computational cost. We demonstrated the importance of parameterization and how it impacts the inductive bias via the initialization — thus conferring desirable properties such as learning rate transfer. Lastly, we empirically demonstrated competitive performance with state-of-the-art methods for Bayesian deep learning on a set of in- and out-of-distribution benchmarks with minimal computational overhead over standard deep learning. In principle, our approach is not restricted to Gaussian variational families and should seamlessly extend to location-scale families, which could further improve performance. Finally, it would be interesting to explore connections between Implicit Bias VI and Bayesian deep learning in function-space [e.g., 37, 54, 74–76].

486 REFERENCES
487

488 [1] M. Goldblum, M. Finzi, K. Rowan, and A. G. Wilson. “The No Free Lunch Theorem, Kol-
489 mogorov Complexity, and the Role of Inductive Biases in Machine Learning”. In: *Inter-490 national Conference on Machine Learning (ICML)*. 2024. DOI: [10.48550/arXiv.2304.05366](https://doi.org/10.48550/arXiv.2304.05366) (cit. on p. 1).

491 [2] M. S. Nacson, R. Mulayoff, G. Ongie, T. Michaeli, and D. Soudry. “The Implicit Bias of
492 Minima Stability in Multivariate Shallow ReLU Networks”. In: *International Conference on*
493 *Learning Representations (ICLR)*. 2023. DOI: [10.48550/arXiv.2306.17499](https://doi.org/10.48550/arXiv.2306.17499) (cit. on
494 p. 1).

495 [3] R. Mulayoff, T. Michaeli, and D. Soudry. “The Implicit Bias of Minima Stability: A View
496 from Function Space”. In: *Advances in Neural Information Processing Systems (NeurIPS)*.
497 2021. URL: <https://proceedings.neurips.cc/paper/2021/hash/944a5ae3483ed5c1e10bbccb7942a279-Abstract.html> (cit. on p. 1).

498 [4] D. Soudry, E. Hoffer, M. S. Nacson, S. Gunasekar, and N. Srebro. “The Implicit Bias of
499 Gradient Descent on Separable Data”. In: *Journal of Machine Learning Research (JMLR)*
500 (2018). DOI: [10.48550/arXiv.1710.10345](https://doi.org/10.48550/arXiv.1710.10345) (cit. on pp. 1, 2, 6, 7, 23, 24, 28, 32).

501 [5] S. Gunasekar, J. Lee, D. Soudry, and N. Srebro. “Characterizing Implicit Bias in Terms of
502 Optimization Geometry”. In: *International Conference on Machine Learning (ICML)*. 2018.
503 DOI: [10.48550/arXiv.1802.08246](https://doi.org/10.48550/arXiv.1802.08246) (cit. on pp. 1–3, 6, 23).

504 [6] M. S. Nacson, J. D. Lee, S. Gunasekar, P. H. P. Savarese, N. Srebro, and D. Soudry. “Con-
505 vergence of Gradient Descent on Separable Data”. In: *International Conference on Artificial*
506 *Intelligence and Statistics (AISTATS)*. 2019. DOI: [10.48550/arXiv.1803.01905](https://doi.org/10.48550/arXiv.1803.01905) (cit.
507 on pp. 1, 6, 7).

508 [7] M. S. Nacson, N. Srebro, and D. Soudry. “Stochastic Gradient Descent on Separable Data:
509 Exact Convergence with a Fixed Learning Rate”. In: *International Conference on Artificial*
510 *Intelligence and Statistics (AISTATS)*. 2019. DOI: [10.48550/arXiv.1806.01796](https://doi.org/10.48550/arXiv.1806.01796) (cit.
511 on pp. 1, 2, 6, 7).

512 [8] B. Wang, Q. Meng, H. Zhang, R. Sun, W. Chen, Z.-M. Ma, and T.-Y. Liu. “Does Momentum
513 Change the Implicit Regularization on Separable Data?” In: *Advances in Neural Information*
514 *Processing Systems (NeurIPS)* (2022) (cit. on pp. 1, 6, 7).

515 [9] H. Jin and G. Montúfar. *Implicit Bias of Gradient Descent for Mean Squared Error Re-516 gression with Two-Layer Wide Neural Networks*. arXiv:2006.07356 [stat]. May 2023. DOI:
517 [10.48550/arXiv.2006.07356](https://doi.org/10.48550/arXiv.2006.07356) (cit. on pp. 1, 6).

518 [10] H. Ravi, C. Scott, D. Soudry, and Y. Wang. “The Implicit Bias of Gradient Descent on Sep-
519 arable Multiclass Data”. In: *Advances in Neural Information Processing Systems (NeurIPS)*.
520 2024. DOI: [10.48550/arXiv.2411.01350](https://doi.org/10.48550/arXiv.2411.01350) (cit. on pp. 1, 6, 7).

521 [11] T. Papamarkou, M. Skouliaridou, K. Palla, L. Aitchison, J. Arbel, D. Dunson, M. Filippone, V.
522 Fortuin, P. Hennig, J. M. Hernández-Lobato, A. Hubin, A. Immer, T. Karaletsos, M. E. Khan,
523 A. Kristiadi, Y. Li, S. Mandt, C. Nemeth, M. A. Osborne, T. G. J. Rudner, D. Rügamer, Y. W.
524 Teh, M. Welling, A. G. Wilson, and R. Zhang. “Position: Bayesian Deep Learning is Needed
525 in the Age of Large-Scale AI”. In: *International Conference on Machine Learning (ICML)*.
526 2024. DOI: [10.48550/arXiv.2402.00809](https://doi.org/10.48550/arXiv.2402.00809) (cit. on p. 1).

527 [12] D. Tran, J. Liu, M. W. Dusenberry, D. Phan, M. Collier, J. Ren, K. Han, Z. Wang, Z. Mariet, H.
528 Hu, N. Band, T. G. J. Rudner, K. Singhal, Z. Nado, J. v. Amersfoort, A. Kirsch, R. Jenatton, N.
529 Thain, H. Yuan, K. Buchanan, K. Murphy, D. Sculley, Y. Gal, Z. Ghahramani, J. Snoek, and
530 B. Lakshminarayanan. *Plex: Towards Reliability using Pretrained Large Model Extensions*.
531 July 15, 2022. DOI: [10.48550/arXiv.2207.07411](https://doi.org/10.48550/arXiv.2207.07411). arXiv: [2207.07411\[cs\]](https://arxiv.org/abs/2207.07411). URL:
532 [http://arxiv.org/abs/2207.07411](https://arxiv.org/abs/2207.07411) (visited on 05/16/2025) (cit. on p. 1).

533 [13] H. Ritter, A. Botev, and D. Barber. “Online Structured Laplace Approximations For Over-
534 coming Catastrophic Forgetting”. In: *Advances in Neural Information Processing Systems*
535 (*NeurIPS*). 2018. DOI: [10.48550/arXiv.1805.07810](https://doi.org/10.48550/arXiv.1805.07810) (cit. on pp. 1, 6).

536 [14] Y. L. Li, T. G. J. Rudner, and A. G. Wilson. “A Study of Bayesian Neural Network Surro-
537 gates for Bayesian Optimization”. In: *International Conference on Learning Representations*
538 (*ICLR*). 2024. DOI: [10.48550/arXiv.2305.20028](https://doi.org/10.48550/arXiv.2305.20028) (cit. on p. 1).

539 [15] V. Fortuin. “Priors in Bayesian Deep Learning: A Review”. In: *International Statistical Re-540 view* 90.3 (2022), pp. 563–591. DOI: [10.1111/insr.12502](https://doi.org/10.1111/insr.12502) (cit. on pp. 1, 9).

540 [16] P. Izmailov, S. Vikram, M. D. Hoffman, and A. G. Wilson. “What Are Bayesian Neural Net-
 541 work Posteriors Really Like?” In: *International Conference on Machine Learning (ICML)*.
 542 2021. DOI: [10.48550/arXiv.2104.14421](https://doi.org/10.48550/arXiv.2104.14421) (cit. on p. 1).

543 [17] B. Adlam, J. Snoek, and S. L. Smith. *Cold Posteriors and Aleatoric Uncertainty*. July 31,
 544 2020. DOI: [10.48550/arXiv.2008.00029](https://doi.org/10.48550/arXiv.2008.00029). arXiv: [2008.00029\[stat\]](https://arxiv.org/abs/2008.00029). URL:
 545 <http://arxiv.org/abs/2008.00029> (visited on 05/15/2025) (cit. on p. 1).

546 [18] T. Cinquin, A. Immer, M. Horn, and V. Fortuin. “Pathologies in priors and inference for
 547 Bayesian transformers”. In: *NeurIPS Bayesian Deep Learning Workshop*. 2021. DOI: [10.48550/arXiv.2110.04020](https://doi.org/10.48550/arXiv.2110.04020) (cit. on p. 1).

548 [19] B. Coker, W. P. Bruinsma, D. R. Burt, W. Pan, and F. Doshi-Velez. “Wide Mean-Field
 549 Bayesian Neural Networks Ignore the Data”. In: *International Conference on Artificial In-
 550 telligence and Statistics (AISTATS)*. 2022. DOI: [10.48550/arXiv.2202.11670](https://doi.org/10.48550/arXiv.2202.11670) (cit. on
 551 p. 1).

552 [20] A. Y. K. Foong, D. R. Burt, Y. Li, and R. E. Turner. “On the Expressiveness of Approximate
 553 Inference in Bayesian Neural Networks”. In: *Advances in Neural Information Processing
 554 Systems (NeurIPS)*. 2020. DOI: [10.48550/arXiv.1909.00719](https://doi.org/10.48550/arXiv.1909.00719) (cit. on p. 1).

555 [21] C. Zhang, S. Bengio, M. Hardt, B. Recht, and O. Vinyals. “Understanding deep learning re-
 556 quires rethinking generalization”. In: *International Conference on Learning Representations
 557 (ICLR)*. 2017. DOI: [10.48550/arXiv.1611.03530](https://doi.org/10.48550/arXiv.1611.03530) (cit. on pp. 2, 3, 6).

558 [22] G. Vardi. “On the Implicit Bias in Deep-Learning Algorithms”. In: *Commun. ACM* 66.6 (May
 559 2023), pp. 86–93. DOI: [10.1145/3571070](https://doi.org/10.1145/3571070) (cit. on pp. 2, 6).

560 [23] B. Vasudeva, P. Deora, and C. Thrampoulidis. *Implicit Bias and Fast Convergence Rates for
 561 Self-attention*. 2024. DOI: [10.48550/arXiv.2402.05738](https://doi.org/10.48550/arXiv.2402.05738) (cit. on p. 2).

562 [24] D. J. C. MacKay. “A Practical Bayesian Framework for Backpropagation Networks”. In: *Neu-
 563 ral Computation* 4 (1992). ISSN: 0899-7667, 1530-888X. DOI: [10.1162/neco.1992.4.
 564 3.448](https://doi.org/10.1162/neco.1992.4.3.448) (cit. on pp. 2, 6, 8).

565 [25] H. Ritter, A. Botev, and D. Barber. “A Scalable Laplace Approximation for Neural Net-
 566 works”. In: *International Conference on Learning Representations (ICLR)*. 2018 (cit. on
 567 pp. 2, 6, 8).

568 [26] E. Daxberger, A. Kristiadi, A. Immer, R. Eschenhagen, M. Bauer, and P. Hennig. “Laplace
 569 Redux – Effortless Bayesian Deep Learning”. In: *Advances in Neural Information Processing
 570 Systems (NeurIPS)*. 2021. DOI: [10.48550/arXiv.2106.14806](https://doi.org/10.48550/arXiv.2106.14806) (cit. on pp. 2, 6, 8, 41).

571 [27] P. Izmailov, D. Podoprikhin, T. Garipov, D. Vetrov, and A. G. Wilson. “Averaging Weights
 572 Leads to Wider Optima and Better Generalization”. In: *Conference on Uncertainty in Arti-
 573 ficial Intelligence (UAI)*. 2018. URL: <https://arxiv.org/abs/1803.05407v3>
 574 (cit. on pp. 2, 6).

575 [28] W. Maddox, T. Garipov, P. Izmailov, D. Vetrov, and A. G. Wilson. “A Simple Baseline for
 576 Bayesian Uncertainty in Deep Learning”. In: *Advances in Neural Information Processing
 577 Systems (NeurIPS)*. 2019. DOI: [10.48550/arXiv.1902.02476](https://doi.org/10.48550/arXiv.1902.02476) (cit. on pp. 2, 6, 8, 42).

578 [29] B. Lakshminarayanan, A. Pritzel, and C. Blundell. “Simple and Scalable Predictive Uncer-
 579 tainty Estimation using Deep Ensembles”. In: *Advances in Neural Information Processing
 580 Systems (NeurIPS)*. 2017. DOI: [10.48550/arXiv.1612.01474](https://doi.org/10.48550/arXiv.1612.01474). URL: <http://arxiv.org/abs/1612.01474> (cit. on pp. 2, 6, 8, 42).

581 [30] A. Graves. “Practical Variational Inference for Neural Networks”. In: *Advances in Neural
 582 Information Processing Systems (NeurIPS)*. 2011. URL: https://papers.nips.cc/paper_files/paper/2011/hash/7eb3c8be3d411e8ebfab08eba5f49632-Abstract.html (cit. on pp. 2, 6, 8, 42).

583 [31] C. Blundell, J. Cornebise, K. Kavukcuoglu, and D. Wierstra. “Weight Uncertainty in Neu-
 584 ral Networks”. In: *International Conference on Machine Learning (ICML)*. 2015. DOI: [10.48550/arXiv.1505.05424](https://doi.org/10.48550/arXiv.1505.05424) (cit. on pp. 2, 6, 8, 42).

585 [32] K. Osawa, S. Swaroop, A. Jain, R. Eschenhagen, R. E. Turner, R. Yokota, and M. E. Khan.
 586 “Practical Deep Learning with Bayesian Principles”. In: *Advances in Neural Information Pro-
 587 cessing Systems (NeurIPS)*. 2019. DOI: [10.48550/arXiv.1906.02506](https://doi.org/10.48550/arXiv.1906.02506) (cit. on pp. 2,
 588 6).

589 [33]

590 [34]

591 [35]

592 [36]

593

594 [33] Y. Shen, N. Daheim, B. Cong, P. Nickl, G. M. Marconi, C. Bazan, R. Yokota, I. Gurevych,
 595 D. Cremers, M. E. Khan, and T. Möllenhoff. “Variational Learning is Effective for Large
 596 Deep Networks”. In: *International Conference on Machine Learning (ICML)*. 2024. DOI:
 597 [10.48550/arXiv.2402.17641](https://doi.org/10.48550/arXiv.2402.17641) (cit. on pp. 2, 6).

598 [34] A. Zellner. “Optimal Information Processing and Bayes’s Theorem”. In: *The American Statistician* 42.4 (1988), pp. 278–280. DOI: [10.2307/2685143](https://doi.org/10.2307/2685143) (cit. on p. 2).

600 [35] P. G. Bissiri, C. Holmes, and S. Walker. “A General Framework for Updating Belief Distributions”. In: *Journal of the Royal Statistical Society: Series B (Statistical Methodology)* 78.5
 601 (Nov. 2016), pp. 1103–1130. ISSN: 1369-7412, 1467-9868. DOI: [10.1111/rssb.12158](https://doi.org/10.1111/rssb.12158)
 602 (cit. on p. 3).

604 [36] J. Knoblauch, J. Jewson, and T. Damoulas. “An Optimization-centric View on Bayes’ Rule:
 605 Reviewing and Generalizing Variational Inference”. In: *Journal of Machine Learning Research (JMLR)* 23.132 (2022), pp. 1–109. ISSN: 1533-7928. URL: <http://jmlr.org/papers/v23/19-1047.html> (cit. on pp. 3, 6).

608 [37] V. D. Wild, R. Hu, and D. Sejdinovic. “Generalized Variational Inference in Function Spaces:
 609 Gaussian Measures meet Bayesian Deep Learning”. In: *Advances in Neural Information Processing Systems (NeurIPS)*. Oct. 2022. DOI: [10.48550/arXiv.2205.06342](https://doi.org/10.48550/arXiv.2205.06342) (cit. on
 610 pp. 3, 6, 9).

612 [38] S. Farquhar, L. Smith, and Y. Gal. “Liberty or Depth: Deep Bayesian Neural Nets Do Not
 613 Need Complex Weight Posterior Approximations”. In: *Advances in Neural Information Processing Systems (NeurIPS)*. 2020. DOI: [10.48550/arXiv.2002.03704](https://doi.org/10.48550/arXiv.2002.03704). URL: <http://arxiv.org/abs/2002.03704> (cit. on pp. 4, 6).

616 [39] M. Sharma, S. Farquhar, E. Nalisnick, and T. Rainforth. “Do Bayesian Neural Networks Need
 617 To Be Fully Stochastic?” In: *International Conference on Artificial Intelligence and Statistics (AISTATS)*. 2023. DOI: [10.48550/arXiv.2211.06291](https://doi.org/10.48550/arXiv.2211.06291) (cit. on pp. 4, 6, 9).

618 [40] B. Hanin and M. Sellke. *Approximating Continuous Functions by ReLU Nets of Minimal
 619 Width*. arXiv:1710.11278 [stat]. Mar. 2018. DOI: [10.48550/arXiv.1710.11278](https://doi.org/10.48550/arXiv.1710.11278). URL:
 620 <http://arxiv.org/abs/1710.11278> (cit. on p. 4).

621 [41] G. Yang, E. J. Hu, I. Babuschkin, S. Sidor, X. Liu, D. Farhi, N. Ryder, J. Pachocki, W. Chen,
 622 and J. Gao. “Tensor Programs V: Tuning Large Neural Networks via Zero-Shot Hyperpara-
 623 meter Transfer”. In: *Advances in Neural Information Processing Systems (NeurIPS)*. 2021.
 624 DOI: [10.48550/arXiv.2203.03466](https://doi.org/10.48550/arXiv.2203.03466) (cit. on pp. 5, 6, 36, 37).

625 [42] A. Bhattacharya, A. Linero, and C. J. Oates. “Grand Challenges in Bayesian Computation”.
 626 In: *Bulletin of the International Society for Bayesian Analysis (ISBA)* 31.3 (Sept. 2024). DOI:
 627 [10.48550/arXiv.2410.00496](https://doi.org/10.48550/arXiv.2410.00496) (cit. on p. 5).

628 [43] G. Yang and E. J. Hu. “Tensor Programs IV: Feature Learning in Infinite-Width Neural Net-
 629 works”. In: *International Conference on Machine Learning (ICML)*. 2021. DOI: [10.48550/arXiv.2011.14522](https://doi.org/10.48550/arXiv.2011.14522) (cit. on pp. 5, 6, 34).

631 [44] G. Zhang, S. Sun, D. Duvenaud, and R. Grosse. *Noisy Natural Gradient as Variational Infer-
 632 ence*. Feb. 26, 2018. DOI: [10.48550/arXiv.1712.02390](https://doi.org/10.48550/arXiv.1712.02390). arXiv: [1712.02390\[cs\]](https://arxiv.org/abs/1712.02390).
 633 URL: <http://arxiv.org/abs/1712.02390> (visited on 05/15/2025) (cit. on p. 6).

634 [45] M.-N. Tran, N. Nguyen, D. Nott, and R. Kohn. *Bayesian Deep Net GLM and GLMM*. May 25,
 635 2018. DOI: [10.48550/arXiv.1805.10157](https://doi.org/10.48550/arXiv.1805.10157). arXiv: [1805.10157\[stat\]](https://arxiv.org/abs/1805.10157). URL:
 636 <http://arxiv.org/abs/1805.10157> (visited on 05/15/2025) (cit. on p. 6).

637 [46] C. Louizos and M. Welling. *Structured and Efficient Variational Deep Learning with Matrix
 638 Gaussian Posteriors*. June 23, 2016. DOI: [10.48550/arXiv.1603.04733](https://doi.org/10.48550/arXiv.1603.04733). arXiv:
 639 [1603.04733\[stat\]](https://arxiv.org/abs/1603.04733). URL: <http://arxiv.org/abs/1603.04733> (visited on
 640 05/15/2025) (cit. on p. 6).

641 [47] A. Mishkin, F. Kunstner, D. Nielsen, M. Schmidt, and M. E. Khan. *SLANG: Fast Structured
 642 Covariance Approximations for Bayesian Deep Learning with Natural Gradient*. Jan. 12,
 643 2019. DOI: [10.48550/arXiv.1811.04504](https://doi.org/10.48550/arXiv.1811.04504). arXiv: [1811.04504\[cs\]](https://arxiv.org/abs/1811.04504). URL: <http://arxiv.org/abs/1811.04504> (visited on 05/15/2025) (cit. on p. 6).

644 [48] J. Harrison, J. Willes, and J. Snoek. “Variational Bayesian Last Layers”. In: *International
 645 Conference on Learning Representations (ICLR)*. Apr. 2024. DOI: [10.48550/arXiv.2404.11599](https://doi.org/10.48550/arXiv.2404.11599) (cit. on p. 6).

648 [49] J. Z. Liu, Z. Lin, S. Padhy, D. Tran, T. Bedrax-Weiss, and B. Lakshminarayanan. “Simple
649 and Principled Uncertainty Estimation with Deterministic Deep Learning via Distance
650 Awareness”. In: *Advances in Neural Information Processing Systems (NeurIPS)*. Oct. 2020.
651 DOI: [10.48550/arXiv.2006.10108](https://doi.org/10.48550/arXiv.2006.10108) (cit. on p. 6).

652 [50] M. E. Khan, A. Immer, E. Abedi, and M. Korzepa. “Approximate Inference Turns Deep
653 Networks into Gaussian Processes”. In: *Advances in Neural Information Processing Systems*
654 (*NeurIPS*). 2019. DOI: [10.48550/arXiv.1906.01930](https://doi.org/10.48550/arXiv.1906.01930) (cit. on p. 6).

655 [51] A. Immer, M. Korzepa, and M. Bauer. “Improving predictions of Bayesian neural nets via lo-
656 cal linearization”. In: *International Conference on Artificial Intelligence and Statistics (AIS-
657 TATS)*. 2021 (cit. on p. 6).

658 [52] E. Daxberger, E. Nalisnick, J. U. Allingham, J. Antorán, and J. M. Hernández-Lobato.
659 “Bayesian Deep Learning via Subnetwork Inference”. In: *International Conference on Ma-
660 chine Learning (ICML)*. 2021. DOI: [10.48550/arXiv.2010.14689](https://doi.org/10.48550/arXiv.2010.14689) (cit. on p. 6).

661 [53] A. Kristiadi, A. Immer, R. Eschenhagen, and V. Fortuin. “Promises and Pitfalls of the Lin-
662 earized Laplace in Bayesian Optimization”. In: *Advances in Approximate Bayesian Inference*
663 (*AABI*). 2023. DOI: [10.48550/arXiv.2304.08309](https://doi.org/10.48550/arXiv.2304.08309) (cit. on p. 6).

664 [54] T. Cinquin, M. Pförtner, V. Fortuin, P. Hennig, and R. Bamler. “FSP-Laplace: Function-Space
665 Priors for the Laplace Approximation in Bayesian Deep Learning”. In: *Advances in Neural*
666 *Information Processing Systems (NeurIPS)*. Oct. 2024. DOI: [10.48550/arXiv.2407.13711](https://doi.org/10.48550/arXiv.2407.13711). URL: <http://arxiv.org/abs/2407.13711> (cit. on pp. 6, 9).

667 [55] S. Fort, H. Hu, and B. Lakshminarayanan. *Deep Ensembles: A Loss Landscape Perspective*.
668 June 25, 2020. DOI: [10.48550/arXiv.1912.02757](https://doi.org/10.48550/arXiv.1912.02757). arXiv: [1912.02757 \[stat\]](https://arxiv.org/abs/1912.02757).
669 URL: <http://arxiv.org/abs/1912.02757> (visited on 05/15/2025) (cit. on p. 6).

670 [56] A. G. Wilson and P. Izmailov. “Bayesian Deep Learning and a Probabilistic Perspective of
671 Generalization”. In: *Advances in Neural Information Processing Systems (NeurIPS)*. 2020.
672 DOI: [10.48550/arXiv.2002.08791](https://doi.org/10.48550/arXiv.2002.08791) (cit. on p. 6).

673 [57] V. D. Wild, S. Ghalebikesabi, D. Sejdinovic, and J. Knoblauch. “A Rigorous Link between
674 Deep Ensembles and (Variational) Bayesian Methods”. In: *Advances in Neural Information*
675 *Processing Systems (NeurIPS)*. 2023. DOI: [10.48550/arXiv.2305.15027](https://doi.org/10.48550/arXiv.2305.15027) (cit. on
676 p. 6).

677 [58] T. Abe, E. K. Buchanan, G. Pleiss, R. Zemel, and J. P. Cunningham. “Deep Ensembles
678 Work, But Are They Necessary?” In: *Advances in Neural Information Processing Systems*
679 (*NeurIPS*). 2022. DOI: [10.48550/arXiv.2202.06985](https://doi.org/10.48550/arXiv.2202.06985) (cit. on p. 6).

680 [59] N. Dern, J. P. Cunningham, and G. Pleiss. *Theoretical Limitations of Ensembles in the Age*
681 *of Overparameterization*. arXiv:2410.16201 [stat]. Oct. 2024. DOI: [10.48550/arXiv.2410.16201](https://doi.org/10.48550/arXiv.2410.16201) (cit. on p. 6).

683 [60] C. Mingard, G. Valle-Pérez, J. Skalse, and A. A. Louis. “Is SGD a Bayesian sampler? Well,
684 almost.” In: *Journal of Machine Learning Research (JMLR)* (2020) (cit. on p. 6).

685 [61] J. A. Lin, J. Antorán, S. Padhy, D. Janz, J. M. Hernández-Lobato, and A. Terenin. “Sampling
686 from Gaussian Process Posteriors using Stochastic Gradient Descent”. In: *Advances in Neural*
687 *Information Processing Systems (NeurIPS)*. 2023. DOI: [10.48550/arXiv.2306.11589](https://doi.org/10.48550/arXiv.2306.11589)
688 (cit. on p. 6).

689 [62] J. Lee, L. Xiao, S. S. Schoenholz, Y. Bahri, R. Novak, J. Sohl-Dickstein, and J. Pennington.
690 “Wide Neural Networks of Any Depth Evolve as Linear Models Under Gradient Descent”. In:
691 *Journal of Statistical Mechanics: Theory and Experiment* 2020.12 (2020). DOI: [10.1088/1742-5468/abc62b](https://doi.org/10.1088/1742-5468/abc62b) (cit. on p. 6).

693 [63] J. Lai, M. Xu, R. Chen, and Q. Lin. *Generalization Ability of Wide Neural Networks on \mathbb{R}* .
694 Feb. 12, 2023. DOI: [10.48550/arXiv.2302.05933](https://doi.org/10.48550/arXiv.2302.05933). arXiv: [2302.05933 \[stat\]](https://arxiv.org/abs/2302.05933).
695 URL: <http://arxiv.org/abs/2302.05933> (visited on 05/15/2025) (cit. on p. 6).

696 [64] G. Yang. “Tensor Programs I: Wide Feedforward or Recurrent Neural Networks of Any Ar-
697 chitecture are Gaussian Processes”. In: *Advances in Neural Information Processing Systems*
698 (*NeurIPS*). 2019. DOI: [10.48550/arXiv.1910.12478](https://doi.org/10.48550/arXiv.1910.12478) (cit. on p. 6).

699 [65] G. Yang. *Tensor Programs II: Neural Tangent Kernel for Any Architecture*. 2020. DOI: [10.48550/arXiv.2006.14548](https://doi.org/10.48550/arXiv.2006.14548) (cit. on p. 6).

702 [66] A. Jacot, F. Gabriel, and C. Hongler. “Neural Tangent Kernel: Convergence and Generaliza-
 703 tion in Neural Networks”. In: *Advances in Neural Information Processing Systems (NeurIPS)*.
 704 2018. DOI: [10.48550/arXiv.1806.07572](https://doi.org/10.48550/arXiv.1806.07572) (cit. on p. 6).

705 [67] V. Muthukumar, A. Narang, V. Subramanian, M. Belkin, D. Hsu, and A. Sahai. “Classification
 706 vs regression in overparameterized regimes: Does the loss function matter?” In: *Journal of*
 707 *Machine Learning Research (JMLR)* (Oct. 2021). DOI: [10.48550/arXiv.2005.08054](https://doi.org/10.48550/arXiv.2005.08054)
 708 (cit. on p. 7).

709 [68] D. Hsu, V. Muthukumar, and J. Xu. *On the proliferation of support vectors in high dimensions*.
 710 2022. DOI: [10.48550/arXiv.2009.10670](https://doi.org/10.48550/arXiv.2009.10670). URL: <http://arxiv.org/abs/2009.10670> (cit. on p. 7).

712 [69] C. Guo, G. Pleiss, Y. Sun, and K. Q. Weinberger. “On Calibration of Modern Neural Net-
 713 works”. In: *International Conference on Machine Learning (ICML)*. 2017. DOI: [10.48550/arXiv.1706.04599](https://doi.org/10.48550/arXiv.1706.04599) (cit. on pp. 8, 33, 41).

715 [70] Y. LeCun, L. Bottou, Y. Bengio, and P. Haffner. “Gradient-based learning applied to doc-
 716 ument recognition”. In: *Proceedings of the IEEE 86.11* (Nov. 1998), pp. 2278–2324. ISSN:
 717 1558-2256. DOI: [10.1109/5.726791](https://doi.org/10.1109/5.726791). URL: <https://ieeexplore.ieee.org/document/726791> (cit. on pp. 8, 39, 40).

719 [71] K. He, X. Zhang, S. Ren, and J. Sun. “Deep Residual Learning for Image Recognition”.
 720 In: *Proceedings of the IEEE/CVF Conference on Computer Vision and Pattern Recognition*
 721 (*CVPR*). IEEE, 2016, pp. 770–778. ISBN: 978-1-4673-8851-1. DOI: [10.1109/CVPR.2016.90](https://doi.org/10.1109/CVPR.2016.90). URL: [http://ieeexplore.ieee.org/document/7780459/](https://ieeexplore.ieee.org/document/7780459/) (cit. on
 722 pp. 8, 41).

724 [72] N. Mu and J. Gilmer. “MNIST-C: A Robustness Benchmark for Computer Vision”. In: *ICML*
 725 *Workshop on Uncertainty and Robustness in Deep Learning*. June 2019. DOI: [10.48550/arXiv.1906.02337](https://doi.org/10.48550/arXiv.1906.02337). URL: <http://arxiv.org/abs/1906.02337> (cit. on pp. 8,
 726 39).

727 [73] D. Hendrycks and T. Dietterich. “Benchmarking Neural Network Robustness to Common
 728 Corruptions and Perturbations”. In: *International Conference on Learning Representations*
 729 (*ICLR*). 2019. DOI: [10.48550/arXiv.1903.12261](https://doi.org/10.48550/arXiv.1903.12261). URL: <http://arxiv.org/abs/1903.12261> (cit. on pp. 8, 39).

731 [74] D. R. Burt, S. W. Ober, A. Garriga-Alonso, and M. van der Wilk. *Understanding Variational*
 732 *Inference in Function-Space*. Nov. 2020. DOI: [10.48550/arXiv.2011.09421](https://doi.org/10.48550/arXiv.2011.09421) (cit. on
 733 p. 9).

734 [75] S. Qiu, T. G. J. Rudner, S. Kapoor, and A. G. Wilson. “Should We Learn Most Likely Func-
 735 tions or Parameters?” In: *Advances in Neural Information Processing Systems (NeurIPS)*.
 736 2023. DOI: [10.48550/arXiv.2311.15990](https://doi.org/10.48550/arXiv.2311.15990) (cit. on p. 9).

737 [76] T. G. J. Rudner, Z. Chen, Y. W. Teh, and Y. Gal. “Tractable Function-Space Variational In-
 738 ference in Bayesian Neural Networks”. In: *Advances in Neural Information Processing Systems*
 739 (*NeurIPS*). 2023. DOI: [10.48550/arXiv.2312.17199](https://doi.org/10.48550/arXiv.2312.17199) (cit. on p. 9).

740 [77] S. P. Boyd and L. Vandenberghe. *Convex optimization*. Cambridge University Press, 2004.
 741 ISBN: 978-0-521-83378-3 (cit. on p. 17).

742 [78] Y. Nesterov. “A method for solving the convex programming problem with convergence rate
 743 $O(\frac{1}{k^2})$ ”. In: *Dokl Akad Nauk SSSR* 269 (1983), p. 543 (cit. on p. 19).

744 [79] B. T. Polyak. “Some methods of speeding up the convergence of iteration methods”. In:
 745 *USSR Computational Mathematics and Mathematical Physics* 4.5 (1964), pp. 1–17. DOI:
 746 [10.1016/0041-5553\(64\)90137-5](https://doi.org/10.1016/0041-5553(64)90137-5) (cit. on p. 19).

747 [80] A. Krizhevsky et al. *Learning multiple layers of features from tiny images*. Tech. rep. 2009
 748 (cit. on p. 39).

749 [81] Y. Le and X. Yang. “Tiny ImageNet Visual Recognition Challenge”. In: *Stanford CS 231N*
 750 (2015). URL: <http://cs231n.stanford.edu/tiny-imagenet-200.zip> (cit.
 751 on p. 39).

752 [82] P. Goyal, P. Dollár, R. Girshick, P. Noordhuis, L. Wesolowski, A. Kyrola, A. Tulloch, Y. Jia,
 753 and K. He. *Accurate, Large Minibatch SGD: Training ImageNet in 1 Hour*. Tech. rep. 2018.
 754 URL: <http://arxiv.org/abs/1706.02677> (cit. on p. 40).

756 [83] S. L. Smith and Q. V. Le. “A Bayesian Perspective on Generalization and Stochastic Gradient
757 Descent”. In: *International Conference on Learning Representations (ICLR)*. 2018. DOI: [10.48550/arXiv.1710.06451](https://doi.org/10.48550/arXiv.1710.06451) (cit. on p. 40).
758

759 [84] S. L. Smith, P.-J. Kindermans, C. Ying, and Q. V. Le. “Don’t Decay the Learning Rate, In-
760 crease the Batch Size”. In: *International Conference on Learning Representations (ICLR)*.
761 2018. DOI: [10.48550/arXiv.1711.00489](https://doi.org/10.48550/arXiv.1711.00489) (cit. on p. 40).
762

763 [85] T. maintainers and contributors. *TorchVision: PyTorch’s Computer Vision library*. <https://github.com/pytorch/vision>. 2016 (cit. on p. 41).
764

765

766

767

768

769

770

771

772

773

774

775

776

777

778

779

780

781

782

783

784

785

786

787

788

789

790

791

792

793

794

795

796

797

798

799

800

801

802

803

804

805

806

807

808

809

810
811
SUPPLEMENTARY MATERIAL812
813
814
815
816
This supplementary material contains additional results and proofs for all theoretical statements.
References referring to sections, equations or theorem-type environments within this document are
prefixed with ‘S’, while references to, or results from, the main paper are stated as is.817
S1 Theoretical Results 16
818 S1.1 Overparametrized Linear Regression 17
819 S1.1.1 Characterization of Implicit Bias (Proof of Theorem 1) 17
820 S1.1.2 Non-Asymptotic Error Analysis 20
821 S1.1.3 Connection to Ensembles 22
822 S1.2 Binary Classification of Linearly Separable Data 23
823 S1.2.1 Preliminaries 24
824 S1.2.2 Gradient Flow for the Expected Loss 24
825 S1.2.3 Complete Proof of Theorem 2 27
826 S1.3 NLL Overfitting and the Need for (Temperature) Scaling 32
827
S2 Parametrization, Feature Learning and Hyperparameter Transfer 33
828 S2.1 Definitions of Stability and Feature Learning 34
829 S2.2 Initialization Scaling for a Linear Network 34
830 S2.3 Proposed Scaling 36
831 S2.4 Details on Hyperparameter Transfer Experiment 37
832
S3 Experiments 38
833 S3.1 Setup and Details 38
834 S3.1.1 Datasets 39
835 S3.1.2 Metrics 39
836 S3.2 Time and Memory-Efficient Training 40
837 S3.3 In- and Out-of-distribution Generalization 40
838 S3.3.1 Architectures, Training, and Methods 40
839 S3.3.2 In-Distribution Generalization and Uncertainty Quantification 43
840 S3.3.3 Robustness to Input Corruptions 44
841 S3.3.4 Comparison to Generalized VI with 2-Wasserstein Regularization 44
842
843
844
S1 THEORETICAL RESULTS845
Lemma S1846
Let $q(\mathbf{w}) = \mathcal{N}(\mathbf{w}; \boldsymbol{\mu}, \boldsymbol{\Sigma})$, $p(\mathbf{w}) = \mathcal{N}(\mathbf{w}; \boldsymbol{\mu}_0, \boldsymbol{\Sigma}_0)$ such that $\boldsymbol{\mu}, \boldsymbol{\mu}_0 \in \mathbb{R}^P$, $\boldsymbol{\Sigma}, \boldsymbol{\Sigma}_0 \in \mathbb{R}^{P \times P}$ positive semi-definite and let $\mathbf{V}_A \in \mathbb{R}^{P \times N}$, $\mathbf{V}_B \in \mathbb{R}^{P \times (P-N)}$ be matrices with pairwise orthonormal columns that together define an orthonormal basis of \mathbb{R}^P , i.e. for $\mathbf{V} = [\mathbf{V}_A \quad \mathbf{V}_B]$ it holds that $\mathbf{V}\mathbf{V}^\top = \mathbf{V}^\top\mathbf{V} = \mathbf{I}$ and $\text{span}(\mathbf{V}) = \mathbb{R}^P$. Assume further that

847
848
849
850
$$\mathbf{V}_A^\top \boldsymbol{\Sigma} \mathbf{V}_A = \mathbf{0}, \quad (\text{S11})$$

851
852
853
then the squared 2-Wasserstein distance is given by

854
855
$$W_2^2(q, p) = \|\mathbf{V}_A^\top \boldsymbol{\mu} - \mathbf{V}_A^\top \boldsymbol{\mu}_0\|_2^2 + W_2^2(\mathcal{N}(\mathbf{V}_B^\top \boldsymbol{\mu}, \mathbf{V}_B^\top \boldsymbol{\Sigma} \mathbf{V}_B), \mathcal{N}(\mathbf{V}_B^\top \boldsymbol{\mu}_0, \mathbf{V}_B^\top \boldsymbol{\Sigma}_0 \mathbf{V}_B)) + C, \quad (\text{S12})$$

856
where the constant C is independent of $(\boldsymbol{\mu}, \boldsymbol{\Sigma})$.857
858
Proof. Consider the matrix

859
860
861
$$\mathbf{V}^\top \boldsymbol{\Sigma} \mathbf{V} = \begin{bmatrix} \mathbf{0}_{N \times N} & \mathbf{V}_A^\top \boldsymbol{\Sigma} \mathbf{V}_B \\ \mathbf{V}_B^\top \boldsymbol{\Sigma} \mathbf{V}_A & \mathbf{V}_B^\top \boldsymbol{\Sigma} \mathbf{V}_B \end{bmatrix}.$$

862
863
Since $\mathbf{V}^\top \boldsymbol{\Sigma} \mathbf{V}$ is symmetric positive semi-definite, its off-diagonal block $\mathbf{V}_A^\top \boldsymbol{\Sigma} \mathbf{V}_B$ satisfies

$$(\mathbf{I} - \mathbf{0}\mathbf{0}^\dagger) \mathbf{V}_A^\top \boldsymbol{\Sigma} \mathbf{V}_B = \mathbf{0} \iff \mathbf{V}_A^\top \boldsymbol{\Sigma} \mathbf{V}_B = \mathbf{0}$$

864 by Boyd and Vandenberghe [A5.5, 77]. Therefore, we have
 865

$$866 \quad \mathbf{V}^T \Sigma \mathbf{V} = \begin{bmatrix} \mathbf{0}_{N \times N} & \mathbf{V}_A^T \Sigma \mathbf{V}_B \\ \mathbf{V}_B^T \Sigma \mathbf{V}_A & \mathbf{V}_B^T \Sigma \mathbf{V}_B \end{bmatrix} = \begin{bmatrix} \mathbf{0}_{N \times N} & \mathbf{0}_{N \times (P-N)} \\ \mathbf{0}_{(P-N) \times N} & \mathbf{V}_B^T \Sigma \mathbf{V}_B \end{bmatrix}. \quad (S13)$$

868 The squared 2-Wasserstein distance between $q(\mathbf{w})$ and $p(\mathbf{w})$ is given by
 869

$$870 \quad W_2^2(q, p) = \|\boldsymbol{\mu} - \boldsymbol{\mu}_0\|_2^2 + \text{tr}(\Sigma - 2(\Sigma^{\frac{1}{2}} \Sigma_0 \Sigma^{\frac{1}{2}})^{\frac{1}{2}} + \Sigma_0).$$

871 For the squared norm term it holds by unitary invariance of $\|\cdot\|_2$ that
 872

$$873 \quad \|\boldsymbol{\mu} - \boldsymbol{\mu}_0\|_2^2 = \|\mathbf{V}^T(\boldsymbol{\mu} - \boldsymbol{\mu}_0)\|_2^2 = \left\| \begin{bmatrix} \mathbf{V}_A^T(\boldsymbol{\mu} - \boldsymbol{\mu}_0) \\ \mathbf{V}_B^T(\boldsymbol{\mu} - \boldsymbol{\mu}_0) \end{bmatrix} \right\|_2^2 = \|\mathbf{V}_A^T \boldsymbol{\mu} - \mathbf{V}_A^T \boldsymbol{\mu}_0\|_2^2 + \|\mathbf{V}_B^T \boldsymbol{\mu} - \mathbf{V}_B^T \boldsymbol{\mu}_0\|_2^2.$$

875 Now for the trace term we have that
 876

$$877 \quad \begin{aligned} & \text{tr}(\mathbf{V} \mathbf{V}^T (\Sigma - 2(\Sigma^{\frac{1}{2}} \Sigma_0 \Sigma^{\frac{1}{2}})^{\frac{1}{2}} + \Sigma_0)) \\ &= \text{tr}(\mathbf{V}^T \Sigma \mathbf{V}) - 2 \text{tr}(\mathbf{V}^T (\Sigma^{\frac{1}{2}} \Sigma_0 \Sigma^{\frac{1}{2}})^{\frac{1}{2}} \mathbf{V}) + \text{tr}(\mathbf{V}^T \Sigma_0 \mathbf{V}) \\ &= \text{tr}(\mathbf{V}_A^T \Sigma \mathbf{V}_A) + \text{tr}(\mathbf{V}_B^T \Sigma \mathbf{V}_B) + \text{tr}(\mathbf{V}_A^T \Sigma_0 \mathbf{V}_A) + \text{tr}(\mathbf{V}_B^T \Sigma_0 \mathbf{V}_B) - 2 \text{tr}(\mathbf{V}^T (\Sigma^{\frac{1}{2}} \Sigma_0 \Sigma^{\frac{1}{2}})^{\frac{1}{2}} \mathbf{V}) \\ &\stackrel{+c}{=} \text{tr}(\mathbf{V}_B^T \Sigma \mathbf{V}_B) + \text{tr}(\mathbf{V}_B^T \Sigma_0 \mathbf{V}_B) - 2 \text{tr}(\mathbf{V}^T (\Sigma^{\frac{1}{2}} \Sigma_0 \Sigma^{\frac{1}{2}})^{\frac{1}{2}} \mathbf{V}) \end{aligned} \quad (S14)$$

882 where we used Eq. (S11) and $\stackrel{+c}{=}$ denotes equality up to constants independent of $(\boldsymbol{\mu}, \Sigma)$.
 883

884 Now by Eq. (S13), we have that $\Sigma = \mathbf{V}_B \mathbf{M} \mathbf{V}_B^T$ for $\mathbf{M} = \mathbf{V}_B^T \Sigma \mathbf{V}_B$ and its unique principal square
 885 root is given by $\Sigma^{\frac{1}{2}} = \mathbf{V}_B \mathbf{M}^{\frac{1}{2}} \mathbf{V}_B^T$ since
 886

$$887 \quad (\mathbf{V}_B \mathbf{M}^{\frac{1}{2}} \mathbf{V}_B^T)(\mathbf{V}_B \mathbf{M}^{\frac{1}{2}} \mathbf{V}_B^T) = \mathbf{V}_B \mathbf{M}^{\frac{1}{2}} \mathbf{I}_{(P-N) \times (P-N)} \mathbf{M}^{\frac{1}{2}} \mathbf{V}_B^T = \Sigma.$$

888 It also holds that the unique principal square root
 889

$$890 \quad (\Sigma^{\frac{1}{2}} \Sigma_0 \Sigma^{\frac{1}{2}})^{\frac{1}{2}} = \mathbf{V}_B (\mathbf{M}^{\frac{1}{2}} \mathbf{V}_B^T \Sigma_0 \mathbf{V}_B \mathbf{M}^{\frac{1}{2}})^{\frac{1}{2}} \mathbf{V}_B^T$$

891 since direct calculation gives
 892

$$893 \quad \begin{aligned} & (\mathbf{V}_B (\mathbf{M}^{\frac{1}{2}} \mathbf{V}_B^T \Sigma_0 \mathbf{V}_B \mathbf{M}^{\frac{1}{2}})^{\frac{1}{2}} \mathbf{V}_B^T)(\mathbf{V}_B (\mathbf{M}^{\frac{1}{2}} \mathbf{V}_B^T \Sigma_0 \mathbf{V}_B \mathbf{M}^{\frac{1}{2}})^{\frac{1}{2}} \mathbf{V}_B^T) \\ &= \mathbf{V}_B \mathbf{M}^{\frac{1}{2}} \mathbf{V}_B^T \Sigma_0 \mathbf{V}_B \mathbf{M}^{\frac{1}{2}} \mathbf{V}_B^T = \Sigma^{\frac{1}{2}} \Sigma_0 \Sigma^{\frac{1}{2}}. \end{aligned}$$

894 Therefore we have that
 895

$$896 \quad \text{tr}(\mathbf{V}^T (\Sigma^{\frac{1}{2}} \Sigma_0 \Sigma^{\frac{1}{2}})^{\frac{1}{2}} \mathbf{V}) = \text{tr}(\mathbf{V}^T \mathbf{V}_B (\mathbf{M}^{\frac{1}{2}} \mathbf{V}_B^T \Sigma_0 \mathbf{V}_B \mathbf{M}^{\frac{1}{2}})^{\frac{1}{2}} \mathbf{V}_B^T \mathbf{V}) = \text{tr}((\mathbf{M}^{\frac{1}{2}} \mathbf{V}_B^T \Sigma_0 \mathbf{V}_B \mathbf{M}^{\frac{1}{2}})^{\frac{1}{2}}).$$

897 Putting it all together we obtain
 898

$$899 \quad \begin{aligned} W_2^2(q, p) &\stackrel{+c}{=} \|\mathbf{V}_A^T \boldsymbol{\mu} - \mathbf{V}_A^T \boldsymbol{\mu}_0\|_2^2 + \|\mathbf{V}_B^T \boldsymbol{\mu} - \mathbf{V}_B^T \boldsymbol{\mu}_0\|_2^2 + \text{tr}(\mathbf{V}_B^T \Sigma \mathbf{V}_B) + \text{tr}(\mathbf{V}_B^T \Sigma_0 \mathbf{V}_B) - 2 \text{tr}(\mathbf{V}^T (\Sigma^{\frac{1}{2}} \Sigma_0 \Sigma^{\frac{1}{2}})^{\frac{1}{2}} \mathbf{V}) \\ &= \|\mathbf{V}_A^T \boldsymbol{\mu} - \mathbf{V}_A^T \boldsymbol{\mu}_0\|_2^2 + \|\mathbf{V}_B^T \boldsymbol{\mu} - \mathbf{V}_B^T \boldsymbol{\mu}_0\|_2^2 + \text{tr}(\mathbf{V}_B^T \Sigma \mathbf{V}_B) + \text{tr}(\mathbf{V}_B^T \Sigma_0 \mathbf{V}_B) - 2 \text{tr}((\mathbf{M}^{\frac{1}{2}} \mathbf{V}_B^T \Sigma_0 \mathbf{V}_B \mathbf{M}^{\frac{1}{2}})^{\frac{1}{2}}) \\ &= \|\mathbf{V}_A^T \boldsymbol{\mu} - \mathbf{V}_A^T \boldsymbol{\mu}_0\|_2^2 + W_2^2(\mathcal{N}(\mathbf{V}_B^T \boldsymbol{\mu}, \mathbf{V}_B^T \Sigma \mathbf{V}_B), \mathcal{N}(\mathbf{V}_B^T \boldsymbol{\mu}_0, \mathbf{V}_B^T \Sigma_0 \mathbf{V}_B)) \end{aligned}$$

900 which completes the proof. \square
 901

905 S1.1 OVERPARAMETRIZED LINEAR REGRESSION

907 S1.1.1 CHARACTERIZATION OF IMPLICIT BIAS (PROOF OF THEOREM 1)

908 Theorem 1 (Implicit Bias in Regression)

909 Let $f_{\mathbf{w}}(\mathbf{x}) = \mathbf{x}^T \boldsymbol{\mu}$ be an overparametrized linear model with $P > N$. Define a Gaussian prior
 910 $p(\mathbf{w}) = \mathcal{N}(\mathbf{w}; \boldsymbol{\mu}_0, \mathbf{S}_0 \mathbf{S}_0^T)$ and likelihood $p(\mathbf{y} | \mathbf{w}) = \mathcal{N}(\mathbf{y}; f_{\mathbf{w}}(\mathbf{X}), \sigma^2 \mathbf{I})$ and assume a variational family $q_{\boldsymbol{\theta}}(\mathbf{w}) = \mathcal{N}(\mathbf{w}; \boldsymbol{\mu}, \mathbf{S} \mathbf{S}^T)$ with $\boldsymbol{\theta} = (\boldsymbol{\mu}, \mathbf{S})$ such that $\boldsymbol{\mu} \in \mathbb{R}^P$ and $\mathbf{S} \in \mathbb{R}^{P \times R}$ where
 911 $R \leq P$. If the learning rate sequence $(\eta_t)_t$ is chosen such that the limit point $\boldsymbol{\theta}_*^{\text{GD}} = \lim_{t \rightarrow \infty} \boldsymbol{\theta}_t^{\text{GD}}$
 912 identified by gradient descent, initialized at $\boldsymbol{\theta}_0 = (\boldsymbol{\mu}_0, \mathbf{S}_0)$, is a (global) minimizer of the expected
 913 log-likelihood $\bar{\ell}(\boldsymbol{\theta})$, then
 914

$$915 \quad \boldsymbol{\theta}_*^{\text{GD}} \in \arg \min_{\substack{\boldsymbol{\theta} = (\boldsymbol{\mu}, \mathbf{S}) \\ s.t. \boldsymbol{\theta} \in \arg \min \bar{\ell}(\boldsymbol{\theta})}} W_2^2(q_{\boldsymbol{\theta}}, p). \quad (7)$$

916 Further, this also holds in the case of stochastic gradient descent and when using momentum.
 917

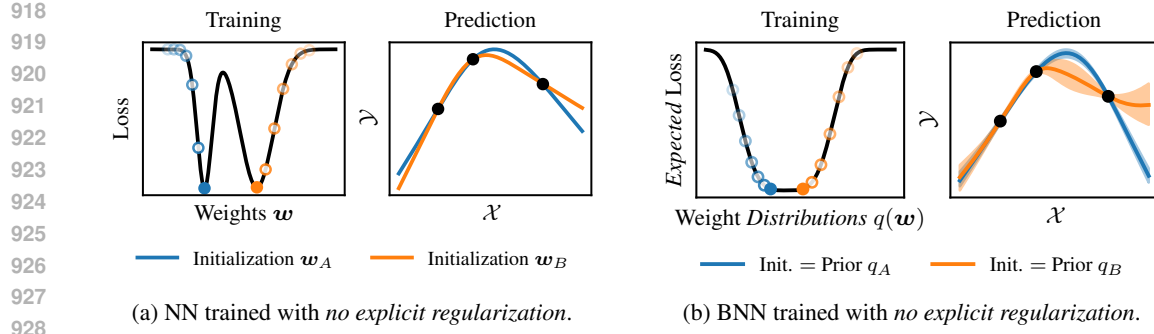


Figure S1: *Implicit regularization in standard neural networks versus in probabilistic networks.* Left panels: A neural network trained without explicit regularization can converge to different global minima of the loss. Optimization of the weights will implicitly regularize towards one or the other. Right panels: Analogously, there are multiple distributions over neural networks that are global minima of the *expected loss*. Optimization of the *distribution* over the weights will implicitly regularize towards one or the other. Our approach uses this implicit regularization instead of an explicit regularization to a prior.

Proof. Let $\theta_* = (\mu_*, S_*)$ be a minimizer of $\bar{\ell}(\theta)$. By assumption it holds that the expected negative log-likelihood is equal to the following non-negative loss function up to an additive constant:

$$\begin{aligned}\bar{\ell}(\theta) &= \mathbb{E}_{q_\theta(\mathbf{w})}(\ell(\mathbf{y}, f_\mathbf{w}(\mathbf{X}))) = \mathbb{E}_{q_\theta(\mathbf{w})}(-\log p(\mathbf{y} \mid \mathbf{w})) \\ &\stackrel{+c}{=} \frac{1}{2\sigma^2} \mathbb{E}_{q_\theta(\mathbf{w})}(\|\mathbf{y} - \mathbf{X}\mathbf{w}\|_2^2) \\ &= \frac{1}{2\sigma^2} (\|\mathbf{y} - \mathbf{X}\mu_*\|_2^2 + \text{tr}(\mathbf{X}\Sigma\mathbf{X}^\top)) \geq 0,\end{aligned}$$

where $\Sigma = \mathbf{S}\mathbf{S}^\top$ and non-negativity follows from Σ being symmetric positive semi-definite. Therefore any (global) minimizer $\theta_* = (\mu_*, \Sigma_*)$ necessarily satisfies

$$\|\mathbf{y} - \mathbf{X}\mu_*\|_2^2 = 0, \quad (\text{S15})$$

$$\text{tr}(\mathbf{X}\Sigma_*\mathbf{X}^\top) = 0. \quad (\text{S16})$$

Let $\mathbf{V} = [\mathbf{V}_{\text{range}} \quad \mathbf{V}_{\text{null}}] \in \mathbb{R}^{P \times P}$ be the orthonormal matrix of right singular vectors of $\mathbf{X} = \mathbf{U}\Lambda\mathbf{V}^\top$, where $\mathbf{V}_{\text{range}} \in \mathbb{R}^{P \times N}$ and $\mathbf{V}_{\text{null}} \in \mathbb{R}^{P \times (P-N)}$. Since $\mathbf{X} \in \mathbb{R}^{N \times P}$ and we are in the overparametrized regime, i.e. $P > N$, the optimal mean parameter decomposes into the least-squares solution and a null space contribution

$$\mu_* = \mathbf{V}_{\text{range}}\mathbf{u}_* + \mathbf{V}_{\text{null}}\mathbf{z} = \mathbf{X}^\dagger\mathbf{y} + \mathbf{V}_{\text{null}}\mathbf{z}. \quad (\text{S17})$$

Furthermore, it holds for positive semi-definite $\Sigma \in \mathbb{R}^{P \times P}$ that

$$\begin{aligned}0 \leq \text{tr}(\mathbf{X}\Sigma\mathbf{X}^\top) &= \text{tr}(\mathbf{U}\Lambda\mathbf{V}^\top\Sigma\mathbf{V}\Lambda\mathbf{U}^\top) = \text{tr}(\Lambda\mathbf{V}^\top\Sigma\mathbf{V}\Lambda) \\ &= \text{tr}([\Lambda_{N \times N} \quad \mathbf{0}] \begin{bmatrix} \mathbf{V}_{\text{range}}^\top \Sigma \mathbf{V}_{\text{range}} & * \\ * & * \end{bmatrix} \begin{bmatrix} \Lambda_{N \times N} \\ \mathbf{0} \end{bmatrix}) \\ &= \text{tr}(\Lambda_{N \times N} \mathbf{V}_{\text{range}}^\top \Sigma \mathbf{V}_{\text{range}} \Lambda_{N \times N}) \\ &= \sum_{i=1}^N \lambda_i^2 [\mathbf{V}_{\text{range}}^\top \Sigma \mathbf{V}_{\text{range}}]_{ii}\end{aligned}$$

where $\lambda_i^2 > 0$ are the squared singular values of \mathbf{X} , which are strictly positive since $\text{rank}(\mathbf{X}) = N$. Therefore using Equation (S16) any global minimizer necessarily satisfies $[\mathbf{V}_{\text{range}}^\top \Sigma_* \mathbf{V}_{\text{range}}]_{ii} = 0$ for $i \in \{1, \dots, N\}$. Now since $\mathbf{V}_{\text{range}}^\top \Sigma_* \mathbf{V}_{\text{range}}$ is symmetric positive semi-definite and its diagonal is zero, so is its trace and therefore the sum of its non-negative eigenvalues is necessarily zero. Thus all eigenvalues are zero and therefore

$$\mathbf{V}_{\text{range}}^\top \Sigma \mathbf{V}_{\text{range}} = \mathbf{0}. \quad (\text{S18})$$

Now by Lemma S1 we have that the squared 2-Wasserstein distance between $q_{\theta_*}(\mathbf{w}) = \mathcal{N}(\mathbf{w}; \boldsymbol{\mu}_*, \boldsymbol{\Sigma}_*)$ and the initialization $p(\mathbf{w}) = \mathcal{N}(\mathbf{w}; \boldsymbol{\mu}_0, \boldsymbol{\Sigma}_0)$ is given up to a constant independent of $(\boldsymbol{\mu}_*, \boldsymbol{\Sigma}_*)$ by

$$\begin{aligned} W_2(q_{\theta_*}, p) &\stackrel{+c}{=} \left\| \mathbf{V}_{\text{range}}^\top \boldsymbol{\mu}_* - \mathbf{V}_{\text{range}}^\top \boldsymbol{\mu}_0 \right\|_2^2 + W_2^2(\mathcal{N}(\mathbf{V}_{\text{null}}^\top \boldsymbol{\mu}_*, \mathbf{V}_{\text{null}}^\top \boldsymbol{\Sigma}_* \mathbf{V}_{\text{null}}), \mathcal{N}(\mathbf{V}_{\text{null}}^\top \boldsymbol{\mu}_0, \mathbf{V}_{\text{null}}^\top \boldsymbol{\Sigma}_0 \mathbf{V}_{\text{null}})) \\ &= \left\| \mathbf{X}^\dagger \mathbf{y} - \mathbf{V}_{\text{range}}^\top \boldsymbol{\mu}_0 \right\|_2^2 + W_2^2(\mathcal{N}(\mathbf{V}_{\text{null}}^\top \boldsymbol{\mu}_*, \mathbf{V}_{\text{null}}^\top \boldsymbol{\Sigma}_* \mathbf{V}_{\text{null}}), \mathcal{N}(\mathbf{V}_{\text{null}}^\top \boldsymbol{\mu}_0, \mathbf{V}_{\text{null}}^\top \boldsymbol{\Sigma}_0 \mathbf{V}_{\text{null}})) \\ &\stackrel{+c}{=} W_2^2(\mathcal{N}(\mathbf{V}_{\text{null}}^\top \boldsymbol{\mu}_*, \mathbf{V}_{\text{null}}^\top \boldsymbol{\Sigma}_* \mathbf{V}_{\text{null}}), \mathcal{N}(\mathbf{V}_{\text{null}}^\top \boldsymbol{\mu}_0, \mathbf{V}_{\text{null}}^\top \boldsymbol{\Sigma}_0 \mathbf{V}_{\text{null}})) \end{aligned}$$

Therefore among variational distributions q_{θ_*} with parameters θ_* that minimize the expected loss $\bar{\ell}(\theta)$, any such θ_* that minimizes the squared 2-Wasserstein distance to the prior satisfies

$$\underbrace{(\mathbf{V}_{\text{null}}^\top \boldsymbol{\mu}_*, \mathbf{V}_{\text{null}}^\top \boldsymbol{\Sigma}_* \mathbf{V}_{\text{null}})}_{=:z} = (\mathbf{V}_{\text{null}}^\top \boldsymbol{\mu}_0, \mathbf{V}_{\text{null}}^\top \boldsymbol{\Sigma}_0 \mathbf{V}_{\text{null}}). \quad (\text{S19})$$

(Stochastic) Gradient Descent It remains to show that (stochastic) gradient descent identifies a minimum of the expected loss $\bar{\ell}(\theta)$, such that the above holds. By assumption we have for the loss on a batch \mathbf{X}_b of data that

$$\begin{aligned} \bar{\ell}(\theta) &= \mathbb{E}_{q_{\theta}(\mathbf{w})}(\ell(\mathbf{y}_b, f_{\mathbf{w}}(\mathbf{X}_b))) = \mathbb{E}_{q_{\theta}(\mathbf{w})}(-\log p(\mathbf{y}_b \mid \mathbf{w})) \\ &\stackrel{+c}{=} \frac{1}{2\sigma^2} (\|\mathbf{y}_b - \mathbf{X}_b \boldsymbol{\mu}\|_2^2 + \text{tr}(\mathbf{X}_b \boldsymbol{\Sigma} \mathbf{X}_b^\top)), \end{aligned}$$

Therefore, at convergence of (stochastic) gradient descent the variational parameters $\boldsymbol{\theta}_\infty = (\boldsymbol{\mu}_\infty, \mathbf{S}_\infty)$ are given by

$$\boldsymbol{\mu}_\infty = \boldsymbol{\mu}_0 - \sum_{t=1}^{\infty} \eta_t \nabla_{\boldsymbol{\mu}} \bar{\ell}_b(\boldsymbol{\theta}_{t-1}) = \boldsymbol{\mu}_0 + \sum_{t=1}^{\infty} \frac{\eta_t}{\sigma^2} \mathbf{X}_b^\top (\mathbf{y}_b - \mathbf{X}_b \boldsymbol{\mu}_{t-1})$$

as well as

$$\mathbf{S}_\infty = \mathbf{S}_0 - \sum_{t=1}^{\infty} \eta_t \nabla_{\mathbf{S}} \bar{\ell}_b(\boldsymbol{\theta}_{t-1}) = \mathbf{S}_0 - \sum_{t=1}^{\infty} \frac{\eta_t}{\sigma^2} \mathbf{X}_b^\top \mathbf{X}_b \mathbf{S}_{t-1}$$

and therefore

$$\begin{aligned} z_\infty &= \mathbf{V}_{\text{null}}^\top \boldsymbol{\mu}_\infty = \mathbf{V}_{\text{null}}^\top \boldsymbol{\mu}_0 + \sum_{t=1}^{\infty} \frac{\eta_t}{\sigma^2} \mathbf{V}_{\text{null}}^\top \underbrace{\mathbf{X}_b^\top (\mathbf{y}_b - \mathbf{X}_b \boldsymbol{\mu}_{t-1})}_{\in \text{range}(\mathbf{X}_b^\top)} = \mathbf{V}_{\text{null}}^\top \boldsymbol{\mu}_0 \\ \mathbf{V}_{\text{null}}^\top \mathbf{S}_\infty &= \mathbf{V}_{\text{null}}^\top \mathbf{S}_0 - \sum_{t=1}^{\infty} \frac{\eta_t}{\sigma^2} \mathbf{V}_{\text{null}}^\top \underbrace{\mathbf{X}_b^\top \mathbf{X}_b \mathbf{S}_{t-1}}_{\text{columns } \in \text{range}(\mathbf{X}_b^\top)} = \mathbf{V}_{\text{null}}^\top \mathbf{S}_0 \end{aligned}$$

where we used continuity of linear maps between finite-dimensional spaces. It follows that

$$\mathbf{M}_\infty = \mathbf{V}_{\text{null}}^\top \boldsymbol{\Sigma}_\infty \mathbf{V}_{\text{null}} = \mathbf{V}_{\text{null}}^\top \mathbf{S}_\infty \mathbf{S}_\infty^\top \mathbf{V}_{\text{null}} = \mathbf{V}_{\text{null}}^\top \mathbf{S}_0 \mathbf{S}_0^\top \mathbf{V}_{\text{null}} = \mathbf{V}_{\text{null}}^\top \boldsymbol{\Sigma}_0 \mathbf{V}_{\text{null}}.$$

Therefore any limit point of (stochastic) gradient descent that minimizes the expected log-likelihood also minimizes the 2-Wasserstein distance to the prior, since $\boldsymbol{\theta}_\infty$ satisfies Equation (S19).

Momentum In case we are using (stochastic) gradient descent with momentum, the updates are given by

$$\begin{aligned} \boldsymbol{\mu}_{t+1} &= \boldsymbol{\mu}_t + \gamma_t \Delta \boldsymbol{\mu}_t - \eta_t \nabla_{\boldsymbol{\mu}} \bar{\ell}_b(\boldsymbol{\theta}_t + \alpha_t \Delta \boldsymbol{\theta}_t) \\ \mathbf{S}_{t+1} &= \mathbf{S}_t + \gamma_t \Delta \mathbf{S}_t - \eta_t \nabla_{\mathbf{S}} \bar{\ell}_b(\boldsymbol{\theta}_t + \alpha_t \Delta \boldsymbol{\theta}_t) \end{aligned} \quad (\text{S20})$$

where

$$\Delta \boldsymbol{\theta}_t = \begin{pmatrix} \Delta \boldsymbol{\mu}_t \\ \Delta \mathbf{S}_t \end{pmatrix} = \boldsymbol{\theta}_t - \boldsymbol{\theta}_{t-1}, \quad \Delta \boldsymbol{\theta}_0 = \mathbf{0}.$$

for parameters $\gamma_t, \alpha_t \geq 0$, which includes Nesterov's acceleration ($\gamma_t = \alpha_t$) [78] and heavy ball momentum ($\alpha_t = 0$) [79].

To prove that the updates of the variational parameters are always orthogonal to the null space of \mathbf{X}_b , we proceed by induction. The base case is trivial since $\Delta\boldsymbol{\theta}_0 = \mathbf{0}$. Assume now that $\mathbf{V}_{\text{null}}^\top \Delta\boldsymbol{\mu}_t = \mathbf{0}$ and $\mathbf{V}_{\text{null}}^\top \Delta\mathbf{S}_t = \mathbf{0}$, then by Equation (S20), we have

$$\mathbf{V}_{\text{null}}^\top \Delta\boldsymbol{\mu}_{t+1} = \mathbf{V}_{\text{null}}^\top (\boldsymbol{\mu}_{t+1} - \boldsymbol{\mu}_t) = \gamma_t \mathbf{V}_{\text{null}}^\top \Delta\boldsymbol{\mu}_t - \eta_t \mathbf{V}_{\text{null}}^\top \nabla_{\boldsymbol{\mu}} \bar{\ell}_b(\boldsymbol{\theta}_t + \alpha_t \Delta\boldsymbol{\theta}_t) = \mathbf{0}$$

$$\mathbf{V}_{\text{null}}^\top \Delta\mathbf{S}_{t+1} = \mathbf{V}_{\text{null}}^\top (\mathbf{S}_{t+1} - \mathbf{S}_t) = \gamma_t \mathbf{V}_{\text{null}}^\top \Delta\mathbf{S}_t - \eta_t \mathbf{V}_{\text{null}}^\top \nabla_{\mathbf{S}} \bar{\ell}_b(\boldsymbol{\theta}_t + \alpha_t \Delta\boldsymbol{\theta}_t) = \mathbf{0}$$

where we used the induction hypothesis and the fact that the gradients are orthogonal to the null space as shown earlier.

Therefore by the same argument as above we have that $\boldsymbol{\theta}_\infty$ computed via (stochastic) gradient descent with momentum satisfies Equation (S19), which directly implies Theorem 1. \square

S1.1.2 NON-ASYMPTOTIC ERROR ANALYSIS

Theorem S3 (Non-Asymptotic Error of Gradient Flow)

Let $f_{\mathbf{w}}(\mathbf{x}) = \mathbf{x}^\top \mathbf{w}$ be a linear model. Define a prior $p(\mathbf{w}) = \mathcal{N}(\mathbf{w}; \boldsymbol{\mu}_0, \mathbf{S}_0 \mathbf{S}_0^\top)$ and assume noise-free observations $y(\cdot) = f_{\mathbf{w}}(\cdot)$ for $\mathbf{w} \sim p(\mathbf{w})$. Further, define a variational distribution $q_{\boldsymbol{\theta}}(\mathbf{w}) = \mathcal{N}(\mathbf{w}; \boldsymbol{\mu}, \mathbf{S} \mathbf{S}^\top)$ with $\boldsymbol{\theta} = (\boldsymbol{\mu}, \mathbf{S})$ such that $\boldsymbol{\mu} \in \mathbb{R}^P$ and $\mathbf{S} \in \mathbb{R}^{P \times R}$ where $R \leq P$. Let $\dot{\boldsymbol{\theta}}(t) = (\dot{\boldsymbol{\mu}}(t), \dot{\mathbf{S}}(t))$ be the variational parameters at time $t \geq 0$ given by the gradient flow of the expected loss

$$\dot{\boldsymbol{\theta}}(t) = -\nabla_{\boldsymbol{\theta}} \bar{\ell}(\boldsymbol{\theta}(t)) \quad (\text{S21})$$

initialized at $\boldsymbol{\theta}(0) = (\boldsymbol{\mu}_0, \mathbf{S}_0)$. Then the expected squared error of the mean prediction

$$\mathbb{E}_{(\mathbf{y}_{\text{test}})} \left((y_{\text{test}} - f_{\boldsymbol{\mu}}(\mathbf{x}_{\text{test}}))^2 \right) = \text{Var}_{\mathbf{w} \sim q_{\boldsymbol{\theta}}(\mathbf{w})} (f_{\mathbf{w}}(\mathbf{x}_{\text{test}})) \quad (\text{S22})$$

at any test point $\mathbf{x}_{\text{test}} \in \mathbb{R}^P$. In other words, assuming the training and test data are drawn from the prior predictive, the predictive error of $f_{\boldsymbol{\mu}(t)}(\cdot)$ at any time $t \geq 0$ is exactly quantified by the predictive uncertainty of the variational distribution, not only at initialization and in the limit $t \rightarrow \infty$.

Proof. The dynamics of the variational parameters as defined by the gradient flow in Equation (S21) are given by

$$\dot{\boldsymbol{\mu}}(t) = -\nabla_{\boldsymbol{\mu}} \bar{\ell}(\boldsymbol{\mu}(t)) = \mathbf{X}^\top (\mathbf{y} - \mathbf{X} \boldsymbol{\mu}(t)) = -\mathbf{X}^\top \mathbf{X} (\boldsymbol{\mu}(t) - \mathbf{w}) = \frac{d}{dt} (\boldsymbol{\mu}(t) - \mathbf{w}),$$

$$\dot{\mathbf{S}}(t) = -\nabla_{\mathbf{S}} \bar{\ell}(\mathbf{S}(t)) = -\mathbf{X}^\top \mathbf{X} \mathbf{S}(t).$$

Since these dynamics are matrix differential equations, the mean and covariance parameters as a function of time are given by

$$\boldsymbol{\mu}(t) = \mathbf{w} + e^{-\mathbf{X}^\top \mathbf{X} t} (\boldsymbol{\mu}_0 - \mathbf{w}), \quad (\text{S23})$$

$$\mathbf{S}(t) = e^{-\mathbf{X}^\top \mathbf{X} t} \mathbf{S}_0. \quad (\text{S24})$$

Thus the expected predictive error at time step $t \geq 0$ is given by

$$\begin{aligned} \mathbb{E}_{(\mathbf{y}_{\text{test}})} \left(\|y_{\text{test}} - f_{\boldsymbol{\mu}(t)}(\mathbf{x}_{\text{test}})\|_2^2 \right) &= \mathbb{E}_{(\mathbf{x}_{\text{test}})}_{\mathbf{w}} \left(\|y_{\text{test}} - \mathbf{x}_{\text{test}}^\top \boldsymbol{\mu}(t)\|_2^2 \right) \\ &= \mathbb{E}_{\mathbf{w}} \left(\left\| \mathbf{x}_{\text{test}}^\top \mathbf{w} - \mathbf{x}_{\text{test}}^\top \left(\mathbf{w} + e^{-\mathbf{X}^\top \mathbf{X} t} (\boldsymbol{\mu}_0 - \mathbf{w}) \right) \right\|_2^2 \right) \\ &= \mathbb{E}_{\mathbf{w}} \left(\left\| \mathbf{x}_{\text{test}}^\top e^{-\mathbf{X}^\top \mathbf{X} t} (\boldsymbol{\mu}_0 - \mathbf{w}) \right\|_2^2 \right) \end{aligned}$$

where we used Equation (S23). We have since $\mathbb{E}(\mathbf{w}) = \boldsymbol{\mu}_0$, that the above

$$\begin{aligned} &= \text{tr} \left(\text{Cov}(\mathbf{w} - \boldsymbol{\mu}_0) e^{-\mathbf{X}^\top \mathbf{X} t} \mathbf{x}_{\text{test}} \mathbf{x}_{\text{test}}^\top e^{-\mathbf{X}^\top \mathbf{X} t} \right) \\ &= \text{tr} \left(\mathbf{x}_{\text{test}}^\top e^{-\mathbf{X}^\top \mathbf{X} t} \mathbf{S}_0 \mathbf{S}_0^\top e^{-\mathbf{X}^\top \mathbf{X} t} \mathbf{x}_{\text{test}} \right) \end{aligned}$$

$$\begin{aligned}
&= \text{tr}(\mathbf{x}_{\text{test}}^\top \mathbf{S}_t \mathbf{S}_t^\top \mathbf{x}_{\text{test}}) \\
&= \text{Var}_{\mathbf{w} \sim q_{\boldsymbol{\theta}(t)}}(f_{\mathbf{w}}(\mathbf{x}_{\text{test}}))
\end{aligned}$$

where we used Equation (S24) in the second-to-last equality. This completes the proof. \square

Theorem S4 (Non-Asymptotic Error of SGD)

Let $f_{\mathbf{w}}(\mathbf{x}) = \mathbf{x}^\top \mathbf{w}$ be a linear model. Define a prior $p(\mathbf{w}) = \mathcal{N}(\mathbf{w}; \boldsymbol{\mu}_0, \mathbf{S}_0 \mathbf{S}_0^\top)$ and assume noise-free observations $y(\cdot) = f_{\mathbf{w}}(\cdot)$ for $\mathbf{w} \sim p(\mathbf{w})$. Further, define a variational distribution $q_{\boldsymbol{\theta}}(\mathbf{w}) = \mathcal{N}(\mathbf{w}; \boldsymbol{\mu}, \mathbf{S} \mathbf{S}^\top)$ with $\boldsymbol{\theta} = (\boldsymbol{\mu}, \mathbf{S})$ such that $\boldsymbol{\mu} \in \mathbb{R}^P$ and $\mathbf{S} \in \mathbb{R}^{P \times R}$ where $R \leq P$. Assume the expected loss is given by $\bar{\ell}(\boldsymbol{\theta}) = \mathbb{E}_{q_{\boldsymbol{\theta}}(\mathbf{w})} \left(\frac{1}{2} \|y - \mathbf{X}\mathbf{w}\|_2^2 \right)$ and let $\boldsymbol{\theta}(t) = (\boldsymbol{\mu}(t), \mathbf{S}(t))$ be the variational parameters at step t of (stochastic) gradient descent with learning rate sequence $(\eta_t)_t$, initialized at $\boldsymbol{\theta}(0) = (\boldsymbol{\mu}_0, \mathbf{S}_0)$. Then the expected squared error of the mean prediction

$$\mathbb{E}_{(\mathbf{y}_{\text{test}})} \left((y_{\text{test}} - f_{\boldsymbol{\mu}(\textcolor{red}{t})}(\mathbf{x}_{\text{test}}))^2 \right) = \text{Var}_{\mathbf{w} \sim q_{\boldsymbol{\theta}(\textcolor{red}{t})}}(f_{\mathbf{w}}(\mathbf{x}_{\text{test}})) \quad (\text{S25})$$

at any test point $\mathbf{x}_{\text{test}} \in \mathbb{R}^P$. In other words, assuming the training and test data are drawn from the prior predictive, the predictive error of $f_{\boldsymbol{\mu}(t)}(\cdot)$ at any optimization step t is exactly quantified by the predictive uncertainty of the variational distribution.

Further, if the learning rate $\eta_t \leq \frac{1}{\lambda_{\max}(\mathbf{X}_t^\top \mathbf{X}_t)}$ for all steps t , then

$$\text{tr}(\text{Cov}_{\mathbf{w} \sim q_{\boldsymbol{\theta}(t+1)}}(\mathbf{w})) \leq \text{tr}(\text{Cov}_{\mathbf{w} \sim q_{\boldsymbol{\theta}(t)}}(\mathbf{w})), \quad (\text{S26})$$

i.e. uncertainty about the parameters decreases monotonically during optimization.

Proof. The expected loss is given up to an additive constant by

$$\bar{\ell}(\boldsymbol{\theta}) = \mathbb{E}_{q_{\boldsymbol{\theta}}(\mathbf{w})}(\ell(\mathbf{y}, f_{\mathbf{w}}(\mathbf{X}))) \stackrel{+c}{=} \frac{1}{2} (\|\mathbf{y} - \mathbf{X}\boldsymbol{\mu}\|_2^2 + \text{tr}(\mathbf{X}\mathbf{S}\mathbf{S}^\top \mathbf{X}^\top)).$$

Now let $(\mathbf{X}_t, \mathbf{y}_t)$ be the minibatch at step $t \geq 1$. Then it holds that

$$f_{\boldsymbol{\mu}(t)}(\mathbf{x}_{\text{test}}) - y_{\text{test}} = \mathbf{x}_{\text{test}}^\top (\boldsymbol{\mu}(t) - \mathbf{w}). \quad (\text{S27})$$

Further, the mean parameters identified by SGD are given by

$$\begin{aligned}
\boldsymbol{\mu}(t) - \mathbf{w} &= \boldsymbol{\mu}(t-1) - \mathbf{w} - \eta_t \nabla_{\boldsymbol{\mu}} \bar{\ell}(\boldsymbol{\theta}(t-1)) \\
&= \boldsymbol{\mu}(t-1) - \mathbf{w} - \eta_t \mathbf{X}_t^\top (\mathbf{X}_t \boldsymbol{\mu}(t-1) - \mathbf{y}_t) \\
&= \boldsymbol{\mu}(t-1) - \mathbf{w} - \eta_t \mathbf{X}_t^\top \mathbf{X}_t (\boldsymbol{\mu}(t-1) - \mathbf{w}) \\
&= (\mathbf{I} - \eta_t \mathbf{X}_t^\top \mathbf{X}_t) (\boldsymbol{\mu}(t-1) - \mathbf{w}) \\
&= \prod_{j=1}^t (\mathbf{I} - \eta_j \mathbf{X}_j^\top \mathbf{X}_j) (\boldsymbol{\mu}(0) - \mathbf{w}), \\
&= \mathbf{B}_t (\boldsymbol{\mu}_0 - \mathbf{w})
\end{aligned}$$

where we defined $\mathbf{B}_t = \prod_{j=1}^t (\mathbf{I} - \eta_j \mathbf{X}_j^\top \mathbf{X}_j)$. The covariance parameters are given by

$$\begin{aligned}
\mathbf{S}(t) &= \mathbf{S}(t-1) - \eta_t \nabla_{\mathbf{S}} \bar{\ell}(\boldsymbol{\theta}(t-1)) \\
&= \mathbf{S}(t-1) - \eta_t \mathbf{X}_t^\top \mathbf{X}_t \mathbf{S}(t-1) \\
&= (\mathbf{I} - \eta_t \mathbf{X}_t^\top \mathbf{X}_t) \mathbf{S}(t-1) \\
&= \prod_{j=1}^t (\mathbf{I} - \eta_j \mathbf{X}_j^\top \mathbf{X}_j) \mathbf{S}(0) \\
&= \mathbf{B}_t \mathbf{S}_0
\end{aligned}$$

Therefore the predictive error at step $t \in \{0, 1, \dots\}$ is given by

$$\mathbb{E}_{(\mathbf{y}_{\text{test}})} \left(\|y_{\text{test}} - f_{\boldsymbol{\mu}(t)}(\mathbf{x}_{\text{test}})\|_2^2 \right) = \mathbb{E}_{(\mathbf{x}_{\text{test}})} \left(\|y_{\text{test}} - \mathbf{x}_{\text{test}}^\top \boldsymbol{\mu}(t)\|_2^2 \right)$$

$$\begin{aligned}
1134 &= \mathbb{E}_{\mathbf{w}} \left(\|\mathbf{x}_{\text{test}}^{\top}(\boldsymbol{\mu}(t) - \mathbf{w})\|_2^2 \right) \\
1135 &= \mathbb{E}_{\mathbf{w}} \left(\|\mathbf{x}_{\text{test}}^{\top} \mathbf{B}_t(\boldsymbol{\mu}_0 - \mathbf{w})\|_2^2 \right)
\end{aligned}$$

1138 We have since $\mathbb{E}(\boldsymbol{\mu}_0 - \mathbf{w}) = \mathbf{0}$, that the above

$$\begin{aligned}
1139 &= \text{tr}(\mathbf{B}_t^{\top} \mathbf{x}_{\text{test}} \mathbf{x}_{\text{test}}^{\top} \mathbf{B}_t \text{Cov}(\mathbf{w} - \boldsymbol{\mu}_0)) \\
1140 &= \text{tr}(\mathbf{x}_{\text{test}}^{\top} \mathbf{B}_t \mathbf{S}_0 \mathbf{S}_0^{\top} \mathbf{B}_t^{\top} \mathbf{x}_{\text{test}}) \\
1141 &= \text{tr}(\mathbf{x}_{\text{test}}^{\top} \mathbf{S}(t) \mathbf{S}(t)^{\top} \mathbf{x}_{\text{test}}) \\
1142 &= \text{Var}_{\mathbf{w} \sim q_{\boldsymbol{\theta}(t)}}(f_{\mathbf{w}}(\mathbf{x}_{\text{test}})).
\end{aligned}$$

1143 This proves Equation (S25).

1144 To prove the second statement, we begin by showing that $\mathbf{I} - \eta_t \mathbf{X}_t^{\top} \mathbf{X}_t$ has a spectrum in the interval
1145 $[0, 1]$. We have by Weyl's theorem, since \mathbf{I} and $\mathbf{C}_{t+1} := -\eta_{t+1} \mathbf{X}_{t+1}^{\top} \mathbf{X}_{t+1}$ are hermitian, that
1146

$$\begin{aligned}
1147 &\lambda_p(\mathbf{I}) + \lambda_{\min}(\mathbf{C}_{t+1}) \leq \lambda_p(\mathbf{I} + \mathbf{C}_{t+1}) \leq \lambda_p(\mathbf{I}) + \lambda_{\max}(\mathbf{C}_{t+1}) \\
1148 &\iff 1 - \eta_{t+1} \lambda_{\max}(\mathbf{X}_{t+1}^{\top} \mathbf{X}_{t+1}) \leq \lambda_p(\mathbf{I} + \mathbf{C}_{t+1}) \leq 1 - \eta_{t+1} \lambda_{\min}(\mathbf{X}_{t+1}^{\top} \mathbf{X}_{t+1}) \\
1149 &\implies 1 - \frac{\lambda_{\max}(\mathbf{X}_{t+1}^{\top} \mathbf{X}_{t+1})}{\lambda_{\max}(\mathbf{X}_{t+1}^{\top} \mathbf{X}_{t+1})} \leq \lambda_p(\mathbf{I} + \mathbf{C}_{t+1}) \leq 1 \\
1150 &\iff 0 \leq \lambda_p(\mathbf{I} + \mathbf{C}_{t+1}) \leq 1
\end{aligned}$$

1151 where we used the assumption on the learning rate that $\forall t : \eta_t \leq \frac{1}{\lambda_{\max}(\mathbf{X}_t^{\top} \mathbf{X}_t)}$. Now by von
1152 Neumann's trace inequality, it holds that
1153

$$\begin{aligned}
1154 \text{tr}(\text{Cov}_{\mathbf{w} \sim q_{\boldsymbol{\theta}(t+1)}}(\mathbf{w})) &= \text{tr}((\mathbf{I} - \eta_{t+1} \mathbf{X}_{t+1}^{\top} \mathbf{X}_{t+1}) \mathbf{S}_t \mathbf{S}_t^{\top} (\mathbf{I} - \eta_{t+1} \mathbf{X}_{t+1}^{\top} \mathbf{X}_{t+1})^{\top}) \\
1155 &= \text{tr}(\mathbf{S}_t \mathbf{S}_t^{\top} (\mathbf{I} - \eta_{t+1} \mathbf{X}_{t+1}^{\top} \mathbf{X}_{t+1}) (\mathbf{I} - \eta_{t+1} \mathbf{X}_{t+1}^{\top} \mathbf{X}_{t+1})) \\
1156 &\leq \sum_{p=1}^P \lambda_p(\mathbf{S}_t \mathbf{S}_t^{\top}) \lambda_p((\mathbf{I} - \eta_{t+1} \mathbf{X}_{t+1}^{\top} \mathbf{X}_{t+1})^2) \\
1157 &= \sum_{p=1}^P \lambda_p(\mathbf{S}_t \mathbf{S}_t^{\top}) \lambda_p((\mathbf{I} - \eta_{t+1} \mathbf{X}_{t+1}^{\top} \mathbf{X}_{t+1}))^2 \\
1158 &\leq \sum_{p=1}^P \lambda_p(\mathbf{S}_t \mathbf{S}_t^{\top}) \\
1159 &= \text{tr}(\text{Cov}_{\mathbf{w} \sim q_{\boldsymbol{\theta}(t)}}(\mathbf{w})).
\end{aligned}$$

1160 \square

1161 S1.1.3 CONNECTION TO ENSEMBLES

1162 Proposition S1 (Connection to Ensembles)

1163 Consider an ensemble of overparametrized linear models $f_{\mathbf{w}}(\mathbf{x}) = \mathbf{x}^{\top} \mathbf{w}$ initialized with weights
1164 drawn from the prior $\mathbf{w}_0^{(i)} \sim \mathcal{N}(\mathbf{w}; \boldsymbol{\mu}_0, \mathbf{S}_0 \mathbf{S}_0^{\top})$. Assume each model is trained independently to
1165 convergence via (S)GD such that $\mathbf{w}_*^{(i)} = \arg \min_{\mathbf{w}} \ell(\mathbf{y}, f_{\mathbf{w}}(\mathbf{X}))$. Then the distribution over the
1166 weights of the trained ensemble $q_{\text{Ens}}(\mathbf{w})$ is equal to the variational approximation $q_{\boldsymbol{\theta}_*}(\mathbf{w})$ learned
1167 via (S)GD initialized at the prior hyperparameters $\boldsymbol{\theta}_0 = (\boldsymbol{\mu}_0, \mathbf{S}_0)$, i.e.
1168

$$1169 q_{\text{Ens}}(\mathbf{w}) = q_{\boldsymbol{\theta}_*^{\text{GD}}}(\mathbf{w}). \quad (\text{S28})$$

1170 The parameters $\mathbf{w}_{\infty}^{(i)}$ of the (independently) trained ensemble members identified via
1171 (stochastic) gradient descent are given by
1172

$$1173 \mathbf{w}_{\infty}^{(i)} = \arg \min_{\mathbf{w} \in F} \|\mathbf{w} - \mathbf{w}_0^{(i)}\|_2$$

1188 where $F = \{\mathbf{w} \in \mathbb{R}^P \mid f_{\mathbf{w}}(\mathbf{X}) = \mathbf{X}\mathbf{w} = \mathbf{y}\}$ is the set of interpolating solutions [5, Sec. 2.1]. Since
1189 we can write F equivalently via the minimum norm solution and an arbitrary null space contribution,
1190 s.t. $F = \{\mathbf{w} = \mathbf{X}^\dagger \mathbf{y} + \mathbf{w}_{\text{null}} \mid \mathbf{w}_{\text{null}} \in \text{null}(\mathbf{X})\}$ we have

$$\begin{aligned} 1191 \quad &= \mathbf{X}^\dagger \mathbf{y} + \arg \min_{\mathbf{w}_{\text{null}} \in \text{null}(\mathbf{X})} \|\mathbf{w}_{\text{null}} - (\mathbf{w}_0^{(i)} - \mathbf{X}^\dagger \mathbf{y})\|_2 \\ 1192 \quad &= \mathbf{X}^\dagger \mathbf{y} + \text{proj}_{\text{null}(\mathbf{X})} \left(\mathbf{w}_0^{(i)} - \underbrace{\mathbf{X}^\dagger \mathbf{y}}_{\in \text{range}(\mathbf{X}^\dagger)} \right) \end{aligned}$$

1193 where we used the characterization of an orthogonal projection onto a linear subspace as the (unique)
1194 closest point in the subspace. Finally, we use that the minimum norm solution is in the range space
1195 of the data and rewrite the projection in matrix form, s.t.

$$1196 \quad = \mathbf{X}^\dagger \mathbf{y} + \mathbf{P}_{\text{null}} \mathbf{w}_0^{(i)}.$$

1200 Therefore the distribution over the parameters $\mathbf{w}_\infty^{(i)}$ of the ensemble members computed via (S)GD
1201 with initial parameters $\mathbf{w}_0 \sim \mathcal{N}(\mathbf{w}; \boldsymbol{\mu}_0, \mathbf{S}_0 \mathbf{S}_0^\top)$ is given by

$$1203 \quad q_{\text{Ens}}(\mathbf{w}) = \mathcal{N} \left(\mathbf{w}; \underbrace{\mathbf{X}^\dagger \mathbf{y} + \mathbf{P}_{\text{null}} \boldsymbol{\mu}_0}_{= \boldsymbol{\mu}_{\text{Ens}}}, \underbrace{\mathbf{P}_{\text{null}} \mathbf{S}_0 \mathbf{S}_0^\top \mathbf{P}_{\text{null}}^\top}_{= \mathbf{S}_{\text{Ens}}} \right).$$

1207 Now the expected negative log-likelihood of the distribution over the parameters of the trained en-
1208 semble members $q_{\text{Ens}}(\mathbf{w})$ with hyperparameters $\boldsymbol{\theta}_{\text{Ens}} = (\boldsymbol{\mu}_{\text{Ens}}, \mathbf{S}_{\text{Ens}})$ is

$$1209 \quad \bar{\ell}(\boldsymbol{\theta}_{\text{Ens}}) \stackrel{c}{=} \frac{1}{2\sigma^2} (\|\mathbf{y} - \mathbf{X}\boldsymbol{\mu}_{\text{Ens}}\|_2^2 + \text{tr}(\mathbf{X} \mathbf{S}_{\text{Ens}} \mathbf{S}_{\text{Ens}}^\top \mathbf{X}^\top)) = 0$$

1210 and therefore $\boldsymbol{\theta}_{\text{Ens}}$ is a minimizer of the expected log-likelihood. Further it holds that

$$1212 \quad \mathbf{z} = \mathbf{V}_{\text{null}}^\top (\mathbf{P}_{\text{null}} \boldsymbol{\mu}_0) = \mathbf{V}_{\text{null}}^\top \boldsymbol{\mu}_0$$

$$1213 \quad \mathbf{M} = \mathbf{V}_{\text{null}}^\top (\mathbf{P}_{\text{null}} \mathbf{S}_0) (\mathbf{P}_{\text{null}} \mathbf{S}_0)^\top \mathbf{V}_{\text{null}} = \mathbf{V}_{\text{null}}^\top \mathbf{S}_0 \mathbf{S}_0^\top \mathbf{V}_{\text{null}} = \mathbf{V}_{\text{null}}^\top \boldsymbol{\Sigma}_0 \mathbf{V}_{\text{null}}$$

1214 and thus by Equation (S19), the distribution of the trained ensemble parameters minimizes the 2-
1215 Wasserstein distance to the prior distribution, i.e.

$$1216 \quad q_{\text{Ens}} = \arg \min_{q(\mathbf{w}) = \mathcal{N}(\mathbf{w}; \boldsymbol{\mu}, \boldsymbol{\Sigma})} W_2^2(q(\mathbf{w}), \mathcal{N}(\mathbf{w}; \boldsymbol{\mu}_0, \boldsymbol{\Sigma}_0)).$$

1218 Combining this with the characterization of the variational posterior in Theorem 1 proves the claim. \square

1221 S1.2 BINARY CLASSIFICATION OF LINEARLY SEPARABLE DATA

1223 In this subsection we provide proofs of claims from Section 4.2. We begin with presenting some
1224 preliminary results from Soudry et al. [4] which will be used throughout the proof. Next, we will
1225 analyze the gradient flow of the expected loss. We extend the results for the gradient flow to gradient
1226 descent and derive the characterization of the implicit bias, completing the proof of Theorem 2.

1227 Theorem 2 (Implicit Bias in Binary Classification)

1228 Let $f_{\mathbf{w}}(\mathbf{x}) = \mathbf{x}^\top \mathbf{w}$ be an (overparametrized) linear model and define a Gaussian prior $p(\mathbf{w}) =$
1229 $\mathcal{N}(\mathbf{w}; \boldsymbol{\mu}_0, \mathbf{S}_0 \mathbf{S}_0^\top)$. Assume a variational distribution $q_{\boldsymbol{\theta}}(\mathbf{w}) = \mathcal{N}(\mathbf{w}; \boldsymbol{\mu}, \mathbf{S} \mathbf{S}^\top)$ over the weights
1230 $\mathbf{w} \in \mathbb{R}^P$ with variational parameters $\boldsymbol{\theta} = (\boldsymbol{\mu}, \mathbf{S})$ such that $\mathbf{S} \in \mathbb{R}^{P \times R}$ and $R \leq P$. Assume we
1231 are using the exponential loss $\ell(u) = \exp(-u)$ and optimize the expected empirical loss $\bar{\ell}(\boldsymbol{\theta})$ via
1232 gradient descent initialized at the prior, i.e. $\boldsymbol{\theta}_0 = (\boldsymbol{\mu}_0, \mathbf{S}_0)$, with a sufficiently small learning rate η .
1233 Then for almost any dataset which is linearly separable (Assumption 1) and for which the support
1234 vectors span the data (Assumption 2), the rescaled gradient descent iterates (rGD)
1235 $\boldsymbol{\theta}_t^{\text{rGD}} = (\boldsymbol{\mu}_t^{\text{rGD}}, \mathbf{S}_t^{\text{rGD}}) = \left(\frac{1}{\log(t)} \boldsymbol{\mu}_t^{\text{GD}} + \mathbf{P}_{\text{null}(\mathbf{X})} \boldsymbol{\mu}_0, \mathbf{S}_t^{\text{GD}} \right)$

1236 converge to a limit point $\boldsymbol{\theta}_*^{\text{rGD}} = \lim_{t \rightarrow \infty} \boldsymbol{\theta}_t^{\text{rGD}}$ for which it holds that

$$1238 \quad \boldsymbol{\theta}_*^{\text{rGD}} \in \arg \min_{\substack{\boldsymbol{\theta} = (\boldsymbol{\mu}, \mathbf{S}) \\ \text{s.t. } \boldsymbol{\theta} \in \Theta_*}} W_2^2(q_{\boldsymbol{\theta}}, p). \quad (10)$$

1240 where the feasible set $\Theta_* = \{(\boldsymbol{\mu}, \mathbf{S}) \mid \mathbf{P}_{\text{range}(\mathbf{X}^\dagger)} \boldsymbol{\mu} = \hat{\mathbf{w}} \text{ and } \forall n : \text{Var}_{q_{\boldsymbol{\theta}}}(f_{\mathbf{w}}(\mathbf{x}_n)) = 0\}$
1241 consists of mean parameters which, if projected onto the training data, are equivalent to the L_2 max
margin vector and covariance parameters such that there is no uncertainty at training data.

1242 S1.2.1 PRELIMINARIES
12431244 Recall that the expected loss is given by
1245

1246
$$\bar{\ell}(\boldsymbol{\theta}) = \sum_{n=1}^N \mathbb{E}_{q_{\boldsymbol{\theta}}(\mathbf{w})}(\ell(y_n \mathbf{x}_n^\top \mathbf{w})) , \quad (\text{S29})$$

1247 and specifically, for the exponential loss, we have
1248

1249
$$\bar{\ell}(\boldsymbol{\theta}) = \bar{\ell}(\boldsymbol{\mu}, \mathbf{S}) = \sum_{n=1}^N \exp(-\mathbf{x}_n^\top \boldsymbol{\mu} + \frac{1}{2} \mathbf{x}_n^\top \mathbf{S} \mathbf{S}^\top \mathbf{x}_n) . \quad (\text{S30})$$

1250 Throughout these proofs, for any mean parameter iterate $\boldsymbol{\mu}_t$, we define the residual as
1251

1252
$$\mathbf{r}_t = \boldsymbol{\mu}_t - \hat{\mathbf{w}} \log t - \tilde{\mathbf{w}} \quad (\text{S31})$$

1253 where $\hat{\mathbf{w}}$ is the solution to the hard margin SVM, and $\tilde{\mathbf{w}}$ is the vector which satisfies
1254

1255
$$\forall n \in \mathcal{S} : \eta \exp(-\mathbf{x}_n^\top \tilde{\mathbf{w}}) = \alpha_n, \quad (\text{S32})$$

1256 where weights α_n are defined through the KKT conditions on the hard margin SVM problem, i.e.
1257

1258
$$\hat{\mathbf{w}} = \sum_{n \in \mathcal{S}} \alpha_n \mathbf{x}_n. \quad (\text{S33})$$

1259 In Lemma 12 (Appendix B) of Soudry et al. [4], it is shown that, for almost any dataset, there are no
1260 more than P support vectors and $\alpha_n \neq 0, \forall n \in \mathcal{S}$. Furthermore, we denote the minimum margin to
1261 a non-support vector as:

1262
$$\kappa = \min_{n \notin \mathcal{S}} \mathbf{x}_n^\top \hat{\mathbf{w}} > 1. \quad (\text{S34})$$

1263 Finally, we define $\mathbf{P}_{\mathcal{S}} \in \mathbb{R}^{P \times P}$ as the orthogonal projection matrix to the subspace spanned by the
1264 support vectors, and $\bar{\mathbf{P}}_{\mathcal{S}} = \mathbf{I} - \mathbf{P}_{\mathcal{S}}$ as the complementary projection.
12651266 S1.2.2 GRADIENT FLOW FOR THE EXPECTED LOSS
12671268 Similar as in Soudry et al. [4], we begin by studying the gradient flow dynamics, i.e. taking the
1269 continuous time limit of gradient descent:
1270

1271
$$\dot{\boldsymbol{\theta}}_t = -\nabla \bar{\ell}(\boldsymbol{\theta}_t), \quad (\text{S35})$$

1272 which can be written componentwise as:
1273

1274
$$\dot{\boldsymbol{\mu}}_t = -\nabla_{\boldsymbol{\mu}} \bar{\ell}(\boldsymbol{\mu}_t, \mathbf{S}_t) = \sum_{n=1}^N \exp\left(-\boldsymbol{\mu}_t^\top \mathbf{x}_n + \frac{1}{2} \mathbf{x}_n^\top \mathbf{S}_t \mathbf{S}_t^\top \mathbf{x}_n\right) \mathbf{x}_n \quad (\text{S36})$$

1275
$$\dot{\mathbf{S}}_t = -\nabla_{\mathbf{S}} \bar{\ell}(\boldsymbol{\mu}_t, \mathbf{S}_t) = -\sum_{n=1}^N \exp\left(-\boldsymbol{\mu}_t^\top \mathbf{x}_n + \frac{1}{2} \mathbf{x}_n^\top \mathbf{S}_t \mathbf{S}_t^\top \mathbf{x}_n\right) \mathbf{x}_n \mathbf{x}_n^\top \mathbf{S}_t. \quad (\text{S37})$$

1276 We begin by showing that the total uncertainty, as measured by the Frobenius norm of the covariance
1277 factor, is bounded during the gradient flow dynamics. To that end, we derive the following dynamics:
1278

1279
$$\frac{d}{dt} \frac{1}{2} \|\mathbf{S}_t\|_F^2 = \text{tr}(\mathbf{S}_t^\top \dot{\mathbf{S}}_t) = -\sum_{n=1}^N \exp\left(-\boldsymbol{\mu}_t^\top \mathbf{x}_n + \frac{1}{2} \mathbf{x}_n^\top \mathbf{S}_t \mathbf{S}_t^\top \mathbf{x}_n\right) \|\mathbf{x}_n^\top \mathbf{S}_t\|^2 \leq 0, \quad (\text{S38})$$

1280 and therefore
1281

1282
$$\|\mathbf{S}_t\|_F^2 \leq \|\mathbf{S}_0\|_F^2. \quad (\text{S39})$$

1283 Finally, by Cauchy-Schwarz inequality, we have that
1284

1285
$$\|\mathbf{S}_t \mathbf{S}_t^\top\|_F \leq \|\mathbf{S}_t\|_F^2 \leq \|\mathbf{S}_0\|_F^2. \quad (\text{S40})$$

1286 We continue by studying the convergence behavior of the mean parameter $\boldsymbol{\mu}_t$.
1287

1296 **Mean parameter** Our goal is to show that $\|\mathbf{r}_t\|$ is bounded. Equation (S31) implies that
1297

$$1298 \quad \dot{\mathbf{r}}_t = \dot{\boldsymbol{\mu}}_t - \frac{1}{t} \hat{\mathbf{w}} = -\nabla_{\boldsymbol{\mu}} \bar{\ell}(\boldsymbol{\mu}_t, \mathbf{S}_t) - \frac{1}{t} \hat{\mathbf{w}}. \quad (S41)$$

1300 This in turn implies that
1301

$$\begin{aligned} 1302 \quad & \frac{1}{2} \frac{d}{dt} \|\mathbf{r}_t\|^2 = \dot{\mathbf{r}}_t^\top \mathbf{r}_t \\ 1303 \quad & = \sum_{n=1}^N \exp \left(-\boldsymbol{\mu}_t^\top \mathbf{x}_n + \frac{1}{2} \mathbf{x}_n^\top \mathbf{S}_t \mathbf{S}_t^\top \mathbf{x}_n \right) \mathbf{x}_n^\top \mathbf{r}_t - \frac{1}{t} \hat{\mathbf{w}}^\top \mathbf{r}_t \\ 1304 \quad & = \sum_{n \in \mathcal{S}} \exp \left(-\log(t) \hat{\mathbf{w}}^\top \mathbf{x}_n - \tilde{\mathbf{w}}^\top \mathbf{x}_n + \frac{1}{2} \mathbf{x}_n^\top \mathbf{S}_t \mathbf{S}_t^\top \mathbf{x}_n - \mathbf{x}_n^\top \mathbf{r}_t \right) \mathbf{x}_n^\top \mathbf{r}_t - \frac{1}{t} \hat{\mathbf{w}}^\top \mathbf{r}_t \\ 1305 \quad & + \sum_{n \notin \mathcal{S}} \exp \left(-\log(t) \hat{\mathbf{w}}^\top \mathbf{x}_n - \tilde{\mathbf{w}}^\top \mathbf{x}_n + \frac{1}{2} \mathbf{x}_n^\top \mathbf{S}_t \mathbf{S}_t^\top \mathbf{x}_n - \mathbf{x}_n^\top \mathbf{r}_t \right) \mathbf{x}_n^\top \mathbf{r}_t \\ 1306 \quad & + \left[\frac{1}{t} \sum_{n \in \mathcal{S}} \exp(-\tilde{\mathbf{w}}^\top \mathbf{x}_n) \left(\exp \left(-\mathbf{x}_n^\top \mathbf{r}_t + \frac{1}{2} \mathbf{x}_n^\top \mathbf{S}_t \mathbf{S}_t^\top \mathbf{x}_n \right) - 1 \right) \mathbf{x}_n^\top \mathbf{r}_t \right] \\ 1307 \quad & + \left[\sum_{n \notin \mathcal{S}} \left(\frac{1}{t} \right)^{\hat{\mathbf{w}}^\top \mathbf{x}_n} \exp \left(-\tilde{\mathbf{w}}^\top \mathbf{x}_n + \frac{1}{2} \mathbf{x}_n^\top \mathbf{S}_t \mathbf{S}_t^\top \mathbf{x}_n \right) \exp(-\mathbf{x}_n^\top \mathbf{r}_t) \mathbf{x}_n^\top \mathbf{r}_t \right]. \end{aligned} \quad (S42)$$

1312 where in last line we used the fact that $\hat{\mathbf{w}}^\top \mathbf{x}_n = 1$ for $n \in \mathcal{S}$ as in (S32), and that
1313 $\sum_{n \in \mathcal{S}} \exp(-\mathbf{x}_n^\top \tilde{\mathbf{w}}) \mathbf{x}_n = \hat{\mathbf{w}}$ as in (S33). We begin by examining the first bracket, studying three
1314 possible cases for each of the summands. First, note that if $\mathbf{x}_n^\top \mathbf{r}_t \leq 0$, then since $\frac{1}{2} \mathbf{x}_n^\top \mathbf{S}_t \mathbf{S}_t^\top \mathbf{x}_n \geq 0$,
1315 we have that

$$1316 \quad \left(\exp \left(-\mathbf{x}_n^\top \mathbf{r}_t + \frac{1}{2} \mathbf{x}_n^\top \mathbf{S}_t \mathbf{S}_t^\top \mathbf{x}_n \right) - 1 \right) \mathbf{x}_n^\top \mathbf{r}_t \leq 0. \quad (S43)$$

1317 Next, by defining $B := \|\mathbf{S}_0\|_F^2 \max_n \|\mathbf{x}_n\|_2$, if $0 < \mathbf{x}_n^\top \mathbf{r}_t < \frac{B}{2}$, we have that
1318

$$1319 \quad \left| \left(\exp \left(-\mathbf{x}_n^\top \mathbf{r}_t + \frac{1}{2} \mathbf{x}_n^\top \mathbf{S}_t \mathbf{S}_t^\top \mathbf{x}_n \right) - 1 \right) \mathbf{x}_n^\top \mathbf{r}_t \right| < \left(\exp \left(\frac{B}{2} \right) - 1 \right) \frac{B}{2}, \quad (S44)$$

1320 and if $\mathbf{x}_n^\top \mathbf{r}_t \geq \frac{B}{2}$, we have that
1321

$$1322 \quad \left(\exp \left(-\mathbf{x}_n^\top \mathbf{r}_t + \frac{1}{2} \mathbf{x}_n^\top \mathbf{S}_t \mathbf{S}_t^\top \mathbf{x}_n \right) - 1 \right) \mathbf{x}_n^\top \mathbf{r}_t \leq 0. \quad (S45)$$

1323 Finally, for arbitrary $\epsilon \geq \max\{B, 1\}$, if $|\mathbf{x}_n^\top \mathbf{r}_t| \geq \epsilon$, we have that
1324

$$1325 \quad \left(\exp \left(-\mathbf{x}_n^\top \mathbf{r}_t + \frac{1}{2} \mathbf{x}_n^\top \mathbf{S}_t \mathbf{S}_t^\top \mathbf{x}_n \right) - 1 \right) \mathbf{x}_n^\top \mathbf{r}_t \leq \left(\exp \left(-\frac{B}{2} \right) - 1 \right) \epsilon < 0, \quad (S46)$$

1326 Furthermore, let $\gamma_* = \min_{n \in \mathcal{S}} \tilde{\mathbf{w}}^\top \mathbf{x}_n$ and $\gamma^* = \max_{n \in \mathcal{S}} \tilde{\mathbf{w}}^\top \mathbf{x}_n$. Now, by taking $\epsilon \geq \max\{B, 1\}$
1327 large enough such that

$$1328 \quad \left| \exp(-\gamma^*) \left(\exp \left(-\frac{B}{2} \right) - 1 \right) \epsilon \right| \geq |\mathcal{S}| \exp(-\gamma_*) \left(\exp \left(\frac{B}{2} \right) - 1 \right) \frac{B}{2}, \quad (S47)$$

1329 if there exists a support vector $n \in \mathcal{S}$ such that $|\mathbf{x}_n^\top \mathbf{r}_t| \geq \epsilon$, then
1330

$$1331 \quad \frac{1}{t} \sum_{n \in \mathcal{S}} \exp(-\tilde{\mathbf{w}}^\top \mathbf{x}_n) \left(\exp \left(-\mathbf{x}_n^\top \mathbf{r}_t + \frac{1}{2} \mathbf{x}_n^\top \mathbf{S}_t \mathbf{S}_t^\top \mathbf{x}_n \right) - 1 \right) \mathbf{x}_n^\top \mathbf{r}_t \leq 0. \quad (S48)$$

1332 The idea of this is that if there exists a support vector such that $|\mathbf{x}_n^\top \mathbf{r}_t|$ is sufficiently big, then the
1333 first bracket in Eq. (S42) is negative.

1350 On the other hand, for the second bracket in Eq. (S42), note that for $n \notin \mathcal{S}$, we have that $\mathbf{x}_n^\top \hat{\mathbf{w}} \geq \kappa$,
 1351 and hence

$$\begin{aligned} 1353 & \sum_{n \notin \mathcal{S}} \left(\frac{1}{t} \right)^{\hat{\mathbf{w}}^\top \mathbf{x}_n} \exp \left(-\tilde{\mathbf{w}}^\top \mathbf{x}_n + \frac{1}{2} \mathbf{x}_n^\top \mathbf{S}_t \mathbf{S}_t^\top \mathbf{x}_n \right) \exp(-\mathbf{x}_n^\top \mathbf{r}_t) \mathbf{x}_n^\top \mathbf{r}_t \\ 1354 & \leq \frac{1}{t^\kappa} \exp \left(\frac{1}{2} \|\mathbf{S}_0\|_F^2 \max_n \mathbf{x}_n^\top \mathbf{x}_n \right) \sum_{n \notin \mathcal{S}} \exp(-\tilde{\mathbf{w}}^\top \mathbf{x}_n) = \mathcal{O} \left(\frac{1}{t^\kappa} \right), \end{aligned} \quad (S49)$$

1358 where in the last line we used that $ze^{-z} \leq 1, \forall z \in \mathbb{R}$ and fact that $\|\mathbf{S}_t \mathbf{S}_t^\top\|_F \leq \|\mathbf{S}_0\|_F^2 < \infty$.
 1359

1360 We will now combine the results from above to show that the residual \mathbf{r}_t is bounded in the following
 1361 way: if there exists a support vector $n \in \mathcal{S}$ such that $|\mathbf{x}_n^\top \mathbf{r}_t| \geq \epsilon$ for big enough $\epsilon > 0$, then
 1362 $\frac{1}{2} \frac{d}{dt} \|\mathbf{r}_t\|^2 = \mathcal{O}(t^{-\kappa})$. If such a support vector does not exist at time t , we will show that \mathbf{r}_t is
 1363 contained inside a compact set. To that end, if $\|\mathbf{P}_{\mathcal{S}} \mathbf{r}_t\| \geq \epsilon_1$, we have that

$$\max_{n \in \mathcal{S}} |\mathbf{x}_n^\top \mathbf{r}_t|^2 \geq \frac{1}{|\mathcal{S}|} \sum_{n \in \mathcal{S}} |\mathbf{x}_n^\top \mathbf{P}_{\mathcal{S}} \mathbf{r}_t|^2 = \frac{1}{|\mathcal{S}|} \|\mathbf{X}_{\mathcal{S}}^\top \mathbf{P}_{\mathcal{S}} \mathbf{r}_t\|^2 \geq \frac{1}{|\mathcal{S}|} \sigma_{\min}^2(\mathbf{X}_{\mathcal{S}}) \epsilon_1^2, \quad (S50)$$

1367 where in the first inequality we used the fact that $\mathbf{P}_{\mathcal{S}}^\top \mathbf{x}_n = \mathbf{x}_n$ for $n \in \mathcal{S}$. Hence by choosing ϵ_1
 1368 such that $\sigma_{\min}^2(\mathbf{X}_{\mathcal{S}}) \epsilon_1^2 / |\mathcal{S}| = \epsilon^2$, where the ϵ is chosen in Eq. (S47), we have that

$$\|\mathbf{P}_{\mathcal{S}} \mathbf{r}_t\| \geq \epsilon_1 \Rightarrow \frac{1}{2} \frac{d}{dt} \|\mathbf{r}_t\|^2 = \mathcal{O}(t^{-\kappa}). \quad (S51)$$

1372 On the other hand, if $\|\mathbf{P}_{\mathcal{S}} \mathbf{r}_t\| \leq \epsilon_1$, recall that

$$\mathbf{r}_t = (\boldsymbol{\mu}_t - \boldsymbol{\mu}_0) + \boldsymbol{\mu}_0 - \hat{\mathbf{w}} \log t - \tilde{\mathbf{w}}, \quad (S52)$$

1374 and since all updates to the mean parameter are in the space spanned by the support vectors (Assumption 2), we have that

$$\bar{\mathbf{P}}_{\mathcal{S}} \mathbf{r}_t = \bar{\mathbf{P}}_{\mathcal{S}} \boldsymbol{\mu}_0 - \bar{\mathbf{P}}_{\mathcal{S}} \tilde{\mathbf{w}}. \quad (S53)$$

1377 We can now conclude that

$$\|\mathbf{P}_{\mathcal{S}} \mathbf{r}_t\| \leq \epsilon_1 \Rightarrow \|\mathbf{r}_t\| \leq \|\mathbf{P}_{\mathcal{S}} \mathbf{r}_t\| + \|\bar{\mathbf{P}}_{\mathcal{S}} \mathbf{r}_t\| \leq \epsilon_1 + \|\bar{\mathbf{P}}_{\mathcal{S}} \boldsymbol{\mu}_0\| + \|\bar{\mathbf{P}}_{\mathcal{S}} \tilde{\mathbf{w}}\| < \infty. \quad (S54)$$

1380 Finally, combining the results from Eq. (S49) and Eq. (S54), recalling that $\kappa > 1$, we have that $\|\mathbf{r}_t\|$
 1381 is bounded for all $t > 0$. This completes the first part of the proof and shows that

$$\boldsymbol{\mu}_t = \hat{\mathbf{w}} \log t + \tilde{\mathbf{w}} + \mathbf{r}_t = \hat{\mathbf{w}} \log t + \mathcal{O}(1), \quad (S55)$$

1384 and in particular

$$\lim_{t \rightarrow \infty} \frac{\boldsymbol{\mu}_t}{\|\boldsymbol{\mu}_t\|} = \frac{\hat{\mathbf{w}}}{\|\hat{\mathbf{w}}\|}. \quad (S56)$$

1387 We proceed by showing that the limit covariance parameter vanishes in the span of the support
 1388 vectors.

1389 **Covariance parameter** We begin by substituting the definition of the residual \mathbf{r}_t (S31) into the
 1390 gradient flow dynamics for the covariance factor \mathbf{S}_t :

$$\begin{aligned} 1392 & \dot{\mathbf{S}}_t = -\nabla_{\mathbf{S}} \bar{\ell}(\boldsymbol{\mu}_t, \mathbf{S}_t) \\ 1393 & = - \sum_{n=1}^N \exp(-\boldsymbol{\mu}_t^\top \mathbf{x}_n + \frac{1}{2} \mathbf{x}_n^\top \mathbf{S}_t \mathbf{S}_t^\top \mathbf{x}_n) \mathbf{x}_n \mathbf{x}_n^\top \mathbf{S}_t. \end{aligned} \quad (S57)$$

1396 Next, we split the sum into contributions from support vectors and non-support vectors. For $n \in \mathcal{S}$,
 1397 we use the property $\mathbf{x}_n^\top \hat{\mathbf{w}} = 1$; for $n \notin \mathcal{S}$, the margin is strictly larger than one, which introduces
 1398 higher-order decay in t :

$$\begin{aligned} 1400 & \dot{\mathbf{S}}_t = - \sum_{n \in \mathcal{S}} \frac{1}{t} \exp(-\tilde{\mathbf{w}}^\top \mathbf{x}_n - \mathbf{r}_t^\top \mathbf{x}_n) \exp(\frac{1}{2} \mathbf{x}_n^\top \mathbf{S}_t \mathbf{S}_t^\top \mathbf{x}_n) \mathbf{x}_n \mathbf{x}_n^\top \mathbf{S}_t \\ 1401 & - \sum_{n \notin \mathcal{S}} \left(\frac{1}{t} \right)^{\mathbf{x}_n^\top \hat{\mathbf{w}}} \exp(-\tilde{\mathbf{w}}^\top \mathbf{x}_n - \mathbf{r}_t^\top \mathbf{x}_n) \exp(\frac{1}{2} \mathbf{x}_n^\top \mathbf{S}_t \mathbf{S}_t^\top \mathbf{x}_n) \mathbf{x}_n \mathbf{x}_n^\top \mathbf{S}_t. \end{aligned} \quad (S58)$$

1404 Since r_t is bounded (from the previous part of the proof), the exponential prefactor is uniformly
 1405 bounded away from zero. We formalize this by defining
 1406

$$1407 \quad C := \min_{n \in [N]} \min_{t \geq 0} \exp(-\tilde{w}^\top x_n - r_t^\top x_n) > 0. \quad (S59)$$

1409 We also let σ_{\min} denote the smallest non-zero eigenvalue of the matrix $\sum_{n \in \mathcal{S}} x_n x_n^\top$. Finally, to
 1410 measure the size of S_t restricted to the support-vector subspace, we define
 1411

$$1412 \quad \Delta_t := \text{tr}(P_S S_t S_t^\top P_S).$$

1413 We now compute the derivative of Δ_t over time. Differentiating and substituting the dynamics of
 1414 S_t yields
 1415

$$1416 \quad \begin{aligned} \frac{1}{2} \frac{d}{dt} \Delta_t &= \text{tr}(P_S \dot{S}_t S_t^\top P_S) \\ 1417 &= -\frac{1}{t} \sum_{n \in \mathcal{S}} \exp(-\tilde{w}^\top x_n - r_t^\top x_n) \exp\left(\frac{1}{2} x_n^\top S_t S_t^\top x_n\right) \text{tr}(P_S x_n x_n^\top S_t S_t^\top P_S) \\ 1418 &\quad + \mathcal{O}\left(\frac{1}{t^\kappa}\right). \end{aligned} \quad (S60)$$

1421 At this point we use two facts: 1. from (S59), the exponential prefactor is bounded below by $C > 0$,
 1422 2. from the definition of σ_{\min} , we can control the quadratic form $\sum_{n \in \mathcal{S}} x_n x_n^\top$. Applying both gives
 1423

$$1424 \quad \frac{1}{2} \frac{d}{dt} \Delta_t \leq -\frac{C \sigma_{\min}}{t} \Delta_t + \mathcal{O}\left(\frac{1}{t^\kappa}\right). \quad (S61)$$

1426 Finally, by Grönwall's lemma, there exists a constant $K > 0$ and a starting time $t_0 > 0$ such that
 1427

$$1428 \quad \Delta_t \leq \Delta_{t_0} \left(\frac{t}{t_0}\right)^{-2C\sigma_{\min}} + \frac{K}{2C\sigma_{\min} + \kappa - 1} t^{-(\kappa-1)}, \quad \forall t \geq t_0. \quad (S62)$$

1430 Since both $|\mathcal{S}|C\sigma_{\min} > 0$ and $\kappa > 1$, we conclude that $\Delta_t \rightarrow 0$ as $t \rightarrow \infty$. In words: the covariance
 1431 factor vanishes when projected onto the span of the support vectors, i.e.
 1432

$$1433 \quad \forall n \in \mathcal{S} : \lim_{t \rightarrow \infty} x_n^\top S_t S_t^\top x_n = 0, \quad (S63)$$

1434 as claimed. □
 1435

1436 1437 S1.2.3 COMPLETE PROOF OF THEOREM 2

1438 We will now extend the results for the gradient flow to gradient descent and then use these results to
 1439 characterize the implicit bias of gradient descent as generalized variational inference.
 1440

1441 Throughout this proof, let
 1442

$$1443 \quad \mathbf{A}_t = \sum_{n=1}^N \exp\left(-\boldsymbol{\mu}_t^\top x_n + \frac{1}{2} x_n^\top S_t S_t^\top x_n\right) x_n x_n^\top \quad (S64)$$

1445 be a positive definite matrix at iteration t . We begin the section with a few lemmata which will be
 1446 used throughout the proof.
 1447

Lemma S2

1448 Suppose that we start gradient descent from $(\boldsymbol{\mu}_0, \mathbf{S}_0)$. If $\eta < \lambda_{\max}(\mathbf{A}_0)^{-1}$, then for the gradient
 1449 descent iterates

$$1450 \quad \mathbf{S}_{t+1} = \mathbf{S}_t - \eta \nabla_{\mathbf{S}} \bar{\ell}(\boldsymbol{\mu}_t, \mathbf{S}_t), \quad (S65)$$

1451 we have that $\|\mathbf{S}_t\|_F \leq \|\mathbf{S}_0\|_F$ for all $t \geq 0$.
 1452

1453 *Proof.* First, note that the gradient descent update for the covariance factor is given by
 1454

$$1455 \quad \mathbf{S}_{t+1} = \mathbf{S}_t (\mathbf{I} - \eta \mathbf{A}_t), \quad (S66)$$

1456 and hence we have that
 1457

$$1458 \quad \|\mathbf{S}_{t+1}\|_F = \|\mathbf{S}_t (\mathbf{I} - \eta \mathbf{A}_t)\|_F \leq \|\mathbf{S}_t\|_F \|\mathbf{I} - \eta \mathbf{A}_t\|_2. \quad (S67)$$

1458 Now, since $\eta \leq \lambda_{\max}(\mathbf{A}_0)^{-1} \leq \lambda_{\max}(\mathbf{A}_t)^{-1}$ for all $t \geq 0$ and noting that $\mathbf{A}_t \succeq 0$, we have that

$$1459 \quad \|(I - \eta \mathbf{A}_t)\|_2 \leq 1, \quad (S68)$$

1460 and therefore

$$1462 \quad \|\mathbf{S}_{t+1}\|_F \leq \|\mathbf{S}_t\|_F. \quad (S69)$$

1463 Finally, we can conclude that $\|\mathbf{S}_t\|_F \leq \|\mathbf{S}_0\|_F$ for all $t \geq 0$, as required. \square

1466 Lemma S3

1467 Suppose that we start gradient descent from $(\boldsymbol{\mu}_0, \mathbf{S}_0)$. If $\eta < \lambda_{\max}(\mathbf{A}_0)^{-1}$, then for the gradient
1468 descent iterates

$$1469 \quad \boldsymbol{\mu}_{t+1} = \boldsymbol{\mu}_t - \eta \nabla_{\boldsymbol{\mu}} \bar{\ell}(\boldsymbol{\mu}_t, \mathbf{S}_t), \quad (S70)$$

1471 we have that $\sum_{u=0}^{\infty} \|\nabla_{\boldsymbol{\mu}} \bar{\ell}(\boldsymbol{\mu}_u, \mathbf{S}_u)\|^2 < \infty$. Consequently, we also have that
1472 $\lim_{t \rightarrow \infty} \|\nabla_{\boldsymbol{\mu}} \bar{\ell}(\boldsymbol{\mu}_t, \mathbf{S}_t)\|^2 = 0$.
1473

1474 *Proof.* Note that our loss function is not globally smooth in $\boldsymbol{\mu}$. However, if we initialize at $(\boldsymbol{\mu}_0, \mathbf{S}_0)$,
1475 the gradient descent iterates with $\eta < \lambda_{\max}(\mathbf{A}_0)^{-1}$ maintain bounded local smoothness. The state-
1476 ment now follows directly from Lemma 10 in Soudry et al. [4]. \square

1477 Lemma S4

1478 By choosing ϵ_1 as in Eq. (S51), if $\|\mathbf{P}_{\mathcal{S}} \mathbf{r}_t\| \geq \epsilon_1$, we have that

$$1479 \quad (\mathbf{r}_{t+1} - \mathbf{r}_t)^T \mathbf{r}_t \leq \mathcal{O}\left(\frac{1}{t^{\kappa}}\right) + \mathcal{O}\left(\frac{1}{t^2}\right) \|\mathbf{r}_t\|. \quad (S71)$$

1482 If $\|\mathbf{P}_{\mathcal{S}} \mathbf{r}_t\| < \epsilon_1$, there exists a constant C such that

$$1484 \quad (\mathbf{r}_{t+1} - \mathbf{r}_t)^T \mathbf{r}_t \leq C. \quad (S72)$$

1486 *Proof.* We follow similar steps as in the gradient flow case. It holds that

$$\begin{aligned} 1487 \quad & (\mathbf{r}_{t+1} - \mathbf{r}_t)^T \mathbf{r}_t \\ 1488 \quad &= (-\eta \nabla_{\boldsymbol{\mu}}(\boldsymbol{\mu}_t, \mathbf{S}_t) - \hat{\mathbf{w}}(\log(t+1) - \log(t)))^T \mathbf{r}_t \\ 1489 \quad &= \eta \sum_{n=1}^N \exp\left(-\boldsymbol{\mu}_t^T \mathbf{x}_n + \frac{1}{2} \mathbf{x}_n^T \mathbf{S}_t \mathbf{S}_t^T \mathbf{x}_n\right) \mathbf{x}_n^T \mathbf{r}_t - \hat{\mathbf{w}}^T \mathbf{r}_t \log(1+t^{-1}) \\ 1490 \quad &= \hat{\mathbf{w}}^T \mathbf{r}_t (t^{-1} - \log(1+t^{-1})) + \eta \sum_{n \notin \mathcal{S}} \exp\left(-\boldsymbol{\mu}_t^T \mathbf{x}_n + \frac{1}{2} \mathbf{x}_n^T \mathbf{S}_t \mathbf{S}_t^T \mathbf{x}_n\right) \mathbf{x}_n^T \mathbf{r}_t \\ 1491 \quad &+ \eta \sum_{n \in \mathcal{S}} \left[-\frac{1}{t} \exp(-\hat{\mathbf{w}}^T \mathbf{x}_n) + \exp\left(-\boldsymbol{\mu}_t^T \mathbf{x}_n + \frac{1}{2} \mathbf{x}_n^T \mathbf{S}_t \mathbf{S}_t^T \mathbf{x}_n\right) \right] \mathbf{x}_n^T \mathbf{r}_t, \end{aligned} \quad (S73)$$

1498 where in the last equality we used Equation (S33) to expand $\hat{\mathbf{w}}^T \mathbf{r}_t$. Furthermore, we can bound all
1499 four terms as follows, beginning with the first term:
1500

$$1501 \quad \hat{\mathbf{w}}^T \mathbf{r}_t (t^{-1} - \log(1+t^{-1})) \leq \|\mathbf{r}_t\| \mathcal{O}\left(\frac{1}{t^2}\right), \quad (S74)$$

1504 where we used that $\log(1+t^{-1}) = t^{-1} + \mathcal{O}(t^{-2})$. For the second term, using the same argument
1505 as in Equation (S49), we derive that

$$1506 \quad \eta \sum_{n \notin \mathcal{S}} \exp\left(-\boldsymbol{\mu}_t^T \mathbf{x}_n + \frac{1}{2} \mathbf{x}_n^T \mathbf{S}_t \mathbf{S}_t^T \mathbf{x}_n\right) \mathbf{x}_n^T \mathbf{r}_t \leq \mathcal{O}\left(\frac{1}{t^{\kappa}}\right). \quad (S75)$$

1509 For the third item, from Eq. (S48) and Eq. (S50), we have that $\|\mathbf{P}_{\mathcal{S}} \mathbf{r}_t\| \geq \epsilon_1$ implies that

$$1511 \quad \eta \sum_{n \in \mathcal{S}} \left[-\frac{1}{t} \exp(-\hat{\mathbf{w}}^T \mathbf{x}_n) + \exp\left(-\boldsymbol{\mu}_t^T \mathbf{x}_n + \frac{1}{2} \mathbf{x}_n^T \mathbf{S}_t \mathbf{S}_t^T \mathbf{x}_n\right) \right] \mathbf{x}_n^T \mathbf{r}_t \leq 0. \quad (S76)$$

1512 The first result follows from combining the above three inequalities.
 1513

1514 Next, if $\|P_S \mathbf{r}_t\| < \epsilon_1$, by defining $B := \|S_0\|_F^2$, following the steps in Eq. (S44), we have that
 1515

$$1516 \eta \sum_{n \notin \mathcal{S}} \exp \left(-\boldsymbol{\mu}_t^\top \mathbf{x}_n + \frac{1}{2} \mathbf{x}_n^\top \mathbf{S}_t \mathbf{S}_t^\top \mathbf{x}_n \right) \mathbf{x}_n^\top \mathbf{r}_t \leq \eta |\mathcal{S}| \left(\exp \left(\frac{B}{2} \right) - 1 \right) \frac{B}{2}, \quad (S77)$$

1518 and hence, combining this with Assumption 2 which implies that \mathbf{r}_t is bounded as in Eq. (S54), one
 1519 can find a constant C such that
 1520

$$(\mathbf{r}_{t+1} - \mathbf{r}_t)^\top \mathbf{r}_t \leq C. \quad (S78)$$

□

1523 Proof of Theorem 2

1525 *Proof.* As in the simple version of the proof, we begin by considering the convergence behavior of
 1526 the mean parameter $\boldsymbol{\mu}_t$.
 1527

1528 **Mean parameter** Our goal is again to show that $\|\mathbf{r}_t\|$ is bounded. To that end, we will provide an
 1529 upper bound to the following equation
 1530

$$\|\mathbf{r}_{t+1}\|^2 = \|\mathbf{r}_{t+1} - \mathbf{r}_t\|^2 + 2(\mathbf{r}_{t+1} - \mathbf{r}_t)^\top \mathbf{r}_t + \|\mathbf{r}_t\|^2 \quad (S79)$$

1532 First, consider the first term in the above equation:
 1533

$$\begin{aligned} 1534 \|\mathbf{r}_{t+1} - \mathbf{r}_t\|^2 \\ 1535 &= \|\boldsymbol{\mu}_{t+1} - \hat{\mathbf{w}} \log(t+1) - \tilde{\mathbf{w}} - \boldsymbol{\mu}_t + \hat{\mathbf{w}} \log(t) + \tilde{\mathbf{w}}\|^2 \\ 1536 &= \|\boldsymbol{\mu}_{t+1} - \hat{\mathbf{w}} \log(t+1) - \tilde{\mathbf{w}}\|^2 \\ 1537 &\leq 2 \left[\eta^2 \|\nabla_{\boldsymbol{\mu}} \bar{\ell}(\boldsymbol{\mu}_t, \mathbf{S}_t)\|^2 + \|\hat{\mathbf{w}}\|^2 \log^2(1+t^{-1}) \right] \\ 1538 &\leq 2 \left[\eta^2 \|\nabla_{\boldsymbol{\mu}} \bar{\ell}(\boldsymbol{\mu}_t, \mathbf{S}_t)\|^2 + \|\hat{\mathbf{w}}\|^2 t^{-2} \right] \\ 1539 \\ 1540 \\ 1541 \end{aligned} \quad (S80)$$

1542 where in the first inequality we used the standard inequality that $(x+y)^2 \leq 2(x^2 + y^2)$, and in the
 1543 second inequality we used the fact that $\log(1+x) \leq x$ for $x \geq 0$. Now, from Lemma S3 and the
 1544 fact that t^{-2} is summable, we conclude that there exists $C_1 < \infty$ such that

$$\sum_{t=1}^{\infty} \|\mathbf{r}_{t+1} - \mathbf{r}_t\|^2 \leq C_1 < \infty. \quad (S81)$$

1548 Next, for the second term, recall that in Lemma S4 we showed that if $\|P_S \mathbf{r}_t\| \geq \epsilon_1$, then, for some
 1549 constants $C_2, C_3 < \infty$, we have that, eventually
 1550

$$(\mathbf{r}_{t+1} - \mathbf{r}_t)^\top \mathbf{r}_t \leq C_2 \frac{1}{t^\kappa} + C_3 \frac{1}{t^2} \|\mathbf{r}_t\|, \quad (S82)$$

1553 and that if $\|P_S \mathbf{r}_t\| < \epsilon_1$, then there exists a constant $C_4 < \infty$ such that
 1554

$$(\mathbf{r}_{t+1} - \mathbf{r}_t)^\top \mathbf{r}_t \leq C_4. \quad (S83)$$

1556 We will show that when $\|P_S \mathbf{r}_t\| < \epsilon_1$, the residual \mathbf{r}_t is contained in a compact set, and when
 1557 $\|P_S \mathbf{r}_t\| \geq \epsilon_1$, the residual \mathbf{r}_t can't escape to infinity. We now formally show this claim.
 1558

1559 Let S_1 be the first time such that $\|P_S \mathbf{r}_t\| \geq \epsilon_1$, if such a time does not exist, we are done since the
 1560 support vectors span the data and hence $\|\mathbf{r}_t\|$ is bounded. Now, let T_1 be the first time after S_1 such
 1561 that $\|P_S \mathbf{r}_t\| < \epsilon_1$, where we allow $T_1 = \infty$ if such a time does not exist. Continuing in this manner,
 1562 we define the sequences $S_1 < T_1 < S_2 < T_2 < \dots$, where we allow $T_i = \infty$ for some i .
 1563

1564 We proceed by showing that $\|\mathbf{r}_t\|$ is uniformly bounded on each of the intervals $[S_i, T_i)$. To that
 1565 end, note that for $t \in [S_i, T_i)$, we have that

$$\|\mathbf{r}_{t+1}\|^2 - \|\mathbf{r}_t\|^2 \leq 2C_2 \frac{1}{t^\kappa} + 2C_3 \frac{1}{t^2} \|\mathbf{r}_t\| + \|\mathbf{r}_{t+1} - \mathbf{r}_t\|^2, \quad (S84)$$

1566 and hence, using the fact that $\kappa > 1$, by the discrete version of Grönwall's lemma, that
 1567

$$1568 \quad \max_{t \in [S_i, T_i]} (\|r_t\|^2 - \|r_{S_i}\|^2) \leq K, \quad (S85)$$

1570 for some constant $K < \infty$ independent of i . Furthermore, we also know from Eq. (S83) that
 1571

$$1572 \quad \|r_{S_i}\| \leq \epsilon_1 + 2C_4 + \|r_{S_i} - r_{S_i-1}\|^2 \leq \epsilon_1 + 2C_4 + \max_{t \geq 0} \|r_{t+1} - r_t\|^2 < \infty, \quad (S86)$$

1574 showing that the first jump outside the ϵ_1 -ball is bounded. Combining the two results, we conclude
 1575 that $\|r_t\|$ is uniformly bounded on each of the intervals $[S_i, T_i]$.
 1576

1577 Finally, by noting that the support vectors span the data, we have that $\|r_t\|$ is uniformly bounded
 1578 on each of the intervals $[T_i, S_{i+1}]$. Combining the two results, we conclude that $\|r_t\|$ is uniformly
 1579 bounded for all $t \geq 0$ and hence we have that
 1580

$$1581 \quad \lim_{t \rightarrow \infty} \frac{\mu_t}{\|\mu_t\|} = \frac{\hat{w}}{\|\hat{w}\|} \quad (S87)$$

1582 and the following lemma.
 1583

Lemma S5

1584 For the mean parameter μ_t , we have that
 1585

$$1586 \quad \mu_t = \log(t)\hat{w} + \mathcal{O}(1). \quad (S88)$$

1588 *Proof.* This follows immediately from the definition of the residual in Equation (S31):
 1589

$$1590 \quad \mu_t = \hat{w} \log t + r_t + \tilde{w}_t,$$

1592 and the fact that r_t and \tilde{w}_t are bounded as we showed above. \square
 1593

1594 We continue with the analysis of the covariance parameter over optimization iterations.
 1595

1597 **Covariance parameter** As before, let $\Delta_t = \text{tr}(\mathbf{P}_S \mathbf{S}_t \mathbf{S}_t^\top \mathbf{P}_S)$ be the trace of the projection of the
 1598 covariance parameter on the space of support vectors in \mathcal{S} . By following the ideas from the gradient
 1599 flow case, we have the following dynamics:
 1600

$$1601 \quad \begin{aligned} \Delta_{t+1} &= \text{tr}(\mathbf{P}_S (\mathbf{I} - \eta \mathbf{A}_t) \mathbf{S}_t \mathbf{S}_t^\top (\mathbf{I} - \eta \mathbf{A}_t)^\top \mathbf{P}_S) \\ 1602 &= \text{tr}(\mathbf{P}_S \mathbf{S}_t \mathbf{S}_t^\top \mathbf{P}_S) - 2\eta \text{tr}(\mathbf{P}_S \mathbf{S}_t \mathbf{S}_t^\top \mathbf{A}_t \mathbf{P}_S) + \eta^2 \text{tr}(\mathbf{P}_S \mathbf{A}_t \mathbf{S}_t \mathbf{S}_t^\top \mathbf{A}_t \mathbf{P}_S) \\ 1603 &\leq \Delta_t - \frac{2\eta}{t} C \sigma_{\min} \text{tr}(\mathbf{P}_S \mathbf{S}_t \mathbf{S}_t^\top \mathbf{P}_S) + \mathcal{O}\left(\frac{1}{t^\kappa}\right) + \mathcal{O}\left(\frac{1}{t^2}\right) \\ 1604 &= \Delta_t - \frac{2\eta}{t} C \sigma_{\min} \Delta_t + \mathcal{O}\left(\frac{1}{t^\kappa}\right) + \mathcal{O}\left(\frac{1}{t^2}\right), \end{aligned} \quad (S89)$$

1608 where we used the same arguments as in Equation (S60) to derive the last inequality, in addition to
 1609 noting that $\lambda_{\max}(\mathbf{A}_t^2) \leq \mathcal{O}\left(\frac{1}{t^2}\right)$ in order to bound the last term. Hence, we can write
 1610

$$1611 \quad \Delta_{t+1} - \Delta_t \leq -\frac{2\eta}{t} C \sigma_{\min} \Delta_t + \mathcal{O}\left(\frac{1}{t^\kappa}\right) + \mathcal{O}\left(\frac{1}{t^2}\right). \quad (S90)$$

1614 Again, by the discrete version of Grönwall's lemma, we derive the equivalent result to Eq. (S62).
 1615 Now, noting that $\sum_t \frac{1}{t}$ diverges, the fact that $\kappa > 1$ and $\eta C \sigma_{\min} > 0$, we conclude that Δ_t converges
 1616 to zero. This implies that the covariance parameter converges to zero in the span of the support
 1617 vectors, i.e.
 1618

$$1619 \quad \forall n \in \mathcal{S} : \lim_{t \rightarrow \infty} \mathbf{x}_n^\top \mathbf{S}_t \mathbf{S}_t^\top \mathbf{x}_n = 0, \quad (S91)$$

as desired.

1620 **Characterization as Generalized Variational Inference** As a final step we need to show that
 1621 the solution identified by gradient descent if appropriately transformed identifies the minimum 2-
 1622 Wasserstein solution in the feasible set. Define the feasible set
 1623

$$\Theta_* = \{(\mu, S) \mid P_S \mu = \hat{w} \text{ and } \forall n \in \mathcal{S} : \text{Var}_{q_\theta}(f_w(x_n)) = 0\} \quad (\text{S92})$$

$$= \{(\mu, S) \mid P_S \mu = \hat{w} \text{ and } \forall n \in \mathcal{S} : x_n^\top S S^\top x_n = 0\} \quad (\text{S93})$$

1626 and the variational parameters identified by rescaled gradient descent as
 1627

$$\theta_*^{\text{rGD}} = \lim_{t \rightarrow \infty} \theta_t^{\text{rGD}} = \lim_{t \rightarrow \infty} \left(\frac{1}{\log(t)} \mu_t + P_{\text{null}(\mathbf{X})} \mu_0, S_t \right). \quad (\text{S94})$$

1630 It holds by Lemma S5 that
 1631

$$P_S \mu_*^{\text{rGD}} = P_S \left(\lim_{t \rightarrow \infty} \frac{1}{\log(t)} \mu_t \right) + \mathbf{0} = P_S \hat{w} = \hat{w} \quad (\text{S95})$$

1632 and additionally by Equation (S91) we have for all $n \in \mathcal{S}$ that
 1633

$$x_n^\top S_*^{\text{rGD}} (S_*^{\text{rGD}})^\top x_n = \lim_{t \rightarrow \infty} x_n^\top S_t (S_t)^\top x_n = 0. \quad (\text{S96})$$

1634 Therefore, the limit point θ_*^{rGD} of rescaled gradient descent is in the feasible set. It remains to show
 1635 that it is also a minimizer of the 2-Wasserstein distance to the prior / initialization. We will first
 1636 show a more general result that does not require Assumption 2.

1637 To that end define $(V_S \ V_{X \perp S} \ V_{\text{null}(\mathbf{X})}) \in \mathbb{R}^{P \times P}$ where $V_S \in \mathbb{R}^{P \times P_S}$ is an orthonormal basis
 1638 of the span of the support vectors $\text{range}(\mathbf{X}_S^\top)$, $V_{X \perp S} \in \mathbb{R}^{P \times (N-P_S)}$ an orthonormal basis of its
 1639 orthogonal complement in $\text{range}(\mathbf{X}^\top)$ and $V_{\text{null}(\mathbf{X})} \in \mathbb{R}^{P \times (P-N)}$ the corresponding orthonormal
 1640 basis of the null space $\text{null}(\mathbf{X})$ of the data. Let $V = (V_S \ V_{\text{null}(\mathbf{X})}) \in \mathbb{R}^{P \times (P-N+P_S)}$ and define
 1641 the projected variational distribution and prior onto the span of the support vectors and the null space
 1642 of the data as
 1643

$$q_\theta^{\text{proj}}(\tilde{w}) = \mathcal{N}(\tilde{w}; P_V \mu, P_V \Sigma P_V^\top) = \mathcal{N}(\tilde{w}; \tilde{\mu}, \tilde{\Sigma}) \quad (\text{S97})$$

$$p^{\text{proj}}(\tilde{w}) = \mathcal{N}(\tilde{w}; P_V \mu_0, P_V \Sigma_0 P_V^\top) = \mathcal{N}(\tilde{w}; \tilde{\mu}_0, \tilde{\Sigma}_0) \quad (\text{S98})$$

1644 where $\tilde{w} \in \mathbb{R}^{P-N+P_S}$. Now earlier we showed that the limit point of rescaled gradient descent is
 1645 in the feasible set, defined in Equation (S94), and thus the same holds for the projected limit point
 1646 of rescaled gradient descent, i.e.
 1647

$$(\tilde{\mu}_*^{\text{rGD}}, \tilde{S}_*^{\text{rGD}}) \in \Theta_* \quad (\text{S99})$$

1648 in particular
 1649

$$P_S \tilde{\mu}_*^{\text{rGD}} = P_S \mu_*^{\text{rGD}} = \hat{w}, \quad (\text{S100})$$

$$\forall n \in \mathcal{S} : x_n^\top \tilde{S}_*^{\text{rGD}} (\tilde{S}_*^{\text{rGD}})^\top x_n = x_n^\top S_*^{\text{rGD}} (S_*^{\text{rGD}})^\top x_n = 0. \quad (\text{S101})$$

1650 Therefore, we have for all $n \in \mathcal{S}$ that
 1651

$$0 = x_n^\top \tilde{S}_*^{\text{rGD}} (\tilde{S}_*^{\text{rGD}})^\top x_n = \|(\tilde{S}_*^{\text{rGD}})^\top x_n\|_2^2 \iff (\tilde{S}_*^{\text{rGD}})^\top x_n = \mathbf{0} \quad (\text{S102})$$

$$\iff (\tilde{S}_*^{\text{rGD}})^\top V_S = \mathbf{0} \quad (\text{S103})$$

1652 and thus $V_S^\top \tilde{S}_*^{\text{rGD}} (\tilde{S}_*^{\text{rGD}})^\top V_S = \mathbf{0}$. Therefore by Lemma S1 it holds for the squared 2-Wasserstein
 1653 distance between the projected limit point of rescaled gradient descent and the projected prior that
 1654

$$\begin{aligned} \text{W}_2^2(q_{\theta_*}^{\text{proj}}, p^{\text{proj}}) &\stackrel{+c}{=} \|V_S^\top \tilde{\mu} - V_S^\top \tilde{\mu}_0\|_2^2 + \text{W}_2^2(\mathcal{N}(V_{\text{null}}^\top \tilde{\mu}, V_{\text{null}}^\top \tilde{\Sigma} V_{\text{null}}), \mathcal{N}(V_{\text{null}}^\top \tilde{\mu}_0, V_{\text{null}}^\top \tilde{\Sigma}_0 V_{\text{null}})) \\ &= \left\| \begin{pmatrix} V_S^\top \tilde{\mu} - V_S^\top \tilde{\mu}_0 \\ \mathbf{0} \end{pmatrix} \right\|_2^2 + \text{W}_2^2(\mathcal{N}(V_{\text{null}}^\top \tilde{\mu}, V_{\text{null}}^\top \tilde{\Sigma} V_{\text{null}}), \mathcal{N}(V_{\text{null}}^\top \tilde{\mu}_0, V_{\text{null}}^\top \tilde{\Sigma}_0 V_{\text{null}})) \\ &= \left\| V \begin{pmatrix} V_S^\top \tilde{\mu} - V_S^\top \tilde{\mu}_0 \\ \mathbf{0} \end{pmatrix} \right\|_2^2 + \text{W}_2^2(\mathcal{N}(V_{\text{null}}^\top \tilde{\mu}, V_{\text{null}}^\top \tilde{\Sigma} V_{\text{null}}), \mathcal{N}(V_{\text{null}}^\top \tilde{\mu}_0, V_{\text{null}}^\top \tilde{\Sigma}_0 V_{\text{null}})) \end{aligned}$$

$$\begin{aligned}
&= \|\mathbf{P}_S \tilde{\boldsymbol{\mu}} - \mathbf{P}_S \tilde{\boldsymbol{\mu}}_0\|_2^2 + W_2^2\left(\mathcal{N}\left(\mathbf{V}_{\text{null}}^T \tilde{\boldsymbol{\mu}}, \mathbf{V}_{\text{null}}^T \tilde{\boldsymbol{\Sigma}} \mathbf{V}_{\text{null}}\right), \mathcal{N}\left(\mathbf{V}_{\text{null}}^T \tilde{\boldsymbol{\mu}}_0, \mathbf{V}_{\text{null}}^T \tilde{\boldsymbol{\Sigma}}_0 \mathbf{V}_{\text{null}}\right)\right) \\
&= \|\hat{\mathbf{w}} - \mathbf{P}_S \tilde{\boldsymbol{\mu}}_0\|_2^2 + W_2^2\left(\mathcal{N}\left(\mathbf{V}_{\text{null}}^T \tilde{\boldsymbol{\mu}}, \mathbf{V}_{\text{null}}^T \tilde{\boldsymbol{\Sigma}} \mathbf{V}_{\text{null}}\right), \mathcal{N}\left(\mathbf{V}_{\text{null}}^T \tilde{\boldsymbol{\mu}}_0, \mathbf{V}_{\text{null}}^T \tilde{\boldsymbol{\Sigma}}_0 \mathbf{V}_{\text{null}}\right)\right) \\
&\stackrel{+c}{=} W_2^2\left(\mathcal{N}\left(\mathbf{V}_{\text{null}}^T \tilde{\boldsymbol{\mu}}, \mathbf{V}_{\text{null}}^T \tilde{\boldsymbol{\Sigma}} \mathbf{V}_{\text{null}}\right), \mathcal{N}\left(\mathbf{V}_{\text{null}}^T \tilde{\boldsymbol{\mu}}_0, \mathbf{V}_{\text{null}}^T \tilde{\boldsymbol{\Sigma}}_0 \mathbf{V}_{\text{null}}\right)\right)
\end{aligned}$$

where we used that $\mathbf{P}_S \tilde{\boldsymbol{\mu}} = \hat{\mathbf{w}}$ for any $(\tilde{\boldsymbol{\mu}}, \tilde{\boldsymbol{\Sigma}})$ in the feasible set Θ_* . Therefore it suffices to show that the projected solution $\tilde{\boldsymbol{\theta}}_*^{\text{GD}}$ minimizes

$$W_2^2\left(\mathcal{N}\left(\mathbf{V}_{\text{null}}^T \tilde{\boldsymbol{\mu}}, \mathbf{V}_{\text{null}}^T \tilde{\boldsymbol{\Sigma}} \mathbf{V}_{\text{null}}\right), \mathcal{N}\left(\mathbf{V}_{\text{null}}^T \tilde{\boldsymbol{\mu}}_0, \mathbf{V}_{\text{null}}^T \tilde{\boldsymbol{\Sigma}}_0 \mathbf{V}_{\text{null}}\right)\right) \geq 0. \quad (\text{S104})$$

We have using the definition of the iterates in Equation (9) that

$$\mathbf{V}_{\text{null}}^T \tilde{\boldsymbol{\mu}}_*^{\text{GD}} = \mathbf{V}_{\text{null}}^T \mathbf{P}_V \left(\lim_{t \rightarrow \infty} \frac{1}{\log(t)} \boldsymbol{\mu}_t + \mathbf{P}_{\text{null}(\mathbf{X})} \boldsymbol{\mu}_0 \right) \quad (\text{S105})$$

$$= \mathbf{V}_{\text{null}}^T (\hat{\mathbf{w}} + \mathbf{P}_{\text{null}(\mathbf{X})} \boldsymbol{\mu}_0) = \mathbf{V}_{\text{null}}^T \boldsymbol{\mu}_0 \quad (\text{S106})$$

where we used $\hat{\mathbf{w}} \in \text{range}(\mathbf{X}_S^T)$. Further, it holds for the gradient of the expected loss (S30) with respect to the covariance factor parameters that

$$\mathbf{V}_{\text{null}}^T \tilde{\boldsymbol{\Sigma}}_*^{\text{GD}} = \mathbf{V}_{\text{null}}^T \mathbf{P}_V \boldsymbol{S}_*^{\text{GD}} = \mathbf{V}_{\text{null}}^T \boldsymbol{S}_*^{\text{GD}} = \mathbf{V}_{\text{null}}^T \left(\mathbf{S}_0 - \underbrace{\sum_{t=1}^{\infty} \eta_t \nabla_{\boldsymbol{S}} \bar{\ell}(\boldsymbol{\mu}_t, \mathbf{S}_t)}_{\in \text{range}(\mathbf{X}^T)} \right) \quad (\text{S107})$$

$$= \mathbf{V}_{\text{null}}^T \mathbf{S}_0 = \mathbf{V}_{\text{null}}^T \mathbf{P}_V \mathbf{S}_0 = \mathbf{V}_{\text{null}}^T \tilde{\boldsymbol{\Sigma}}_0. \quad (\text{S108})$$

Therefore we have that

$$W_2^2\left(\mathcal{N}\left(\mathbf{V}_{\text{null}}^T \tilde{\boldsymbol{\mu}}_*^{\text{GD}}, \mathbf{V}_{\text{null}}^T \tilde{\boldsymbol{\Sigma}}_*^{\text{GD}} \mathbf{V}_{\text{null}}\right), \mathcal{N}\left(\mathbf{V}_{\text{null}}^T \tilde{\boldsymbol{\mu}}_0, \mathbf{V}_{\text{null}}^T \tilde{\boldsymbol{\Sigma}}_0 \mathbf{V}_{\text{null}}\right)\right) = 0 \quad (\text{S109})$$

and thus the projected variational parameters $\tilde{\boldsymbol{\theta}}_*^{\text{GD}}$ are both feasible (S99) and minimize the squared 2-Wasserstein distance to the projected initialization / prior (S104). This completes the proof for the generalized version of Theorem 2 without Assumption 2, which we state here for convenience.

Lemma S6

Given the assumptions of Theorem 2, except for Assumption 2 meaning the support vectors \mathbf{X}_S do not necessarily span the data, it holds for the limit point of rescaled gradient descent that

$$\boldsymbol{\theta}_*^{\text{GD}} \in \arg \min_{\substack{\boldsymbol{\theta} = (\boldsymbol{\mu}, \boldsymbol{S}) \\ \text{s.t. } \boldsymbol{\theta} \in \Theta_*}} W_2^2\left(q_{\boldsymbol{\theta}}^{\text{proj}}, p^{\text{proj}}\right). \quad (\text{S110})$$

If in addition Assumption 2 holds, i.e. the support vectors span the training data \mathbf{X} , such that

$$\text{span}(\{\mathbf{x}_n\}_{n \in [N]}) = \text{span}(\{\mathbf{x}_n\}_{n \in \mathcal{S}}), \quad (\text{S111})$$

then the orthogonal complement of the support vectors in $\text{range}(\mathbf{X}^T)$ has dimension $N - P_S = 0$ and thus the projection $\mathbf{P}_V = \mathbf{I}_{P_S \times P_S}$ is the identity and therefore

$$q_{\boldsymbol{\theta}}^{\text{proj}} = q_{\boldsymbol{\theta}} \quad \text{and} \quad p^{\text{proj}} = p. \quad (\text{S112})$$

This completes the proof of Theorem 2. □

S1.3 NLL OVERFITTING AND THE NEED FOR (TEMPERATURE) SCALING

In Theorem 2, we assume we rescale the mean parameters. This is because the exponential loss can be made arbitrarily small for a mean vector that is aligned with the L_2 max-margin vector simply by increasing its magnitude. In fact, the sequence of mean parameters identified by gradient descent diverges to infinity at a logarithmic rate $\boldsymbol{\mu}_t^{\text{GD}} \approx \log(t) \hat{\mathbf{w}}$ as we show⁴ in Lemma S5 and illustrate in Figure S2 (right panel).

⁴This has been observed previously in the deterministic case (see Theorem 3 of Soudry et al. [4]) and thus naturally also appears in our probabilistic extension.

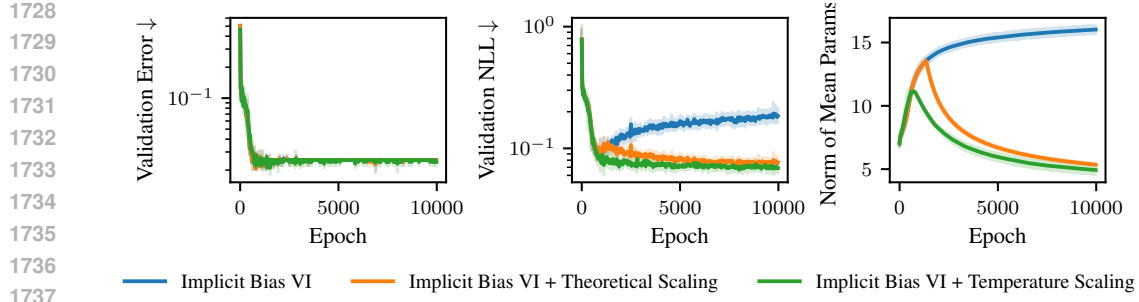


Figure S2: *NLL overfitting in classification due to implicit bias of the mean parameters.* As shown here for a two-hidden layer neural network on synthetic data, when training with vanilla SGD the mean parameters diverge to infinity $\|\mu_t\|_2 \approx \mathcal{O}(\log(t))$ (right) and thus the classifier will eventually overfit in terms of negative log-likelihood (left and middle). Rescaling the GD iterates as in Theorem 2 or using temperature scaling [69] avoids overfitting.

This bias of the mean parameters towards the max-margin solution does not impact the train loss or validation error, but leads to overfitting in terms of validation NLL (see Figure S2) as long as there is at least one misclassified datapoint \mathbf{x} , since then the (average) validation NLL is given by

$$\begin{aligned} \bar{\ell}(\boldsymbol{\theta}_t^{\text{GD}}) &= \mathbb{E}_{q_{\boldsymbol{\theta}_t^{\text{GD}}}(\mathbf{w})}(\exp(-\mathbf{y}\mathbf{x}^T\mathbf{w})) = \exp(\mathbf{x}^T\boldsymbol{\mu}_t^{\text{GD}} + \frac{1}{2}\mathbf{x}^T\mathbf{S}_t^{\text{GD}}(\mathbf{S}_t^{\text{GD}})^T\mathbf{x}) \\ &\approx \exp(\log(t)\mathbf{x}^T\hat{\mathbf{w}} + \frac{1}{2}\mathbf{x}^T\mathbf{S}_t^{\text{GD}}(\mathbf{S}_t^{\text{GD}})^T\mathbf{x}) \rightarrow \infty \quad \text{as } t \rightarrow \infty. \end{aligned} \quad (\text{S113})$$

However, by rescaling the mean parameters as we do in Theorem 2, this can be prevented as Figure S2 (middle panel) illustrates for a two-hidden layer neural network on synthetic data. Such overfitting in terms of NLL has been studied extensively empirically with the perhaps most common remedy being Temperature Scaling (TS) [69]. As we show empirically in Figure S2, instead of using the theoretical rescaling, using temperature scaling performs very well, especially in the non-asymptotic regime, which is why we also adopt it for our experiments in Section 5.

The aforementioned divergence of the mean parameters to infinity also explains the need for the projection of the prior mean parameters in Equation (9), since any bias from the initialization vanishes in the limit of infinite training. At first glance the additional projection seems computationally prohibitive for anything but a zero mean prior, but close inspection of the implicit bias of the covariance parameters \mathbf{S} in Theorem 2 shows that at convergence

$$\forall n : \text{Var}_{q_{\boldsymbol{\theta}}}(f_{\mathbf{w}}(\mathbf{x}_n)) = \mathbf{x}_n^T \mathbf{S} \mathbf{S}^T \mathbf{x}_n = 0 \implies \text{range}(\mathbf{S}) \subset \text{null}(\mathbf{X}) \quad (\text{S114})$$

Meaning we can approximate a basis of the null space of the training data by computing a QR decomposition of the covariance factor in $\mathcal{O}(PR^2)$ once at the end of training. For $R = P$ the inclusion becomes an equality and the projection can be computed exactly.

S2 PARAMETRIZATION, FEATURE LEARNING AND HYPERPARAMETER TRANSFER

Notation For this section we need a more detailed neural network notation. Denote an L -hidden layer, width- D feedforward neural network by $f(\mathbf{x}) \in \mathbb{R}_{\text{out}}^D$, with inputs $\mathbf{x} \in \mathbb{R}^{D_{\text{in}}}$, weights $\mathbf{W}^{(l)}$, pre-activations $\mathbf{h}^{(l)}(\mathbf{x}) \in \mathbb{R}^{D^{(l)}}$, and post-activations (or ‘‘features’’) $\mathbf{g}^{(l)}(\mathbf{x}) \in \mathbb{R}^{D^{(l)}}$. That is, $\mathbf{h}^{(1)}(\mathbf{x}) = \mathbf{W}^{(1)}\mathbf{x}$ and, for $l \in 1, \dots, L-1$,

$$\mathbf{g}^{(l)}(\mathbf{x}) = \phi\left(\mathbf{h}^{(l)}(\mathbf{x})\right), \quad \mathbf{h}^{(l+1)}(\mathbf{x}) = \mathbf{W}^{(l+1)}\mathbf{g}^{(l)}(\mathbf{x}),$$

and the network output is given by $f(\mathbf{x}) = \mathbf{W}^{(L+1)}\mathbf{g}^{(L)}(\mathbf{x})$, where $\phi(\bullet)$ is an activation function.

For convenience, we may abuse notation and write $\mathbf{h}^{(0)}(\mathbf{x}) = \mathbf{x}$ and $\mathbf{h}^{(L+1)}(\mathbf{x}) = f(\mathbf{x})$. Throughout we use $\bullet^{(l)}$ to indicate the layer, subscript \bullet_t to indicate the training time (i.e., epoch), $\Delta\bullet_t = \bullet_t - \bullet_0$ to indicate the change since initialization, and $[\bullet]_i$, $[\bullet]_{ij}$ to indicate the component within a vector or matrix.

1782 S2.1 DEFINITIONS OF STABILITY AND FEATURE LEARNING
17831784 The following definitions extend those of Yang and Hu [43] to the variational setting.
17851786 **Definition S1** (*bc* scaling)
17871788 In layer l , the variational parameters are initialized as
1789

1790
$$[\boldsymbol{\mu}_0^{(l)}]_i \sim \mathcal{N}(0, D^{-2b^{(l)}}), \quad [\boldsymbol{S}_0^{(l)}]_{ij} \sim \mathcal{N}(0, D^{-2\tilde{b}^{(l)}})$$

1791 and the learning rates for the mean and covariance parameters, respectively, are set to
1792

1793
$$\eta^{(l)} = \eta D^{-c^{(l)}}, \tilde{\eta}^{(l)} = \eta D^{-\tilde{c}^{(l)}}.$$

1794 The hyperparameter η represents a global learning rate that can be tuned, as for example in the
1795 hyperparameter transfer experiment from Section 3.4.
17961797 For the next two definitions, let $m_r(X) = \mathbb{E}_z((X - \mathbb{E}_z(X))^r)$ denote the r th central moment
1798 moment of a random variable X with respect to z , which represents all reparameterization noise in
1799 the random variable X . All Landau notation in Section S2 refers to asymptotic behavior in width D
1800 in probability over reparameterization noise z . We say that a vector sequence $\{\boldsymbol{v}_D\}_{D=1}^\infty$, where each
1801 $\boldsymbol{v}_D \in \mathbb{R}^D$, is $\mathcal{O}(D^{-a})$ if the scalar sequence $\{\sqrt{\frac{1}{D} \|\boldsymbol{v}_D\|^2}\}_{D=1}^\infty = \{\text{RMSE}(\boldsymbol{v}_D)\}_{D=1}^\infty$ is $\mathcal{O}(D^{-a})$.
18021803 **Definition S2** (Stability of Moment r)
18041805 A neural network is *stable in moment r* , if all of the following hold for all \boldsymbol{x} and $l \in \{1, \dots, L\}$.
18061807 1. At initialization ($t = 0$):
18081809 (a) The pre- and post-activations are $\Theta(1)$:
1810

1811
$$m_r(\boldsymbol{h}_0^{(l)}(\boldsymbol{x})), m_r(\boldsymbol{g}_0^{(l)}(\boldsymbol{x})) = \Theta(1)$$

1812 (b) The function is $\mathcal{O}(1)$:
1813

1814
$$m_r(f_0(\boldsymbol{x})) = \mathcal{O}(1)$$

1815 2. At any point during training $t > 0$:
18161817 (a) The change from initialization in the pre- and post-activations are $\mathcal{O}(1)$:
1818

1819
$$\Delta m_r(\boldsymbol{h}_t^{(l)}(\boldsymbol{x})), \Delta m_r(\boldsymbol{g}_t^{(l)}(\boldsymbol{x})) = \mathcal{O}(1)$$

1820 (b) The function is $\mathcal{O}(1)$:
1821

1822
$$m_r(f_t(\boldsymbol{x})) = \mathcal{O}(1)$$

1823 **Definition S3** (Feature Learning of Moment r)
18241825 *Feature learning* occurs in moment r in layer l if, for any $t > 0$, the change from initialization is
1826 $\Omega(1)$:
1827

1828
$$\Delta m_r(\boldsymbol{g}_t^{(l)}(\boldsymbol{x})) = \Omega(1).$$

1829 As we will see later, Figure S5 and Figure S6 investigate feature learning for the first two moments.
18301831 S2.2 INITIALIZATION SCALING FOR A LINEAR NETWORK
18321833 In this section we illustrate how the initialization scaling $\{(b^{(l)}, \tilde{b}^{(l)})\}$ can be chosen for stability.
1834 For simplicity, we consider a linear feedforward network of width D evaluated on a single input
1835 $\boldsymbol{x} \in \mathbb{R}_{\text{in}}^D$. We assume a Gaussian variational family that factorizes across layers. This implies the
1836 hidden units evolve as $\boldsymbol{h}_t^{(l+1)} = \boldsymbol{W}_t^{(l+1)} \boldsymbol{h}_t^{(l)}$ and the weights are linked to the variational parameters
1837 by $\text{vec}(\boldsymbol{W}_t^{(l)}) = \boldsymbol{\mu}_t^{(l)} + \boldsymbol{S}_t^{(l)} \boldsymbol{z}$.
18381839 Therefore, the mean and variance of the i th component hidden units in layer $l \in \{1, \dots, L+1\}$,
1840 where $i \in \{1, \dots, D^{(l)}\}$, are given by
1841

1842
$$\mathbb{E}_z([\boldsymbol{h}_t^{(l)}]_i) = [\boldsymbol{\mu}_t^{(l)}]_i^\top \mathbb{E}_z(\boldsymbol{h}_t^{(l-1)})$$

$$\text{Var}_z\left(\left[\mathbf{h}_t^{(l)}\right]_i\right) = [\boldsymbol{\mu}_t^{(l)}]_I^\top \mathbf{C}_t^{(l-1)} [\boldsymbol{\mu}^{(l)}]_I + \text{tr}([\mathbf{S}_t^{(l)}]_{I,:}^\top \mathbf{A}_t^{(l-1)} [\mathbf{S}_t^{(l)}]_{I,:}),$$

where $I = \{iD^{(l-1)}, \dots, (i+1)D^{(l-1)}\}$ and the second moment of and covariance of layer- l hidden units are denoted by

$$\begin{aligned}\mathbf{A}_t^{(l)} &= \mathbb{E}_z\left(\mathbf{h}_t^{(l)} \mathbf{h}_t^{(l)\top}\right) \\ \mathbf{C}_t^{(l)} &= \mathbf{A}_t^{(l)} - \mathbb{E}_z\left(\mathbf{h}_t^{(l)}\right) \mathbb{E}_z\left(\mathbf{h}_t^{(l)}\right)^\top.\end{aligned}$$

Mean We start with the mean of the hidden units, which conveniently depends only on the mean variational parameters and the previous layer hidden units.

$$\begin{aligned}\mathbb{E}_z\left(\left[\mathbf{h}_0^{(l)}\right]_i\right) &= \sum_{j=1}^{D^{(l-1)}} [\boldsymbol{\mu}_0^{(l)}]_{I,j} \mathbb{E}_z\left(\left[\mathbf{h}_0^{(l-1)}\right]_j\right) \\ &= \mathcal{O}\left(\sqrt{D^{(l-1)}} \cdot D^{-b^{(l)}} \cdot 1\right) \\ &= \begin{cases} \mathcal{O}\left(D^{-b^{(1)}}\right) & l = 1 \\ \mathcal{O}\left(D^{-\left(b^{(l)} - \frac{1}{2}\right)}\right) & l \in \{2, \dots, L+1\} \end{cases}.\end{aligned}$$

Therefore, we require $b^{(1)} \geq 0$ and $b^{(l)} \geq \frac{1}{2}$ for $l \in \{2, \dots, L+1\}$.

Variance Next we examine the variance of hidden units. Consider the first term, which represents the contribution of the mean parameters.

$$\begin{aligned}[\boldsymbol{\mu}_0^{(l)}]_I^\top \mathbf{C}_0^{(l-1)} [\boldsymbol{\mu}^{(l)}]_I &= \sum_{j=1}^{D^{(l-1)}} [\boldsymbol{\mu}_0^{(l)}]_{I,j}^2 [\mathbf{C}_0^{(l-1)}]_{j,j} + \sum_{j \neq j'} [\boldsymbol{\mu}_0^{(l)}]_{I,j} [\mathbf{C}_0^{(l-1)}]_{j,j'} [\boldsymbol{\mu}_0^{(l)}]_{I,j'} \\ &= \mathcal{O}\left(D^{(l-1)} \cdot D^{-2b^{(l)}} \cdot 1\right) + \mathcal{O}\left(\sqrt{D^{(l-1)}(D^{(l-1)} - 1)} \cdot D^{-b^{(l)}} \cdot 1 \cdot D^{-b^{(l)}}\right) \\ &= \mathcal{O}\left(D^{(l-1)} \cdot D^{-2b^{(l)}}\right) \\ &= \begin{cases} \mathcal{O}\left(D^{-2b^{(1)}}\right) & l = 1 \\ \mathcal{O}\left(D^{-\left(2b^{(l)} - 1\right)}\right) & l \in \{2, \dots, L+1\} \end{cases}.\end{aligned}$$

Therefore, we require $b^{(1)} \geq 0$ and $b^{(l)} \geq \frac{1}{2}$ for $l \in \{2, \dots, L+1\}$. Notice these are the same requirements as above for the mean of the hidden units. We summarize the scaling for the mean parameters as

$$b^{(l)} \geq \begin{cases} 0 & l = 1 \\ \frac{1}{2} & l \in \{2, \dots, L+1\} \end{cases} \quad (\text{S115})$$

Now consider the second term in the variance of the hidden units. Assume the rank scales with the input and output dimension of a layer as $R^{(l)} = (D^{(l-1)}D^{(l)})^{p^{(l)}}$, where $p^{(l)} \in [0, 1]$.

$$\begin{aligned}\text{tr}([\mathbf{S}_0^{(l)}]_{I,:}^\top \mathbf{A}_0^{(l-1)} [\mathbf{S}_0^{(l)}]_{I,:}) &= \sum_{r=1}^{R^{(l)}} [\mathbf{S}_0^{(l)}]_{I,r}^\top \mathbf{A}_0^{(l-1)} [\mathbf{S}_0^{(l)}]_{I,r} \\ &= \sum_{r=1}^{R^{(l)}} \left(\sum_{j=1}^{D^{(l-1)}} [\mathbf{S}_0^{(l)}]_{I,j,r}^2 [\mathbf{A}_0^{(l-1)}]_{j,j} + \sum_{j \neq j'}^{D^{(l-1)}} [\mathbf{S}_0^{(l)}]_{I,j,r} [\mathbf{A}_0^{(l-1)}]_{j,j'} [\mathbf{S}_0^{(l)}]_{I,j',r} \right) \\ &= \mathcal{O}\left(R^{(l)} D^{(l-1)} \cdot D^{-2\tilde{b}^{(l)}} \cdot 1\right) + \mathcal{O}\left(\sqrt{R^{(l)} D^{(l-1)}(D^{(l-1)} - 1)} \cdot D^{-\tilde{b}^{(l)}} \cdot 1 \cdot D^{-\tilde{b}^{(l)}}\right) \\ &= \mathcal{O}\left(R^{(l)} D^{(l-1)} D^{-2\tilde{b}^{(l)}}\right)\end{aligned}$$

$$\begin{aligned}
&= \begin{cases} \mathcal{O}\left(D^{-(2\tilde{b}^{(1)} - p^{(1)})}\right) & l = 1 \\ \mathcal{O}\left(D^{-(2\tilde{b}^{(l)} - 1 - 2p^{(l)})}\right) & l \in \{2, \dots, L\} \\ \mathcal{O}\left(D^{-(2\tilde{b}^{(L+1)} - 1 - p^{(L+1)})}\right) & l = L + 1. \end{cases}
\end{aligned}$$

Therefore we require $\tilde{b}^{(0)} \geq \frac{p^{(1)}}{2}$, $\tilde{b}^{(l)} \geq \frac{1}{2} + p^{(l)}$ for $l \in \{2, \dots, L\}$, and $\tilde{b}^{(L+1)} \geq \frac{1}{2} + \frac{p^{(L+1)}}{2}$. Notice we can write these conditions in terms of the mean scaling as

$$\tilde{b}^{(l)} \geq b^{(l)} + \begin{cases} \frac{p^{(l)}}{2} & l = 1 \\ p^{(l)} & l \in \{2, \dots, L\} \\ \frac{p^{(l)}}{2} & l = L + 1. \end{cases} \quad (S116)$$

S2.3 PROPOSED SCALING

The previous section derives the necessary conditions for stability at initialization. Recall from Section 3.4 that we propose scaling the contribution of the covariance parameters to the forward pass, i.e. the Sz term, by $R^{-1/2}$ since each element in the term is a sum over R random variables, where R is the rank of S . In the more detailed notation of this section, the proposed scaling implies the forward pass in a linear layer is given by

$$[\mathbf{h}_t^{(l)}]_i = [\mathbf{W}_t]_{:,i} \mathbf{h}_t^{(l-1)} = \left([\boldsymbol{\mu}_t^{(l)}]_I + R^{-1/2} [\mathbf{S}_t^{(l)}]_I \mathbf{z}^{(l)}\right) \mathbf{h}_t^{(l-1)}. \quad (S117)$$

In practice, rather than scaling $[\mathbf{S}_t^{(l)}]_I \mathbf{z}^{(l)}$ by $R^{-1/2}$ in the forward pass, we apply Lemma J.1 from Yang et al. [41] to instead scale the initialization by $R^{-1/2}$ and, in SGD, the learning rate by R^{-1} . Scaling by the rank allows treating the mean and covariance parameters as if they were weights parameterized by μP in a non-probabilistic network, inheriting any scaling that has already been derived for that architecture.

From Table 3 of Yang et al. [41], we therefore scale the mean parameters as

$$b^{(l)} = \begin{cases} 0 & l = 1 \\ 1/2 & l \in \{2, \dots, L\} \\ 1 & l = L + 1 \end{cases} \quad \text{and} \quad c^{(l)} = \begin{cases} -1 & l = 1 \\ 0 & l \in \{2, \dots, L\} \\ 1 & l = L + 1. \end{cases} \quad (S118)$$

Assuming $R^{(l)} = (D^{(l-1)} D^{(l)})^{p^{(l)}}$ as before, where $p^{(l)} \in [0, 1]$, we scale the covariance parameters as

$$\tilde{b}^{(l)} = b^{(l)} + \begin{cases} \frac{p^{(l)}}{2} & l = 1 \\ p^{(l)} & l \in \{2, \dots, L\} \\ \frac{p^{(l)}}{2} & l = L + 1 \end{cases} \quad \text{and} \quad \tilde{c}^{(l)} = c^{(l)} + \begin{cases} p^{(l)} & l = 1 \\ 2p^{(l)} & l \in \{2, \dots, L\} \\ p^{(l)} & l = L + 1. \end{cases} \quad (S119)$$

By comparing to Equations S115 and S116, we see the mean and covariance parameters in all but the output layer are initialized as large as possible while still maintaining stability. The output layer parameters scale to zero faster, since, as in μP for the weights of non-probabilistic networks, we set $b^{(L+1)}$ to 1 instead of $1/2$.

Note that in Section S2.2 we did not consider input and output dimensions that scaled with the width D for simplicity. For our experiments, we take the exact μP initialization and learning rate scaling from Yang et al. [41] — which includes, for example, a $1/\text{fan_in}$ scaling in the input layer — for the means and then make the rank adjustment for the covariance parameters as described above.

We investigate the proposed scaling in Figures S4 and S5. We train two-hidden-layer ($L = 2$) MLPs of hidden sizes 8, 16, 32, and 64 on a single observation $(x, y) = (1, 1)$ using a squared error loss. We use SGD with a learning rate of 0.05. For the variational networks, we assume a multivariate Gaussian variational family with a full rank covariance.

Figures S3 and S4 show the RMSE of the change in the hidden units from initialization, $\Delta \mathbf{g}_t^{(l)}(x) = \mathbf{g}_t^{(l)}(x) - \mathbf{g}_0^{(l)}(x)$, as a function of the hidden size. The RMSE of the hidden units *at* initialization,

$g_0^{(l)}$ is also shown in blue. Each panel corresponds to a layer of the network, so the first two panels correspond to features $g_t^{(1)}(x)$ and $g_t^{(2)}(x)$, respectively, while the third panel corresponds to the output of the network, $g_t^{(3)}(x) = f_t(x)$. The difference between the figures is the parameterization. Figure S3 uses standard parameterization (SP) while Figure S4 uses maximal update parameterization (μ P). We observe that (a) the features change more under μ P than SP and (b) training is more stable across hidden sizes under μ P than SP, especially for smaller networks.

Figures S5 and S6 show the analogous results for a variational network. The top row shows the change in the mean of the hidden units, while the bottom row shows the change in the standard deviation. As in the non-probabilistic case, we observe that (a) both the mean and standard deviation of the features change more under μ P than SP and (b) training is more stable across hidden sizes under μ P than SP, especially for smaller networks.

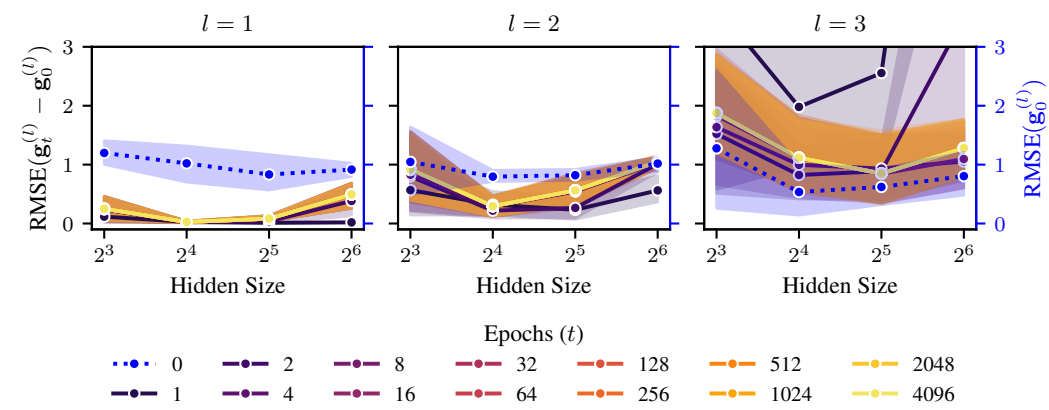


Figure S3: *MLP, Standard Parameterization.* RMSE of the change in the hidden units and, in blue, their initial values. Shaded region represents 95% confidence interval over 5 random initializations. The MLP is trained under SP.

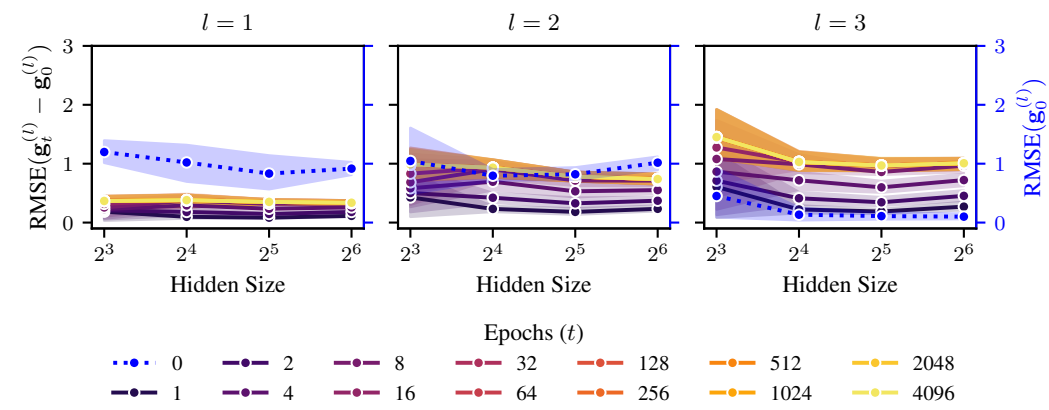


Figure S4: *MLP, Maximal Update Parameterization.* RMSE of the change in the hidden units and, in blue, their initial values. Shaded region represents 95% confidence interval over 5 random initializations. The MLP is trained under μ P.

S2.4 DETAILS ON HYPERPARAMETER TRANSFER EXPERIMENT

As discussed in Section 3.4 we train two-hidden-layer MLPs of width 128, 256, 512, 1024, and 2048 on CIFAR-10. For comparability to Figure 3 in Tensor Programs V [41] we use the same hyperpa-

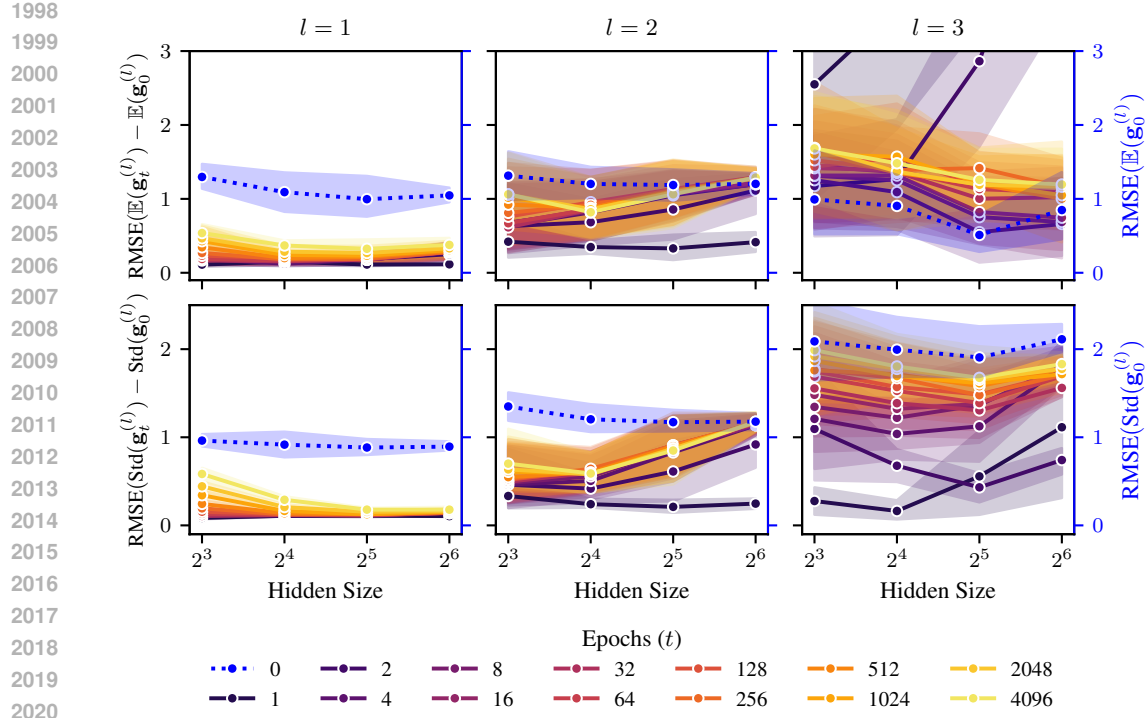


Figure S5: *Variational MLP, Standard Parameterization*. RMSE of the change in the hidden units and, in blue, their initial values. Shaded region represents 95% confidence interval over 5 random initializations. The variational MLP is trained under SP with a full rank covariance in each layer.

rameters but applied to the mean parameters.⁵ For the input layer, we scale the mean parameters at initialization by a factor of 16 and in the forward pass by a factor of 1/16. For the output layer, we scale the mean parameters by 0.0 at initialization and by 32.0 in the forward pass. We use 20 epochs, batch size 64, and a grid of global learning rates ranging from 2^{-8} to 2^0 with cosine annealing during training. For the grid search results shown in the right panel of Figure 3, we use validation NLL for model selection and then evaluate the relative test error compared to the best performing model for that width across parameterizations and learning rates.

S3 EXPERIMENTS

This section outlines in more detail the experimental setup, including datasets (Section S3.1.1), metrics (Section S3.1.2), architectures, the training setup and method details (Section S3.3.1). It also contains additional experiments to the ones in the main paper (Sections S3.2, S3.3.2 and S3.3.3).

S3.1 SETUP AND DETAILS

In all of our experiments we used the following datasets and metrics.

⁵Specifically, we used the hyperparameters as indicated here: <https://github.com/microsoft/mup/blob/main/examples/MLP/demo.ipynb>

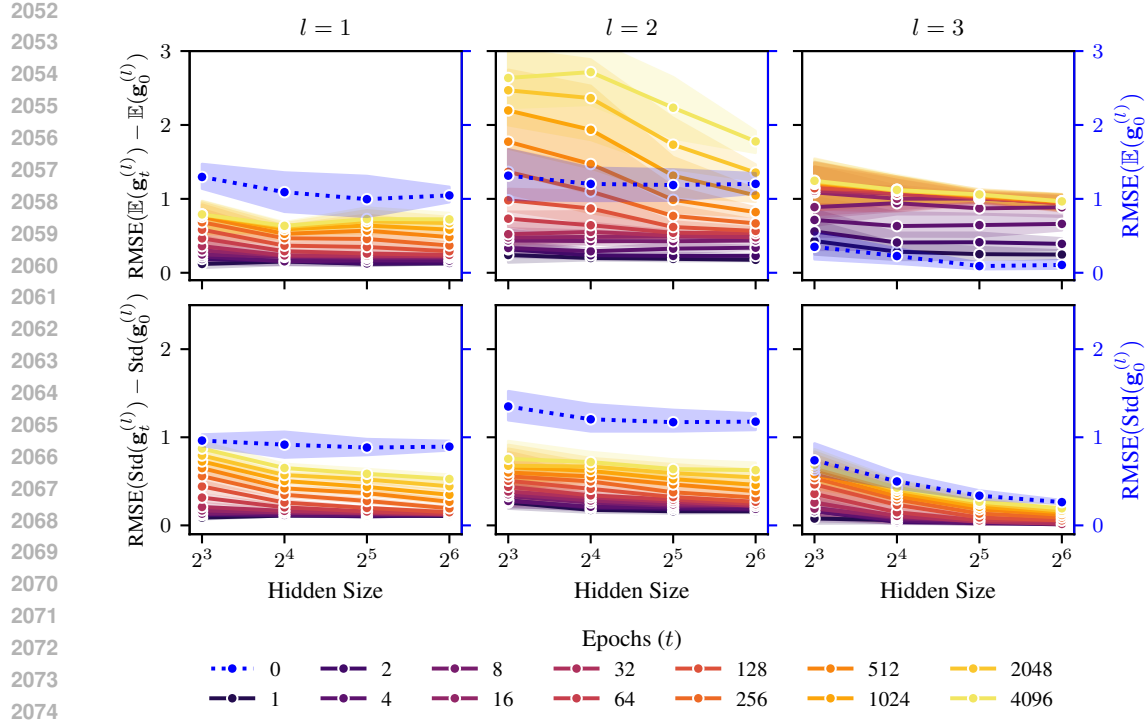


Figure S6: *Variational MLP, Maximal Update Parametrization*. RMSE of the change in the hidden units and, in blue, their initial values. Shaded region represents 95% confidence interval over 5 random initializations. The variational MLP is trained under μ P with a full rank covariance in each layer.

S3.1.1 DATASETS

Table S1: *Benchmark datasets used in our experiments*. All corrupted datasets are only intended for evaluation and thus only have test sets consisting of 15 different corruptions of the original test set.

Dataset	N	N_{test}	D_{in}	C	Train / Validation Split
MNIST [70]	60 000	10 000	28×28	10	(0.9, 0.1)
CIFAR-10 [80]	50 000	10 000	$3 \times 32 \times 32$	10	(0.9, 0.1)
CIFAR-100 [80]	50 000	10 000	$3 \times 32 \times 32$	100	(0.9, 0.1)
TinyImageNet [81]	100 000	10 000	$3 \times 64 \times 64$	200	(0.9, 0.1)
MNIST-C [72]	-	150 000	28×28	10	-
CIFAR-10-C [73]	-	150 000	$3 \times 32 \times 32$	10	-
CIFAR-100-C [73]	-	150 000	$3 \times 32 \times 32$	100	-
TinyImageNet-C [73]	-	150 000	$3 \times 64 \times 64$	200	-

S3.1.2 METRICS

Accuracy The (top-k) accuracy is defined as

$$\text{Accuracy}_k(\mathbf{y}, \hat{\mathbf{y}}) = \frac{1}{N_{\text{test}}} \sum_{n=1}^{N_{\text{test}}} \mathbf{1}_{(y_n \in \hat{y}_n^{1:k})}. \quad (\text{S120})$$

Negative Log-Likelihood (NLL) The (normalized) negative log likelihood for classification is given by

$$\text{NLL}(\mathbf{y}, \hat{\mathbf{y}}) = -\frac{1}{N_{\text{test}}} \sum_{n=1}^{N_{\text{test}}} \log \hat{p}_{\hat{y}_n}, \quad (\text{S121})$$

2106 where $\hat{p}_{\hat{y}_n}$ is the probability a model assigns to the predicted class \hat{y}_n .
 2107

2108 **Expected Calibration Error (ECE)** The expected calibration error measures how well a model
 2109 is calibrated, i.e. how closely the predicted class probability matches the accuracy of the model.
 2110 Assume the predicted probabilities of the model on the test set are binned into a given binning of the
 2111 unit interval. Compute the accuracy a_j and average predicted probability \hat{p}_j of each bin, then the
 2112 expected calibration error is given by

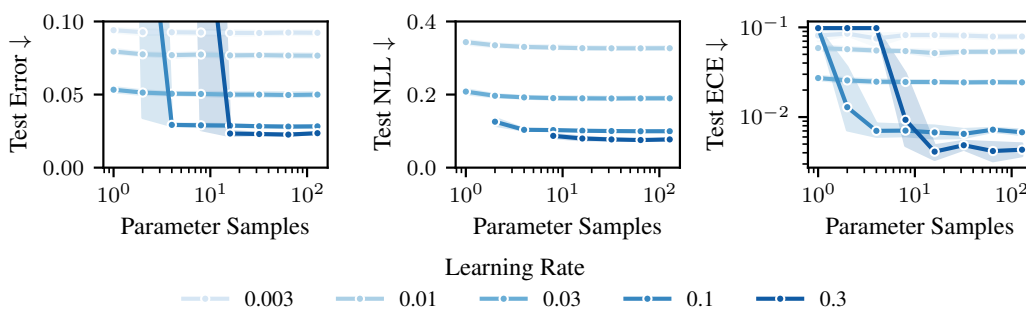
$$2113 \quad 2114 \quad \text{ECE} = \sum_{j=1}^J b_j |a_j - \hat{p}_j|, \quad (S122)$$

2116 where b_j is the fraction of datapoints in bin $j \in \{1, \dots, J\}$.
 2117

2118 S3.2 TIME AND MEMORY-EFFICIENT TRAINING

2120 To keep the time and memory overhead low during training, we would like to draw as few samples
 2121 of the parameters as possible to evaluate the training objective $\ell(\theta)$. Drawing M parameter samples
 2122 for the loss increases the time and memory overhead of a forward and backward pass M times
 2123 (disregarding parallelism). Therefore it is paramount for efficiency to use as few parameter samples
 2124 as possible, ideally $M = 1$.

2125 When drawing fewer samples from the variational distribution, the variance in the training loss and
 2126 gradients increases. In practice this means one has to potentially choose a smaller learning rate to
 2127 still achieve good performance. This is analogous to the previously observed linear relationship
 2128 $N_b \propto \eta$ between the optimal batch size N_b and learning rate η [e.g., 82–84]. Figure S7 shows this
 2129 relationship between the number of parameter samples used for training and the learning rate on
 2130 MNIST for a two-hidden layer MLP of width 128.



2143 Figure S7: *Generalization versus number of parameter samples*. For a fixed number of epochs and
 2144 batch size, fewer samples require a smaller learning rate. For a fixed learning rate, generalization
 2145 performance quickly plateaus with more parameter samples.

2146 As Figure S8 shows, when using momentum, generalization performance tends to increase, but only
 2147 if either the number of samples is increased, or the learning rate is decreased accordingly. A similar
 2148 relationship between noise in the objective and the use of momentum has previously been observed
 2149 by Smith and Le [83], which propose and empirically verify a scaling law for the optimal batch size
 2150 $N_b \propto \frac{\eta}{1-\gamma}$ as a function of the momentum parameter $\gamma > 0$.

2152 S3.3 IN- AND OUT-OF-DISTRIBUTION GENERALIZATION

2154 This section recounts details of the methods we benchmark in Section 5, how they are trained and
 2155 additional experimental results.

2157 S3.3.1 ARCHITECTURES, TRAINING, AND METHODS

2159 **Architectures** We use convolutional architectures for all experiments in Section 5. For MNIST,
 we use a standard LeNet-5 [70] with ReLU activations. For CIFAR-10, CIFAR-100 and TinyIma-

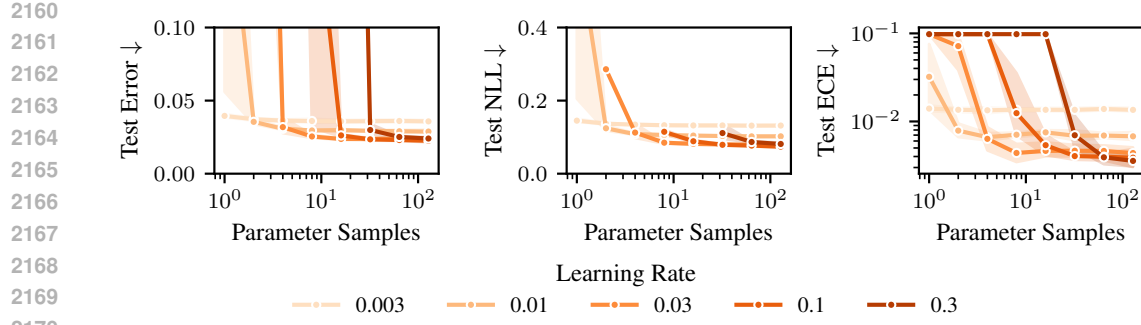


Figure S8: *Generalization versus number of parameter samples when using momentum.* Using momentum improves generalization performance, but when using fewer parameter samples, a smaller learning rate is necessary than for vanilla SGD as predicted by ??.

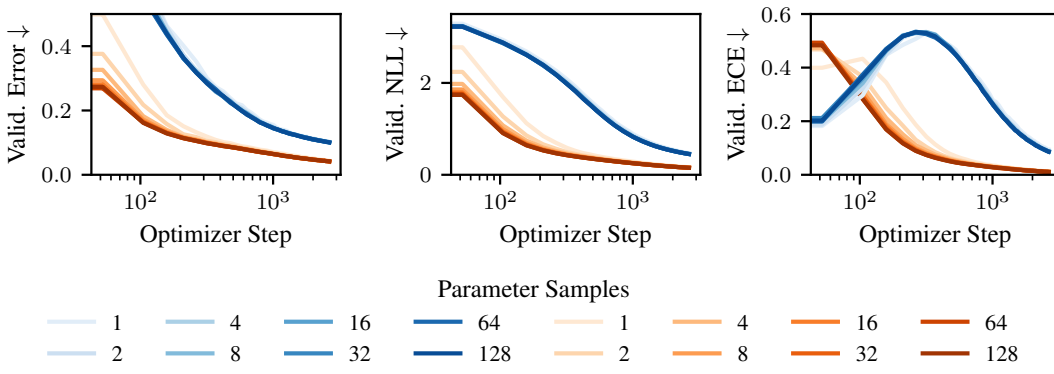


Figure S9: *Validation error during training for different numbers of parameter samples.* The difference in generalization error between different number of parameter samples vanishes with more optimization steps both for SGD (—) and when using momentum (—), if the learning rate is sufficiently small (in this example $\eta = 0.003$).

geNet we use a ResNet-34 [71] where the first layer is a 2D convolution with `kernel_size=3, stride=1` and `padding=1` to account for the image resolution of CIFAR and TinyImageNet and the normalization layers are `GroupNorm` layers. We use pretrained weights from ImageNet for all but the first and last layer of the ResNets from `torchvision` [85] and fully finetune all parameters during training.

Training We train all models using SGD with momentum ($\gamma = 0.9$) with batch size $N_b = 128$ and learning rate $\eta = 0.005$ for 200 epochs. We do not use a learning rate scheduler since we found that neither cosine annealing nor learning rate warm-up improved the results.

Temperature Scaling [69] For temperature scaling we optimize the scalar temperature parameter in the last layer on the validation set via the L-BFGS implementation in `torch` with an initial learning rate $\eta_{TS} = 0.1$, a maximum number of 100 iterations per optimization step and `history_size=100`.

Laplace Approximation (Last-Layer, GS + ML) [26] As recommended by Daxberger et al. [26] we use a post-hoc KFAC last-layer Laplace approximation with a GGN approximation to the Hessian. We tune the hyperparameters post-hoc using type-II maximum likelihood (ML). As an alternative we also do a grid search (GS) for the prior scale, which we found to be somewhat more robust in our experiments. Finally, we compute the predictive using an (extended) probit approximation. Our implementation of the Laplace approximation is a thin wrapper of `laplace` [26] and we use its default hyperparameters throughout.

2214
 2215 **Weight-space VI (Mean-field) [30, 31]** For variational inference, we used a mean-field variational
 2216 family and trained via an ELBO objective with a weighting of the Kullback-Leibler regularization
 2217 term to the prior. We chose a unit-variance Gaussian prior with mean that was set to the pretrained
 2218 weights, except for the in- and output layer which had zero mean. We found that using a KL weight
 2219 and more than a single sample (here $M = 8$) was necessary to achieve competitive performance.
 2220 The KL weight was chosen to be inversely proportional to the number of parameters of the model, for
 2221 which we observed better performance than a KL weight that was independent of the architecture.
 2222 At test time we compute the predictive by averaging logits using 32 samples.

2223 **Implicit Bias VI [ours]** For all architectures in Section 5 we use a Gaussian in- and output layer
 2224 with a low-rank covariance ($R = 10, 20$). We train with a single parameter sample $M = 1$ through-
 2225 out and do temperature scaling at the end of training on the validation set with the same settings as
 2226 when just performing temperature scaling. We do temperature scaling in classification due to the
 2227 specific form of the implicit bias in classification as described in Section S1.3. Since IBVI trains
 2228 by optimizing a minibatch approximation of the expected negative log-likelihood (an average over
 2229 log-probabilities with respect to parameter samples), we also average log-probabilities at test-time
 2230 to compute the predictive distribution over class probabilities. Although we did not see a significant
 2231 difference between averaging log-probabilities, probabilities or logits. Like for WSVI we use 32
 2232 samples at test time.

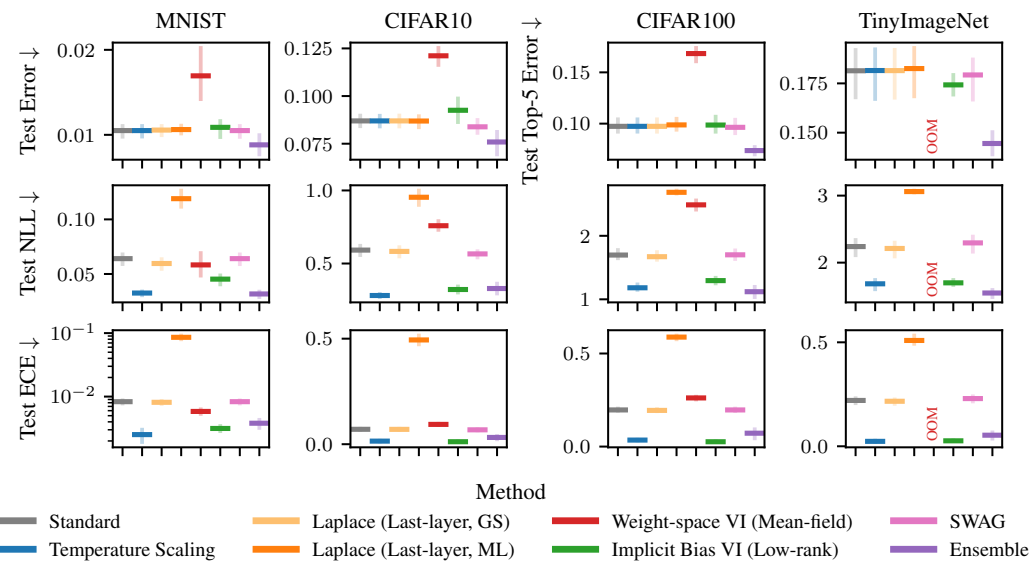
2233 **SWAG** [28] We used a slightly modified implementation of SWAG based on
 2234 `torch-uncertainty` and the original implementation by Maddox et al. [28]. The begin-
 2235 ning of the averaging cycle set to half the number of total epochs and a cycle length of one, i.e.
 2236 SWAG updates happen every epoch. For all other hyperparameters we use the default settings.

2237 **Deep Ensembles** [29] We use five ensemble members initialized and trained independently. We
 2238 compute the predictive by averaging the predicted probabilities of the ensemble members in line with
 2239 standard practice [29]. We did not see a significant difference in performance between averaging
 2240 logits or averaging class probabilities.

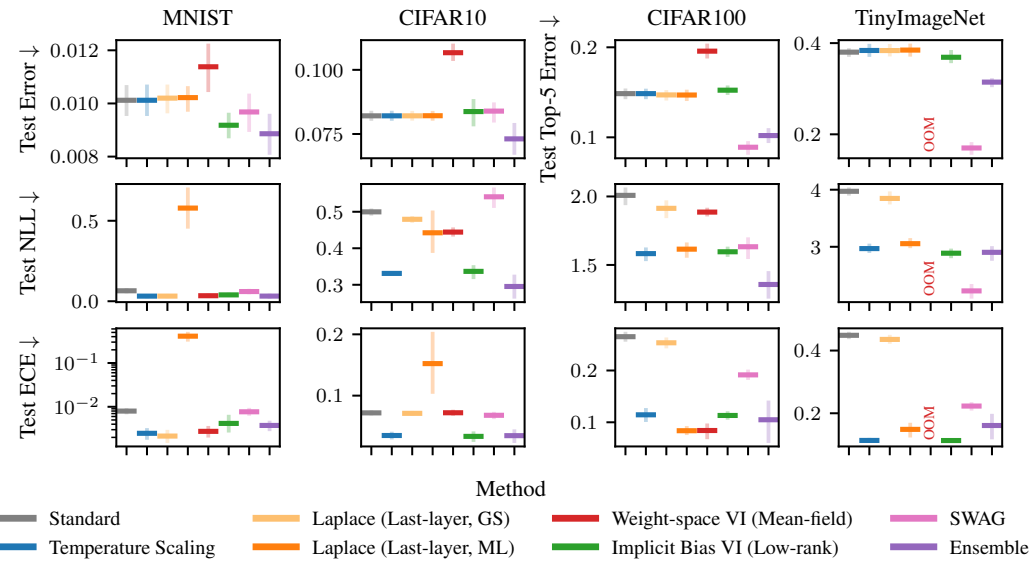
2241
 2242
 2243
 2244
 2245
 2246
 2247
 2248
 2249
 2250
 2251
 2252
 2253
 2254
 2255
 2256
 2257
 2258
 2259
 2260
 2261
 2262
 2263
 2264
 2265
 2266
 2267

2268 S3.3.2 IN-DISTRIBUTION GENERALIZATION AND UNCERTAINTY QUANTIFICATION
2269

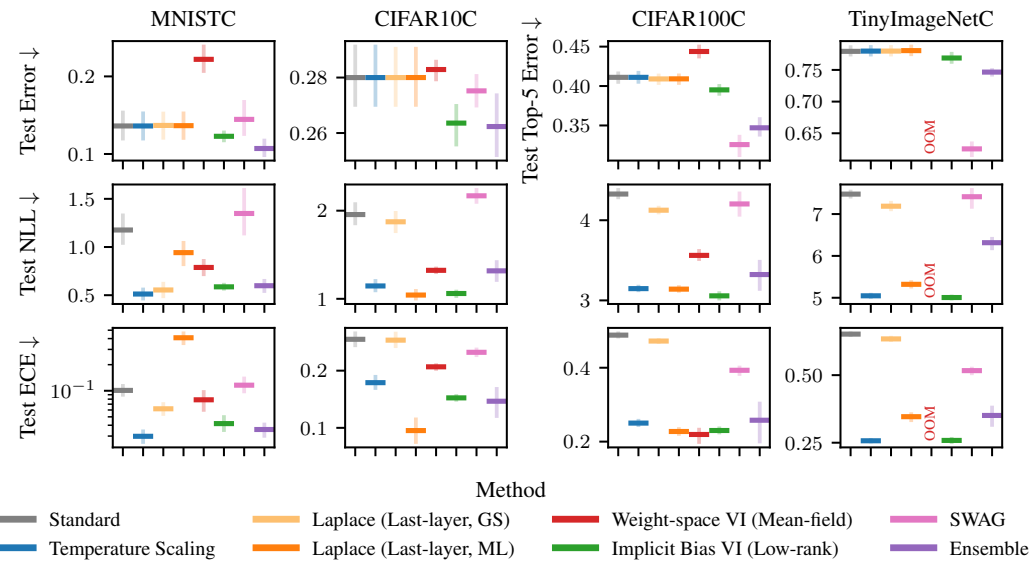
2270 The full results from the in-distribution generalization experiment in Section 5 can be found in
2271 Figure S10. The same experiment but done in the Maximal Update parametrization is depicted in
2272 Figure S11. When finetuning a pretrained model, we found that on some datasets (CIFAR-100,
2273 TinyImageNet) μ P resulted in somewhat lower performance, contrary to the results in Section 3.4,
2274 where we trained from scratch. This suggests that, when pretraining, there may be a modification to
2275 the parametrization that could improve generalization.



2296 Figure S10: *In-distribution generalization and uncertainty quantification (Standard parametriza-
2297 tion).*



2319 Figure S11: *In-distribution generalization and uncertainty quantification (Maximal Update
2320 parametrization).*

2322 S3.3.3 ROBUSTNESS TO INPUT CORRUPTIONS
23232324 Besides the benchmark in Figure S11, we also evaluated the models trained using the Maximal
2325 Update parametrization on the corrupted datasets. The results can be found in Figure S12.2345 Figure S12: Generalization on robustness benchmark problems (Maximal Update parametrization).
23462347 S3.3.4 COMPARISON TO GENERALIZED VI WITH 2-WASSERSTEIN REGULARIZATION
23482349 Theorems 1 and 2 characterize the implicit bias of gradient descent for an overparametrized
2350 linear model as a preference for distributions minimizing the expected loss, which are closest in 2-
2351 Wasserstein distance to the initialization. Given this characterization, by the KKT conditions there
2352 exists a Lagrange multiplier $\lambda \geq 0$ such that the optimal variational parameters θ_*^{GD} define a sta-
2353 tionary point of the following unconstrained optimization objective:

2354
$$\bar{\ell}_r(\theta) = \bar{\ell}(\theta) + \lambda W_2^2(q_\theta, p). \quad (\text{S123})$$

2355

2356 In other words, Implicit Bias VI is equivalent to Generalized VI (GVI) with a 2-Wasserstein regu-
2357 larizer and some regularization strength $\lambda \geq 0$ for overparametrized linear models.
23582359 **Experiment Results** To understand the difference in performance between **IBVI** and **Generalized**
2360 **VI** with a 2-Wasserstein regularizer for *deep neural networks*, we trained models via the GVI ob-
2361 jective in Equation (S123) for different regularization strengths $\lambda \geq 0$ with the same setup as in
2362 Section 5. The results on in-distribution test data can be found in Figure S13 and the results for
2363 corrupted test data are in Figure S14. Both on in- and out-of-distribution data **GVI** performs similar
2364 or worse than **IBVI** for all regularization strengths we tested in terms of test error. **IBVI** and **GVI**
2365 perform roughly similar in terms of uncertainty quantification with **GVI** only performing better for
2366 regularization strengths that harm accuracy.
2367
2368
2369
2370
2371
2372
2373
2374
2375

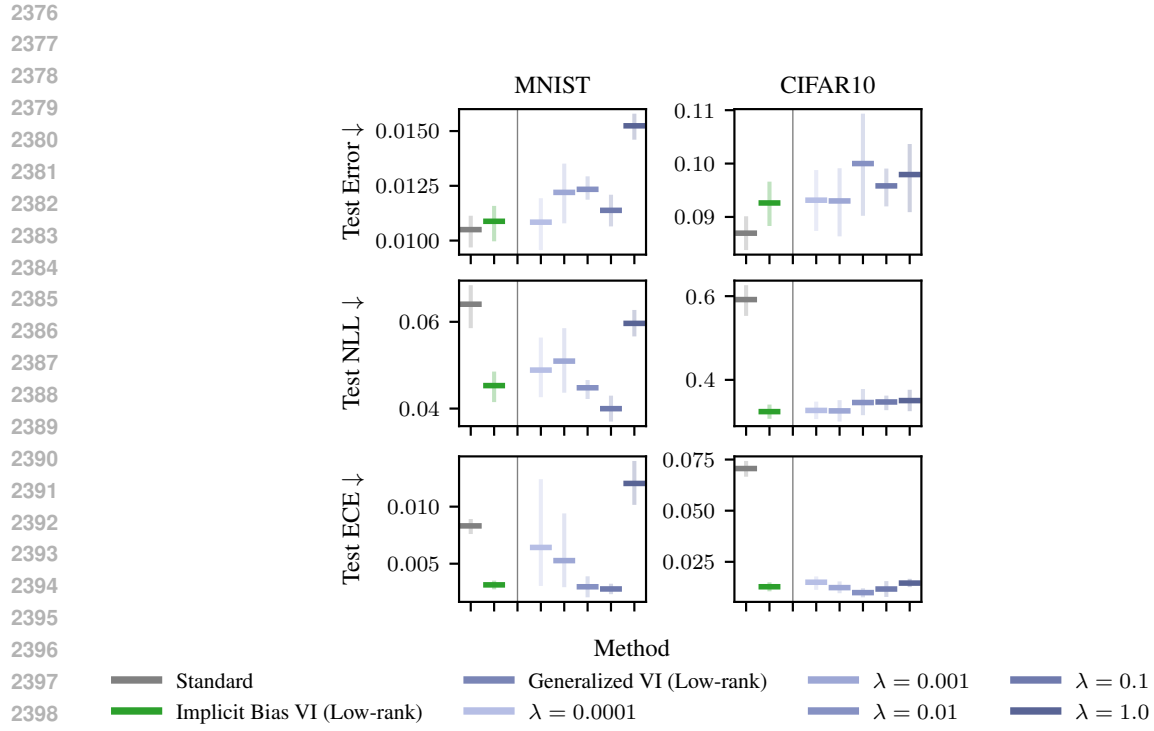


Figure S13: *In-distribution generalization and uncertainty quantification of IBVI and GVI.*

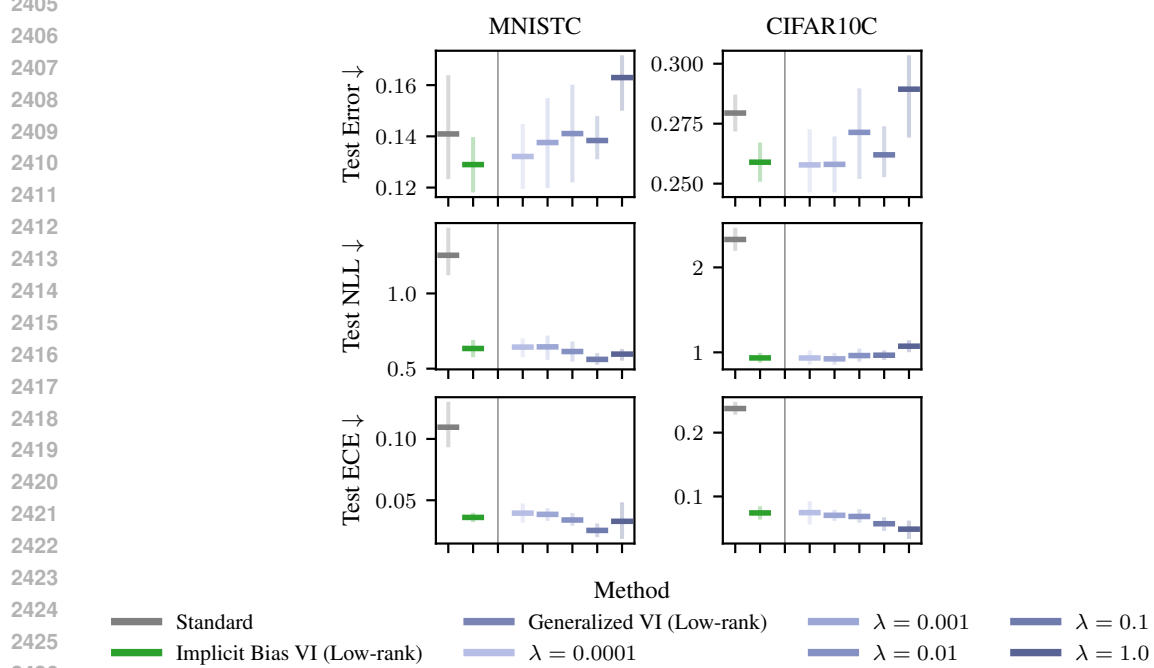


Figure S14: *Out-of-distribution generalization and uncertainty quantification of IBVI and GVI.*